

University of Memphis

University of Memphis Digital Commons

Electronic Theses and Dissertations

4-24-2014

Fungal and Bacterial Infection Mitigation with Antibiotic and Antifungal Loaded Biopolymer Sponges

Ashley Cox Parker

Follow this and additional works at: <https://digitalcommons.memphis.edu/etd>

Recommended Citation

Parker, Ashley Cox, "Fungal and Bacterial Infection Mitigation with Antibiotic and Antifungal Loaded Biopolymer Sponges" (2014). *Electronic Theses and Dissertations*. 939.
<https://digitalcommons.memphis.edu/etd/939>

This Dissertation is brought to you for free and open access by University of Memphis Digital Commons. It has been accepted for inclusion in Electronic Theses and Dissertations by an authorized administrator of University of Memphis Digital Commons. For more information, please contact khhgerty@memphis.edu.

FUNGAL AND BACTERIAL INFECTION MITIGATION WITH ANTIBIOTIC AND
ANTIFUNGAL LOADED BIOPOLYMER SPONGES

by

Ashley Cox Parker

A Dissertation

Submitted in Partial Fulfillment of the

Requirements for the Degree of

Doctor of Philosophy

Major: Biomedical Engineering

The University of Memphis

May 2014

Copyright © 2014 Ashley Cox Parker
All rights reserved

DEDICATION

I would like to dedicate this dissertation to my loving and supportive parents, Tommy and Michelle Cox, and my wonderful husband, David Parker. My parents have always been there for me and without their support and encouragement, I never would have made it where I am today. My loving husband has been a steady influence and support for me throughout my graduate education, always encouraging and cheering me on through the good and tough times.

ACKNOWLEDGEMENTS

First and foremost, I would like to thank my committee chair, advisor, and mentor, Dr. Warren Haggard, whose inspiration and guidance was critical to my success in graduate school and the completion of this work. Additionally, I would like to thank my graduate committee members, Drs. Joel Bumgardner, Ernö Lindner, William Mihalko, Tomoko Fujiwara, and Harry Courtney for their insight and valuable guidance. Because I would not have successfully completed this dissertation without their help, I would like to thank the following individuals: Dr. Jessica Amber Jennings for research guidance and input; Dr. Scott Noel for his early development of the chitosan sponge; Drs. Mark Smeltzer and Karen Beenken at University of Arkansas for Medical Sciences for their collaborative efforts on animal models; Dr. Mark Shirtliff and Lauren Hittle at the University of Maryland at Baltimore for their collaboration on fungal activity assays; Dr. Karyl Buddington and Donny Ray for help with multiple animal models; Patty Lott at the University of Alabama at Birmingham for histological processing; Lou Boykins from the Integrated Microscopy Center for her help with microscopy; Dr. Sanjay Misra for crystallinity testing; Mr. Nathan Webb for help with spectroscopy; Cheyenne Rhoades for histological imaging and grading; Stephen Gilley for viscometry analysis; Alex Hoban for help with *in vitro* testing; and Melanie James and Hope Clippinger for their administrative and moral support. I would also like to thank my fellow graduate students and Keaton Smith for his hard work and invaluable input on cooperative research projects, without which this work might not have been accomplished. Last but not least, I would like to acknowledge and thank my parents, Mr. and Mrs. Tommy and Michelle

Cox, my brother, Brandon Cox, my husband David Parker and his parents, Mrs. Betty Lou Parker and the late Mr. David Parker, for their love and continued moral support.

PREFACE

This dissertation is comprised of several manuscripts which have been or will be submitted for publication to various peer reviewed journals. The manuscript in Chapter 2 entitled “Effects of Sodium Acetate Buffer on Chitosan Sponge Properties and *In Vivo* Degradation in a Rat Intramuscular Model” has been submitted to the Journal for Biomedical Materials Research Part B Applied Biomaterials (January 2014). The research in Chapter 2 was funded by the Department of Defense Medical Research and Development grant number W81XWH-12-2-0020. The manuscript in Chapter 3 entitled “Preliminary Evaluation of Chitosan and Polyethylene Glycol Blended Sponges for the *In Vitro* Local Delivery of Amphotericin B and *In Vivo* Degradation in a Rat Intramuscular Model” will be submitted to the Journal for Biomedical Materials Research Part B Applied Biomaterials. The manuscript in Chapter 4 entitled “Characterization of Local Delivery with Amphotericin B and Vancomycin from Modified Chitosan Sponges and Functional Biofilm Evaluation” will be submitted to the Journal of Orthopaedic Research. The manuscript in Appendix C entitled “Evaluation of Two Sources of Calcium Sulfate for a Local Drug Delivery System: A Pilot Study” has been published in Clinical Orthopaedics and Related Research (May 2011). The manuscript in Appendix D entitled “A Daptomycin-Xylitol-loaded Polymethylmethacrylate Bone Cement How Much Xylitol Should Be Used?” has been published in Clinical Orthopaedics and Related Research (September 2013). All of the work in this dissertation was supported by a National Science Foundation Graduate Research Fellowship.

ABSTRACT

Parker, Ashley Cox. PhD. The University of Memphis. May 2014. Fungal and Bacterial Infection Mitigation with Antibiotic and Antifungal Loaded Biopolymer Sponges. Major Professor: Warren O. Haggard.

Musculoskeletal injuries are some of the most prevalent injuries in both civilian and military populations and their infections can be difficult to treat, often resulting in multiple surgeries and increased costs. In both previous and recent military operations, extremity injuries have been the most common battlefield injuries and many involve complex, open fractures. These extremity injuries are especially susceptible to multiple pathogenic, and sometimes drug resistant, bacteria and fungi. Fungal infections have recently become increasingly problematic in both military and civilian populations and have significantly higher amputation rates than those from bacterial infections. Many of these bacterial and fungal strains adhere to tissue and implanted orthopaedic hardware within wounds, forming biofilms. These problematic, often polymicrobial, infections threaten the health of the patient, but the risk also exists of spreading within hospitals to become prominent resistant infections. Local antimicrobial delivery releases high levels of antimicrobials directly to injured wound tissue, overcoming sub-bactericidal or sub-fungicidal antimicrobial levels present in the avascular wound zones. This research will determine the ability of modified chitosan sponges, buffered with sodium acetate or blended with polyethylene glycol (PEG), to act as short term adjunctive therapies to initial surgical treatment for delivering both antibiotics and/or antifungals for early abatement of infection. The objective of this work was to evaluate both types of modified sponges for *in vitro* and *in vivo* material characteristics and device functionality. *In vitro* analysis demonstrated both the buffered and PEG modified chitosan sponges

exhibited increased degradation and functional cytocompatibility. The chitosan/PEG sponges were able to be loaded with hydrophobic antifungals and the sponges released *in vitro* biologically active concentrations, alone or in combination with the antibiotic vancomycin. Both types of modified sponges exhibited good biocompatibility and slight, but not complete, degradation in an *in vivo* rat intramuscular degradation and biocompatibility model. In an *in vivo* bacteria biofilm infection prevention mouse model, vancomycin loaded chitosan/PEG sponges also cleared more bacteria than the unmodified chitosan sponges. These experimental results led to the conclusion that with additional research and *in vivo* studies, the buffered and PEG blended chitosan sponge local delivery systems exhibit potential for use as adjunctive bacterial or fungal infection prevention therapies to standard surgical treatment of musculoskeletal wounds.

TABLE OF CONTENTS

Chapter		Page
1	Introduction	1
	Background	1
	Hypothesis	7
2	Effects of Sodium Acetate Buffer on Chitosan Sponge Properties and <i>In Vivo</i> Degradation in a Rat Intramuscular Model	8
	Introduction	8
	Materials and Methods	10
	Results	15
	Discussion	28
	References	33
3	Preliminary Evaluation of Chitosan and Polyethylene Glycol Blended Sponges for the <i>In Vitro</i> Local Delivery of Amphotericin B and <i>In Vivo</i> Degradation in a Rat Intramuscular Model	37
	Introduction	37
	Materials and Methods	39
	Results	46
	Discussion	67
	References	73
4	Characterization of Local Delivery with Amphotericin B and Vancomycin from Modified Chitosan Sponges and Functional Biofilm Evaluation	77
	Introduction	77
	Methods	79
	Results	85
	Discussion	97
	References	100
5	Conclusions	104
6	Recommendations for Future Work	107
	References	108
	Appendices	113
	A. Preliminary Formulation Research	113
	B. Additional Cytocompatibility Evaluations	119

C. Evaluation of Two Sources of Calcium Sulfate for a Local Drug Delivery System: A Pilot Study	125
Introduction	125
Materials and Methods	127
Results	132
Discussion	139
References	145
D. A Daptomycin-Xylitol-loaded Polymethylmethacrylate Bone Cement How Much Xylitol Should Be Used?	148
Introduction	148
Materials and Methods	149
Results	156
Discussion	161
References	165
E. Animal Use Protocol Approvals	170

LIST OF TABLES

Table	Page
2.1. Physicochemical properties of buffered and unbuffered chitosan sponges and raw material	18
2.2. Quantitative and qualitative analysis of satellite animal rat tissue histology after 14, 21, and 28 days of sponge implantation	27
3.1. Differential scanning calorimetry results of chitosan/PEG and chitosan sponges, as well as chitosan, PEG 6000, and PEG 8000 powder	51
3.2. Quantitative and qualitative analysis of satellite animal rat tissue histology after 14, 21, and 28 days of sponge implantation	66
4.1. Formulation variables and swelling ratios (n = 3) of blended chitosan/PEG and chitosan sponges	86
4.2. Activity of vancomycin released (both single loaded and dual loaded with amphotericin B) from blended chitosan/PEG and control chitosan sponges against <i>S. aureus</i>	91
A.1. Chitosan and polyethylene glycol sponge formulation variables tested	113
C.1. Average percent daptomycin loaded in pellets and released in elution testing	138
C.2. The average activity for 5% loaded daptomycin (1:10 dilution) against of <i>Staphylococcus aureus</i>	139
C.3. Comparisons of present study with previous research on CaSO ₄ and PMMA	142,143
D.1. Summary of values of cement properties	158
D.2. Summary of activity test results	160
D.3. Summary of the objective functions (that is, best-fit relationships between each of the properties determined and the xylitol loading (X))	161

LIST OF FIGURES

Figure	Page
2.1. <i>In vitro</i> enzymatic mediated degradation profiles	16
2.2. X-ray diffraction spectra	17
2.3. Attenuated total reflectance Fourier transform infrared spectroscopy spectra	19
2.4. Scanning electron microscopy images	21
2.5. Cell culture viability results	22
2.6. Gross and histological tissue images	23
2.7. Percent of implant remaining per histological defect area	25
2.8. Percent of fibrous tissue present per histological defect area	26
2.9. Graded histological inflammatory response	28
3.1. Attenuated total reflectance Fourier transform infrared spectroscopy spectra	48
3.2. X-ray diffraction spectra	50
3.3. Scanning electron microscopy images	53
3.4. <i>In vitro</i> enzymatic mediated degradation profile and sponge viscosity after degradation	55
3.5. <i>In vitro</i> amphotericin B elution profiles	58
3.6. Amphotericin B concentration from zone of inhibition assay	59
3.7. <i>In vitro</i> cytocompatibility results	60
3.8. Quantitative histological analysis of percent implant area per defect area	62
3.9. Quantitative histological analysis of percent fibrous tissue area per defect area	63
3.10. Qualitative graded inflammatory responses of rat tissue	65
4.1. <i>In vitro</i> release profiles of sodium deoxycholate amphotericin B	87
4.2. <i>In vitro</i> vancomycin release profiles	88

4.3. Amphotericin B concentration from zone of inhibition assay	90
4.4. <i>In vitro</i> cytocompatibility of amphotericin B eluates	92
4.5. <i>In vitro</i> cytocompatibility of vancomycin eluates	93
4.6. <i>In vitro</i> cytocompatibility of combination vancomycin and amphotericin B eluates	94
4.7. Bacteria counts from <i>in vivo</i> mouse study	96
A.1. <i>In vitro</i> enzyme mediated degradation profiles	114
A.2. Amphotericin B elution profiles	115
A.3. Chitosan and PEG sponge swelling	116
A.4. Enzyme mediated degradation profiles	117
B.1. Live/Dead stained cells after contact with sponges	120
B.2. Cytocompatibility of amphotericin B and vancomycin standards	124
B.3. Cytocompatibility of stock amphotericin B, vancomycin, and dual solutions	124
C.1. Experimental flow chart	128
C.2. Enzymatic mediated degradation without daptomycin	133
C.3. Enzymatic mediated degradation with daptomycin	134
C.4. <i>In vitro</i> daptomycin elution profiles	136
C.5. Cumulative <i>in vitro</i> daptomycin release	137
D.1. Experimental study design	151
D.2. Daptomycin release profiles	157
D.3. Fatigue test results	159

KEYS TO SYMBOLS OR ABBREVIATIONS

Abbreviation	Meaning	Page
α	alpha	15
°C	degrees Celsius	10
μ	linear attenuation coefficient	155
μL	microliters	43
ALABC	Antibiotic loaded acrylic bone cement	148
ANOVA	Analysis of variance	15
<i>Aspergillus</i> spp	<i>Aspergillus</i> species	2
ATR	Attenuated total reflectance	13
ATR-FTIR	Attenuated total reflectance fourier transform infrared spectroscopy	13
Au/Pd	Gold/ Palladium	13
<i>C. albicans</i>	<i>Candida albicans</i>	2
CaSO ₄	Calcium sulfate	9
cc	cubic centimeter	84
CDC	Center for Disease Control	100
CFU	Colony forming unit	83
cm	centimeter	10
CO ₂	Carbon dioxide	13
DDA	Degree of deacetylation	5
D _{dapt}	Coefficient of diffusion for outflow of Daptomycin	150
DMEM	Dulbecco's Modified Eagle Medium	13

DMSO	Dimethylsulfoxide	43
dn/dc	specific refractive index increment	12
D_{PBS}	Coefficient of diffusion for intake of PBS	155
DSC	Differential scanning calorimetry	12
FBS	Fetal bovine serum	13
FTIR	Fourier transform infrared spectroscopy	13
g	grams	129
g/mol	grams/mole	40
GPC	Gel permeation chromatography	12
HPLC	High pressure liquid chromatography	81
I	Inhibition index	154
IACUC	Institutional Animal Care and Use Committee	14
IFI	Invasive fungal infections	3
$K\alpha$ Cu	K alpha copper	12
k'	Cement polymerization rate	158
$K_2\text{SO}_4$	Potassium sulfate	127
kDa	kilodaltons	10
kGy	kilogray	14
K_{IC}	Fracture toughness	151
kV	kilovolt	12
lyo	Lyophilization	45
M	molar	10
mA	milliamps	12

mg	milligrams	11
MIC	Minimum inhibitory concentration	2
min	minute	13
mL	milliliters	2
mm	millimeters	13
mM	millimolar	81
MRSA	Methillicin sensitive <i>Staphylococcus aureus</i>	2
MW	Molecular weight	10
NaOH	Sodium hydroxide	9
NHDF	Normal human dermal fibroblasts	13
NIH	National Institute of Health	84
nm	nanometers	13
OD	Optical density	155
<i>P. aeruginosa</i>	<i>Pseudomonas aeruginosa</i>	2
PBS	Phosphate buffered saline	11
PEG	Polyethylene glycol	6
PJI	Periprosthetic joint infection	148
PMMA	Polymethylmethacrylate	4
PTFE	Polytetrafluoroethylene	84
R	Radiopacity	155
R'	Normalized radiopacity	155
<i>S. aureus</i>	<i>Staphylococcus aureus</i>	84
SD	Standard deviation	132

SEM	Scanning electron microscopy	30
TCP	Tissue culture plastic	83
TIDOS	Trauma Infectious Disease Outcome Study	3
TJA	Total joint arthroplasty	148
TSB	Trypticase soy broth	83
USD	United States Dollar	148
UV-Vis	Ultraviolet-visible spectroscopy	82
v/v	volume/ volume	10
w/v	weight/volume	10
XRD	X-ray diffraction	12

CHAPTER 1

INTRODUCTION

Background

Musculoskeletal trauma, which is an injury to bone and/or muscle tissue, is one of the most prevalent types of injuries in the United States.¹ More than three out of five of the unintentional injuries occurring annually in the U.S. are musculoskeletal injuries.¹ In 2004, approximately 57.2 million musculoskeletal injuries occurred in the U.S. and 20,000 of the injured patients died.¹ The economic cost of these injuries is high due to medical (hospitalization, post operative care, therapy, etc.) costs and salary loss; out of the musculoskeletal injuries that occurred in 2004, 1.04 million people were hospitalized for an average of 4.7 days, resulting in total estimated hospital costs of \$26.65 billion and \$25,000 per patient.¹

Infection associated with these musculoskeletal related injuries also has a significant impact on patient morbidity and mortality and can be a devastating complication.² Infection and osteomyelitis, a bone infection caused by bacteria or a fungus, are especially troublesome in open fractures, which are caused by high energy trauma and typically result in both skeletal and soft tissue injury. The infection rates of orthopaedic surgery (total hip arthroplasty) have been reported as 0.8-1.2% while the reported infection rates of closed and open fractures are 3.6-8.1% and 17.5-21.2%, respectively.³ Based on injuries through May 2003, the rate of infection was reported to be 26.5% in soldiers with battlefield complex trauma.⁴ During the Vietnam War, infectious complications occurred in 3.9% of casualties and septic shock was determined to be a leading cause of mortality.⁵

In the Iraq and Afghanistan wars (Operation Iraqi and Enduring Freedom), extremity injuries were the most common combat injuries. These extremity injuries are especially susceptible to multiple pathogenic, and sometimes drug resistant bacteria or fungi, such as methicillin resistant *Staphylococcus aureus* (MRSA), *Pseudomonas aeruginosa*, *Acinetobacter baumannii*, *Escherichia coli*, *Aspergillus* spp, or *Candida albicans* (*C. albicans*).^{6,7} In addition to the presence of multidrug resistant bacteria or fungi, the presence of necrotic tissue, debris, and fixation devices or implants creates a favorable environment for the development of biofilms and corresponding infection.⁸ According to an estimate by the CDC, approximately 65% of bacterial infections are associated with biofilms.⁹ Biofilms are adherent (sessile) bacterial populations of single or mixed colonies with protective mechanisms that enable them to communicate between themselves and resist antibiotic and antimicrobial agents.^{8,10} In biofilms, the metabolic activity of the bacteria is reduced, resulting in less susceptibility to antimicrobials and an increased minimal inhibitory concentration (MIC).¹⁰ Researchers have found the MIC for nonadherent *P. aeruginosa* to be 1 µg/ml tobramycin, but adherent *P. aeruginosa* in biofilms on urinary catheters remained viable after 12 hours of exposure to tobramycin at levels as high as 1,000 µg/ml.^{8,11} Systemic antibiotics cannot reach such a high concentration at a localized site without toxicity, thereby becoming ineffective against the biofilms.¹⁰

Invasive fungal infections have become recently troublesome for both military and civilian populations, with high mortality rates and high healthcare costs.^{2,12,13} The British Military has recently reported higher rates of fungal wound infections in casualties from the Helmand Province in Afghanistan.¹⁴ In a 2011 Trauma Infectious

Disease Outcome Study (TIDOS), it was determined that 36 cases of invasive fungal infections (IFI) were found in Operation Enduring Freedom soldiers with blast injuries in Afghanistan from June 2009 to December 2010, and 78% of the wounded warriors with IFI required lower extremity amputations.¹⁵ An outbreak of cutaneous mucormycosis was also recently reported in victims from the 2011 tornado in Joplin, Missouri.¹⁶ *Apophysomyces trapeziformis* was identified in all 13 infected patients and 10 patients required admission to intensive care, but 5 of the infected patients died.^{16,17} While invasive fungal infections can be rare in patients without risk factors, higher incidences have been found in transplant patients, African Americans, and babies younger than one year old.^{18,19} Invasive *Candida* infection is the third most common cause of hospital-acquired bloodstream infections and is five times more prevalent in children than invasive *Aspergillus* infection.^{19,20}

Effective wound management often provides faster and more comfortable wound healing, which increases patients' quality of life. The common steps utilized in wound management with orthopaedic injuries and surgical sites are debridement, irrigation, dressings, fixation, closure, and systemic antibiotic therapy.²¹ All of these steps are utilized by surgeons in order to prevent further damage to the tissues, amputation, or even death. Because systemic antibiotics cannot be administered at very high concentrations to fight localized bacteria, local antimicrobial delivery can be an effective route for treating wounds and minimizing bacterial infections, when used as an adjunctive therapy to systemic dosing.²² In addition to issues with antibiotic resistance, toxicity issues can arise with systemic drug delivery because drugs are delivered to the entire body.²² Local antibiotic or antifungal delivery releases high levels of antibiotics directly to injured

wound tissue, overcoming sub-bactericidal antibiotic levels present in the avascular wound zones.^{22,10,23}

Several materials are currently being utilized as local antibiotic delivery systems, but many of these materials have disadvantages, including the need for a removal surgery, the inability to load antibiotics directly in the operating room, and limited time of delivery. Polymethylmethacrylate (PMMA) bone cement is one of the most common materials used as a local antibiotic carrier for musculoskeletal infection prevention or treatment.²⁴ While bone cement has shown to reduce infection in severe open fractures, some major disadvantages of the material are the need for surgical removal, possible biofilm formation, and the development of antibiotic resistant bacteria.^{10,25} Calcium sulfate is another commonly used local antibiotic delivery material and is a biocompatible, biodegradable material with osteoconductive properties.^{26,27} Although calcium sulfate exhibits an antibiotic bolus release followed by extended drug release from several hours to weeks, wounds treated with calcium sulfate can develop sterile draining sinuses that mimic infected draining sinuses and antibiotic choices and dosages can be limited.²⁶⁻²⁹ The collagen sponge is also a degradable drug delivery system, but despite the degradable nature and high local antibiotic release of these sponges, the high initial level of antibiotics has been reported to generate toxic antibiotic serum levels and potential immunogenic responses to the collagen sources can be another problem.^{10,30}

While antibiotics have been studied extensively in local delivery, antifungals have not been successfully locally delivered from as many degradable delivery systems because of their hydrophobicity for loading and distribution. The hydrophobic antifungal, amphotericin B, has also been incorporated into a few local delivery systems,

including poly(methyl methacrylate) bone cement, a hydroxyapatite and chitosan composite, a Pluronic® based copolymer gel, and dextran hydrogels.³¹⁻³⁵ A drawback to these developed local antifungal delivery systems is that most are pre-loaded with antifungal and are not easily customized by the clinician. There is a clear need for a degradable local delivery system alternative, such as a chitosan device, that can be loaded with multiple antimicrobials, including antibiotics and antifungals, at the point of care to provide clinicians with a viable adjunctive therapy to systemic antibiotic and antifungal delivery.

Chitosan, a positively charged linear polysaccharide composed of β -(1-4)-2-amino-2-D-glucosamine (deacetylated) and β -(1-4)-2-acetamido-2-D-glucosamine (acetylated) units, has been studied extensively in bioadhesion, drug delivery and tissue engineering research and demonstrates promising properties for such biomedical applications.³⁶⁻⁴⁰ Chitosan is produced by deacetylation of the naturally occurring chitin from crustacean shells, which is the second most abundant naturally occurring polymer.^{40,41} Advantages of chitosan include low cost, biodegradability, high biocompatibility, availability, and functional groups that allow for easy chemical modification.⁴²

Chitin and chitosan have different degrees of deacetylation (DDA); chitin typically has DDA of less than 50% and chitosan has a DDA greater than 50%.³⁸ The degree of deacetylation of chitosan affects degradation; as DDA increases, chitosan becomes more resistant to degradation.⁴¹ While in the human body, chitosan is degraded by lysozyme, lipasases, chitosanases, and N-acetyl-o-glucosamindase.⁴³ Lysozyme degrades chitosan through cleavage of glycosidic bonds and has also shown to quickly

degrade chitosan *in vitro*.⁴⁴ Chitosan's degradation products, glucosamines and saccharides, do not elicit chronic foreign body reactions because the human body gradually absorbs them.⁴⁵

When used as a drug delivery system, chitosan effectively carries antibiotics and exhibits biodegradation and predictable elution rates.⁴⁶ However, wide variations in *in vivo* degradation of chitosan have been reported; Ma et al. found chitosan scaffolds to exhibit minimal degradation after subcutaneous implantation, but Noel and researchers reported rapid degradation of chitosan after use as a wound dressing.^{47,48} Previous research conducted at the University of Memphis has yielded a topical, porous, degradable chitosan sponge that provides an adaptable antibiotic delivery system in which tailored dosing and degradation can be achieved.^{48,49} This system can be loaded with antibiotics immediately prior to use, allowing for clinician selected antibiotic loading, as well as combination loading.^{48,49} However, in order to load hydrophobic antifungals into the chitosan sponges, the sponges must be modified, possibly with other polymers that have previously shown antifungal solubility.

The water soluble polymer, polyethylene glycol (PEG) has been found to function as a solvent system for a hydrophobic fatty acid, cis-2-decenoic acid, allowing for point of care loading of the fatty acid into the chitosan sponges.⁵⁰ Polyethylene glycol exhibits protein resistance, which is the resistance of protein accumulation on surfaces, low toxicity and immunogenicity; when added to chitosan films, PEG also enhanced protein adsorption, cell adhesion, growth, and proliferation.⁵¹ In addition to films, PEG has been used to modify chitosan fibers and hydrogels.⁵¹⁻⁵⁴ Modification of chitosan with PEG can occur through blending, copolymerization, or by using PEG simply as the drug solvent.⁵²⁻

⁵⁴ Polyethylene glycol has also been utilized as a solvent system, either as liposomes or nanoparticles, for amphotericin B in systemic delivery.⁵⁵⁻⁵⁸

For the modified chitosan sponges investigated in this body of work, sodium acetate buffered and PEG blended chitosan sponges were fabricated and evaluated for *in vitro* material properties and functionality as degradable, biocompatible, local antibiotic and/or antifungal delivery systems. The modified chitosan sponges were also investigated *in vivo* to confirm biocompatibility, degradation, and infection prevention.

Hypothesis

Chitosan sponges, modified with either a buffer or polyethylene glycol (PEG) will form a degradable local delivery system, capable of point of care loading of multiple antibiotics and/or hydrophobic antifungals, for use as adjunctive therapy to reduce bacterial and fungal wound contamination and biofilms in acute musculoskeletal trauma injuries.

CHAPTER 2

EFFECTS OF SODIUM ACETATE BUFFER ON CHITOSAN SPONGE PROPERTIES AND *IN VIVO* DEGRADATION IN A RAT INTRAMUSCULAR MODEL

Introduction

Musculoskeletal injuries are some of the most prevalent injuries in both civilian and military populations and their infections can be difficult to treat, often resulting in multiple surgeries, as well as increased patient morbidity, treatment time, and costs.¹ In military operations, extremity injuries are the most frequent and many involve complex, open fractures where bone is exposed to environmental contamination.² Extremity injuries are especially susceptible to multiple pathogenic, and sometimes multidrug resistant bacteria, such as methicillin resistant *Staphylococcus aureus* (MRSA), *Pseudomonas aeruginosa*, *Acinetobacter baumannii*, and *Escherichia coli*.^{3,4} Up to 25% of open fractures develop osteomyelitis, bone infection caused by bacteria or fungus, and treatment failure rates are higher when either MRSA or *P. aeruginosa* are the infecting organisms.⁵⁻⁷

The current standard of care for extremity wounds includes debridement and irrigation of the affected area, as well as fracture stabilization, with serial debridement and irrigation steps to follow.¹ Systemic antibiotics are the current standard method of prophylaxis and treatment for infections. Due to the avascular nature of traumatic wound sites, delivery of inhibitory concentrations of antibiotics to affected tissue through the bloodstream requires high dosing which carries risks ranging from allergic reaction to ototoxicity or kidney failure.²⁻⁴ Local antibiotic delivery, used as an adjunctive therapy to systemic dosing, can overcome the issues of sub-bactericidal antibiotic concentrations in

the avascular zones of wound sites by providing high levels of antibiotics directly to the injured tissues.

Two of the most commonly used local antibiotic delivery systems in clinical practice include antibiotic-loaded polymethylmethacrylate (PMMA) and calcium sulfate (CaSO_4). Antibiotic loaded PMMA beads provide a predictable release of antibiotic for several weeks and reduce the infection rate in severe open fractures, but disadvantages include the possibility for surgical removal and long term, sub-inhibitory antibiotic concentrations which may encourage antibiotic resistant bacteria strains and/or biofilm formation on the implant's surface.⁵⁻¹⁰ CaSO_4 is a degradable material with characteristic, high initial antibiotic burst-release in the local wound site, elevated wound drainage, and limited antibiotic choices and dosages.¹¹⁻¹⁴

Porous chitosan sponges have been previously developed for rapid local drug delivery as an adjunctive therapy during extremity wound debridement and irrigation.^{15,16} These biocompatible sponges can be loaded at the point of care with physician selected antibiotics and then release a high local dose of antibiotic to reduce bacterial levels.^{15,16} However, one problem is that these sponges do not degrade quickly and can persist in the wound, after the sponges have delivered the antibiotic. This delayed degradation is a problem because remaining chitosan may act as a nidus for secondary infection.

One approach to increase chitosan degradation is to decrease crystallinity of the chitosan polymer.²⁴ Crystallization of the chitosan sponges occurs during sodium hydroxide (NaOH) washes, used in the neutralization process. Using different solutions for residual acid removal without inducing crystallization could help to increase sponge degradation. In this investigation, sodium acetate buffers were used after a NaOH wash

of the chitosan sponges and were compared to neutral sponges with NaOH washes only. We hypothesized *in vitro* and *in vivo* analysis would reveal that modification of sponges using the buffering step in fabrication would increase sponge degradation while not affecting biocompatibility, compared to neutral chitosan sponges. The first aim of this study was to evaluate whether the buffering procedure affected *in vitro* degradation and biocompatibility, as well as thermal, crystalline, spectroscopic, and morphologic properties. We then evaluated the *in vivo* degradation and biocompatibility of the chitosan sponges in a rat dorsal muscle pouch model through both quantitative and qualitative histological assessment of the implant sites.

Materials and Methods

Fabrication. Chitosan sponges were manufactured using previously described double lyophilization methods.^{15,17,18} Chitopharm S chitosan was purchased from Chitinor AS (Tromsø, Norway) having a 82.5 ± 1.7 degree of deacetylation (DDA), 251 ± 17 kDa weight-average molecular weight (MW) and 2.013 ± 0.145 polydispersity index. All acids and buffer solutions were obtained from Fisher Scientific (Pittsburg, PA) First, the chitosan was dissolved at 1% (w/v) in a 1% (v/v) blended acid solvent (3:1 ratio of lactic to acetic acid). The dissolved chitosan solution was cast (250 mL) in an 11×20 cm container, frozen at -20°C, and lyophilized in a Labconco (Kansas City, MO) FreeZone 2.5 Liter Benchtop Freeze Dry System. The dehydrated, acidic chitosan sponges were then either neutralized in NaOH or neutralized in NaOH and soaked in one of two different acetate buffer treatments to create neutralized or buffered sponges, respectively. For the NaOH neutralization treatment, the sponges were rinsed in 250 mL of 0.6 M NaOH for approximately seven minutes, washed with copious amounts of ultrapure water

until a neutral pH was reached, and then re-frozen at -20°C and re-lyophilized. Based on prior work and preliminary screening using multiple variations of acetate buffer pH, concentration, and hydration times, the buffered sponges were fabricated by gently compressing the hydrated sponge and then soaking the sponge in approximately 500 mL of a 0.25 M acetate buffer at either 4.6 or 5.6 pH. After 30 minutes of hydration in the buffer solution, excess buffer solution was removed and the buffered sponge was re-frozen at -20°C and re-lyophilized. After the second lyophilization the neutral, 4.6 pH buffered and 5.6 pH buffered chitosan sponges were stored in a desiccator cabinet until subsequent analyses.

In Vitro Degradation. Degradation of neutralized, 4.6 pH, and 5.6 pH buffered chitosan sponges was determined based on mass loss using a protocol previously reported.^{18,19}

Briefly, triplicate samples of each sponge formulation were trimmed to similar sizes and weighed on a Mettler Toledo (Columbus, OH) XS205 Dual Range scale to establish an initial weight. Samples were placed in a 125 mL Nalgene (Rochester, NY) container and hydrated with 35 mL of 1 mg/mL 2× crystallized chicken egg white lysozyme and penicillin (100 units/mL), streptomycin (100 mg/mL), amphotericin B (0.25 µg/mL), both from MP Biomedicals (Solon, OH), in 1× phosphate buffered saline (PBS).

Degradation samples were placed on a rocking shaker in an incubator at 37°C and the degradation solution was exchanged every 24 hours over 10 days. At each 24 hour interval, three replicate chitosan sponge samples from each sponge variation were removed from the degradation solution and rinsed in ultrapure water. Sponge samples were then placed in a vacuum oven at 60°C for two days until dry and were weighed for a

final sponge weight. The percent remaining of the sponge was calculated using equation 1.

$$\text{Percent remaining (\%)} = \left(\frac{\text{Sponge weight at x days}}{\text{Initial dry sponge weight}} \right) \times 100 \quad (1)$$

The gentle, vacuum drying process eliminated the option of utilizing that individual samples a second time, and therefore separate samples were analyzed for each replicate and time point.

Molecular Weight. Molecular weight was determined by gel permeation chromatography (GPC), using a TOSOH Bioscience (King of Prussia, PA) TSKgel G5000PWxl column at 30°C, coupled with a Wyatt (Santa Barbara, CA) DAWN HELEOS II multi-angle light scattering detector and Varian Prostar 450 refractive index detector. Chitosan samples were dissolved at 1 mg/mL in the mobile phase solution of 0.15 M acetic acid and 0.1 M sodium acetate at pH 5. An injection volume of 50 μ L and a specific refractive index increment (dn/dc) for chitosan of 0.163 mL/g were used.²⁰

Crystallinity. X-ray diffraction (XRD) was used to characterize the crystal structure of the raw chitosan material, as well as neutral, 4.6 pH, and 5.6 pH buffered chitosan sponges. XRD patterns were determined using multiple scans from a Bruker AXS (Madison, WI) Advanced D8 X-ray diffractometer with $K\alpha$ Cu radiation source at 40 kV and 40 mA over a 2θ range from 5° to 40° with a step size of 0.05° and a time/step of 0.2 seconds.

Thermal Analysis. A Netzsch (Selb, Germany) 200 PC differential scanning calorimeter (DSC) was used to evaluate the thermal properties of the three chitosan sponge

formulations and chitosan powder (n = 3). Samples were scanned from 40 to 400°C at 20°C/min in order to assess variations in endothermic and exothermic peak temperatures.

Spectral Analysis. In order to evaluate sponge differences, chitosan sponge sample functional group chemistries were compared (n = 3) using attenuated total reflectance Fourier transform infrared spectrometry (ATR-FTIR) with a ThermoScientific (Waltham, MA) Nicolet iS10 FTIR spectrometer with a diamond ATR crystal. Absorbance spectra were acquired using 64 scans with a resolution of 4 cm⁻¹ and processed using the Thermo Scientific OMNIC™ Software Suite.

Morphology. Surface morphology of the three chitosan sponge formulations (n = 3) was assessed using a FEI/Philips XL30 Environmental Scanning Electron Microscope at 15kV and samples sputter-coated with 30 nm of Au/Pd. Images were visually inspected for differences between sponge groups such as surface texture and porosity.

Direct Contact Biocompatibility. A protocol modified from ASTM F813-07 “Standard Practice for Direct Contact Cell Culture Evaluation of Materials for Medical Devices” was followed in order to assess the direct contact biocompatibility between the chitosan sponge variations and normal human dermal fibroblasts (NHDF) purchased from Lonza (Walkersville, MD). NHDF cells (passages 4 through 6) were seeded at 6×10⁴ cells/mL and allowed proliferate to confluence on BD Falcon (Franklin Lake, NJ) 12-well polystyrene tissue culture plates in Dulbecco’s Modified Eagle’s Medium (DMEM) supplemented with 10% fetal bovine serum (FBS) and penicillin (100 units/mL), streptomycin (100 mg/mL), amphotericin B (0.25 µg/mL), all purchased from Fisher Scientific, under standard cell culture conditions (37°C and 5% CO₂ atmosphere). Cell culture medium was aspirated and refreshed with 1 mL of fresh medium before a single 8

mm diameter test specimen (n = 5) of either a neutralized chitosan sponge, 4.6 pH buffered chitosan sponge, 5.6 pH buffered chitosan sponge or a polyurethane sponge (control) was gently placed in a well in direct contact with the cell monolayer. Cultures were incubated for either one or three days before biocompatibility was assessed with the Cell Titer-Glo® Luminescent Cell Viability assay (Promega, Madison, WI). The luminescent signal, which corresponded to the amount of adenosine triphosphate and the number of viable cells through a standard dilution of known concentrations of cells, was recorded at 590 nm using a BioTek (Winooski, VT) FLx-800 Fluorescence Microplate Reader.

In vivo Degradation. A total of 23, three month old male Sprague-Dawley rats (average weight of 398 g) were utilized for this study. This pre-clinical study was approved by institutional review boards at the University of Memphis (IACUC protocol #0720) and the Army Medical Research and Material Command (Protocol DM 090455.02) and followed guidelines set forth by both organizations. Rats were anesthetized with 2% isoflurane in an environmental chamber and given a sub-cutaneous injection of carprofen in the rat flank. The rat was prepared for sterile surgery with anesthesia maintained using 4 to 5% isoflurane. Two 1.5 cm incisions were made through the skin on each side of the midline (4 incisions total). In each incision, a 1.25 cm pouch was created in the *latissimus dorsi* muscle. One disc shaped implant, 9.5 mm in diameter and approximately 5 mm thick, was implanted bilaterally in each muscle pouch. Test groups included gamma irradiation sterilized (25.0 to 40.0 kGy dosage) neutralized chitosan sponge, 4.6 pH buffered chitosan sponge, 5.6 pH buffered chitosan sponge and an absorbable gelatin sponge (Gelfoam®, Pfizer, New York City, NY) as a positive control. Each rat received

one of each implant, randomized among the four incision sites. After implantation, the muscle incision was sutured while the skin was closed with one to three staples. Carprofen was also administered for two days post-operatively. Ten rats were sacrificed at the 4 and 10 day time points (n = 10). Satellite animals were sacrificed at the 14, 21 and 28 day time points (n = 1) for preliminary investigation of prolonged degradation. Satellite animal degradation data was used for selecting degradation time points for future *in vivo* studies. After each sacrifice the implanted region and surrounding tissue were excised (see figure 5A) and placed in 10% phosphate buffered formalin for two days. Tissue sections were then bisected across the implant for quantitative and qualitative histological evaluation (paraffin-embedded and H&E stained). The percentages of sponge and fibrous tissue in the defect area of the stained tissue sections were measured and calculated using a Nikon inverted microscope Eclipse TE300 and BIOQUANT® OSTEO II image analysis software, and cellular response was graded by three blinded reviewers.

Statistical Analysis. *In vitro* degradation testing was analyzed by least squares regression. Thermal analysis was analyzed using one-way ANOVA with Tukey's post hoc analysis. *In vitro* biocompatibility samples were compared using an independent, two sample t-test. Statistical analyses on the histological results were performed initially with ANOVA and Holm Sidak post hoc analysis was used for the percent of fibrous tissue in the defect and tissue response. Statistical significance level was set at $\alpha = 0.05$.

Results

***In vitro* degradation.** The percentage of sponge remaining over time in the *in vitro* degradation study is shown in Figure 1. Both the pH 4.6 and 5.6 buffered chitosan sponge formulations exhibited significant differences in degradation, 71 and 44% respectively,

from the neutral chitosan sponge. Although the pH 4.6 buffered chitosan sponge had a lower percentage of sponge remaining, there was no significant difference between the pH 4.6 and pH 5.6 sponge ($p = 0.087$). There was a significant decrease over time for the 4.6 pH buffered chitosan sponge ($p = 0.0001$) and 5.6 pH buffered chitosan sponge ($p = 0.024$) groups, but there was no change over time for the neutral sponge group ($p = 0.592$).

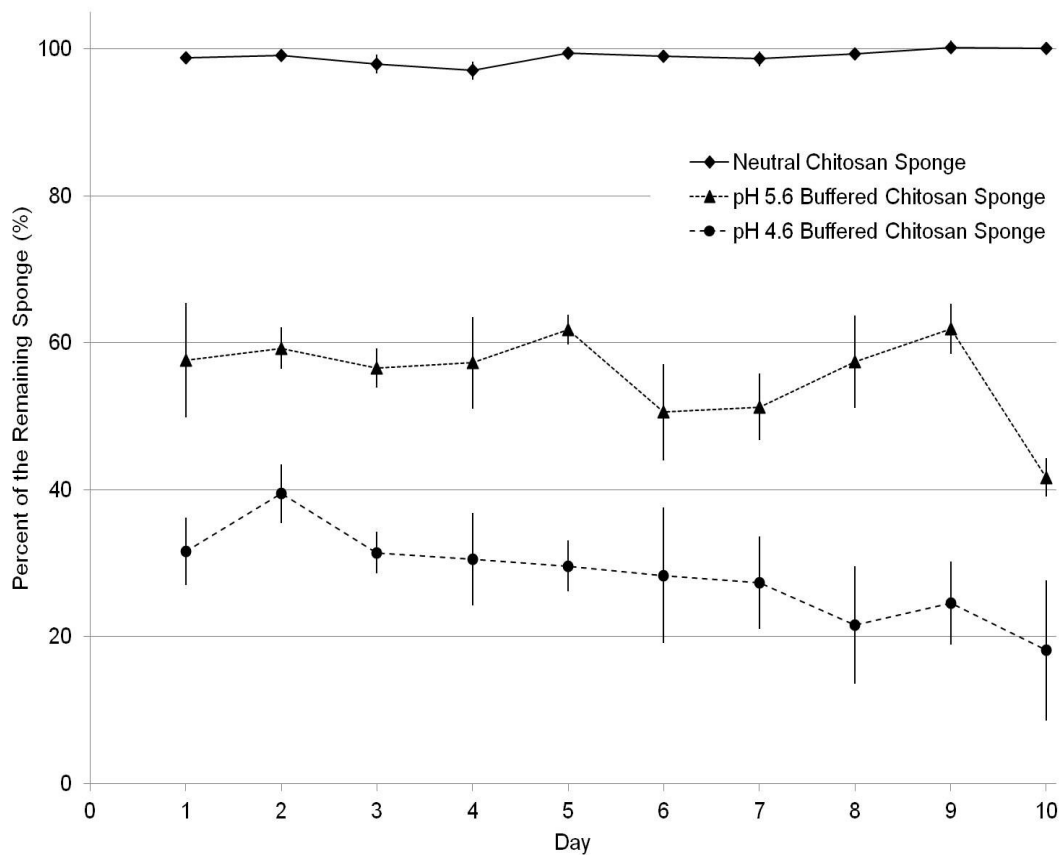


Figure 1. Results for the enzymatic-mediated degradation of neutral (◆), pH 5.6 buffered (▲), and pH 4.6 buffered (●) chitosan sponges represented as mean \pm standard deviation for the percent by weight of the chitosan sponge remaining over time ($n = 3$).

Molecular Weight, Crystallinity, and Thermal Analysis. X-ray diffraction spectra (Figure 2) reveal differences between the chitosan powder, neutralized chitosan sponge, and buffered chitosan sponges. Characteristic diffraction peaks for chitosan powder appeared at 2θ of 10.5° and 20° . After manufacturing the powder into a neutralized chitosan sponge, the 2θ of 20° peak was reduced to a minimum and subsequent manufacturing into both buffered sponge versions eliminated this peak altogether. The $2\theta = 10.5^\circ$ diffraction peak intensity varied between the sponge groups, but all of the group's $2\theta = 10.5^\circ$ peak were lower than the chitosan powder's.

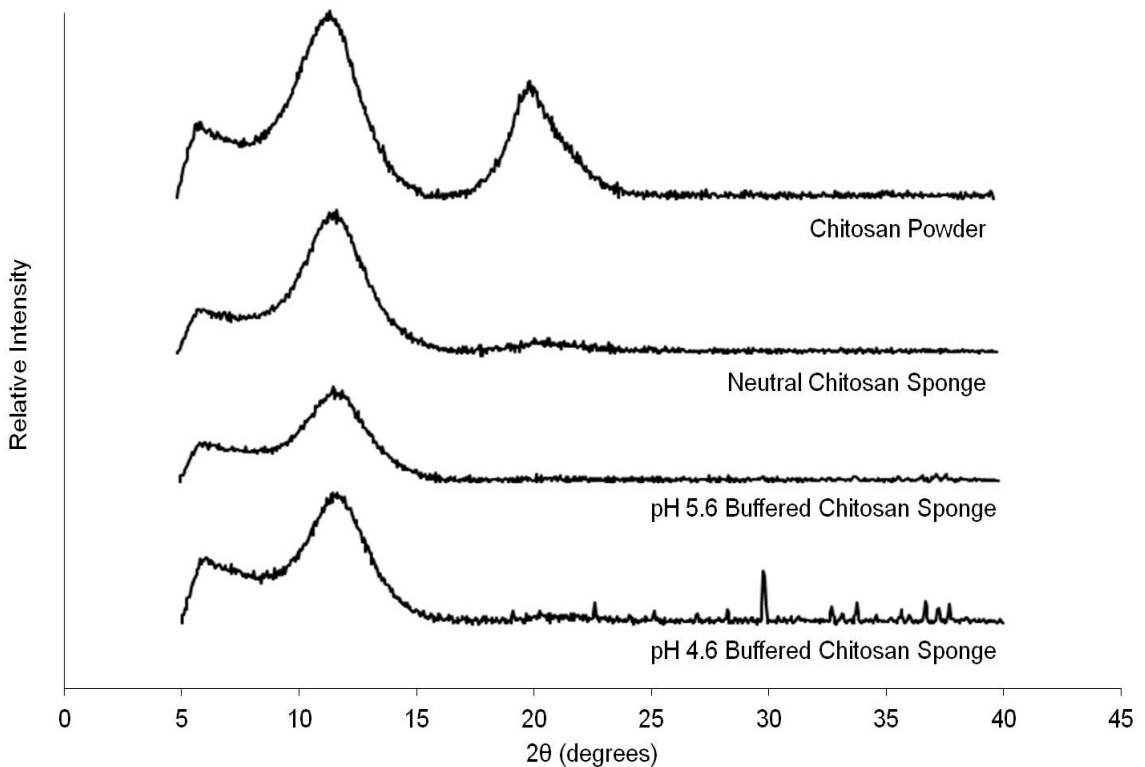


Figure 2. Stacked x-ray diffraction (XRD) spectra in the 2θ range from 5° to 40° of (top to bottom) the chitosan powder, neutral chitosan sponge, pH 5.6 buffered chitosan sponge, and pH 4.6 buffered chitosan sponge.

The initial molecular weight and thermal analysis of chitosan powder and neutralized and buffered chitosan sponges is shown in Table 1. Analysis of DSC data for the chitosan samples revealed that endothermic and exothermic peaks appeared at 105-111°C and 291-326°C, respectively. The endothermic peak corresponds to water loss and the exothermic peak can be attributed to polymer decomposition, possibly of amine units.²¹⁻²³ The chitosan powder exhibited the highest exothermic peak temperature; after processing chitosan into a neutral sponge, the exothermic peak temperature decreased ($p < 0.001$). Buffering the chitosan sponges at pH 5.6 and 4.6 lowered the exothermic peak temperature by 23.4 and 30.2°C, respectively, from the neutral chitosan sponge's peak temperature ($p < 0.001$).

Table 1. Physicochemical Properties of Buffered and Unbuffered Chitosan Sponges and Raw Material (n = 3).

<i>Material</i>	<i>Molecular Weight (kDa)</i>	<i>Thermal Analysis</i>	
		<i>Endotherm Peak Temp. (°C)</i>	<i>Exotherm Peak Temp. (°C)</i>
Chitosan Powder	250.6 ± 16.60	111.6 ± 4.9	326.0 ± 0.1*
Neutral Chitosan Sponge	172.0 ± 20.76	110.1 ± 2.5	321.4 ± 0.2*
pH 5.6 Buffered Chitosan Sponge	220.1 ± 30.79	105.7 ± 2.4	291.2 ± 1.2*
pH 4.6 Buffered Chitosan Sponge	171.0 ± 28.55	105.7 ± 1.9	298.0 ± 0.8*

* represents $p < 0.05$ vs. all

Spectral Analysis. As shown in Figure 3, several peaks characteristic of chitosan were identified at the following wavenumbers: H-bonded, O-H stretching at the broad peak centralized at 3350 cm^{-1} ; alkane, C-H stretching vibrations at 2910 and 2850 cm^{-1} ; amide I band C=O stretching at 1640 cm^{-1} ; amine and amide II band N-H bending at 1550 cm^{-1} ; C-H rocking at and just below 1400 cm^{-1} ; ether group C-O stretching at 1010 cm^{-1} . All peaks present are typical to chitosan functional groups and buffered groups showed increased peak intensities and peaks shifting downward, indicative of acetate's presence in these sponges.

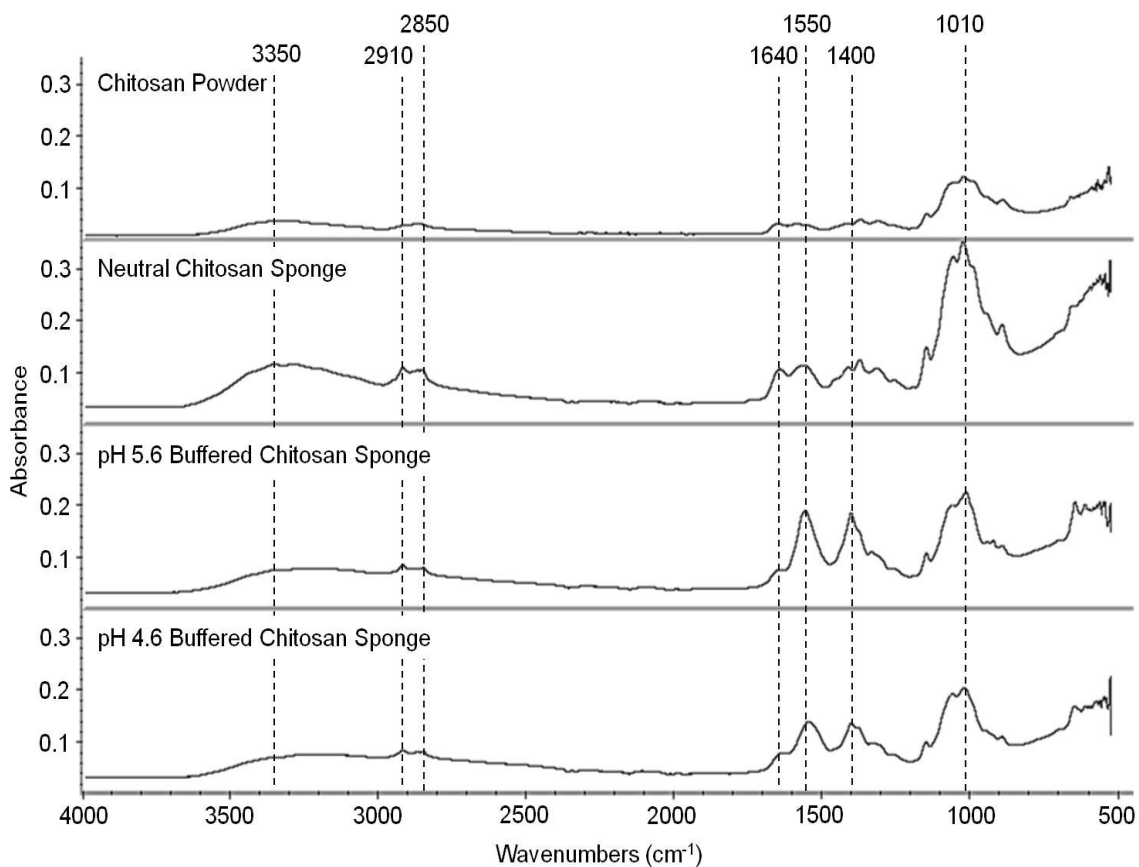


Figure 3. Stacked and averaged ($n = 3$) ATR-FTIR absorbance spectra for chitosan powder, and neutral, pH 5.6 buffered and pH 4.6 buffered chitosan sponges.

Morphology. The morphology of the chitosan powder before processing into sponges can be seen in Figure 4A, while the surface of the neutral, pH 5.6 and pH 4.6 buffered chitosan sponges can be seen in Figures 4B, C, and D, respectively. Upon inspection, the surfaces of both buffered chitosan sponge appear to have greater surface roughness than the neutral sponge. The morphology of both the pH 5.6 and 4.6 buffered chitosan sponges appears similar.

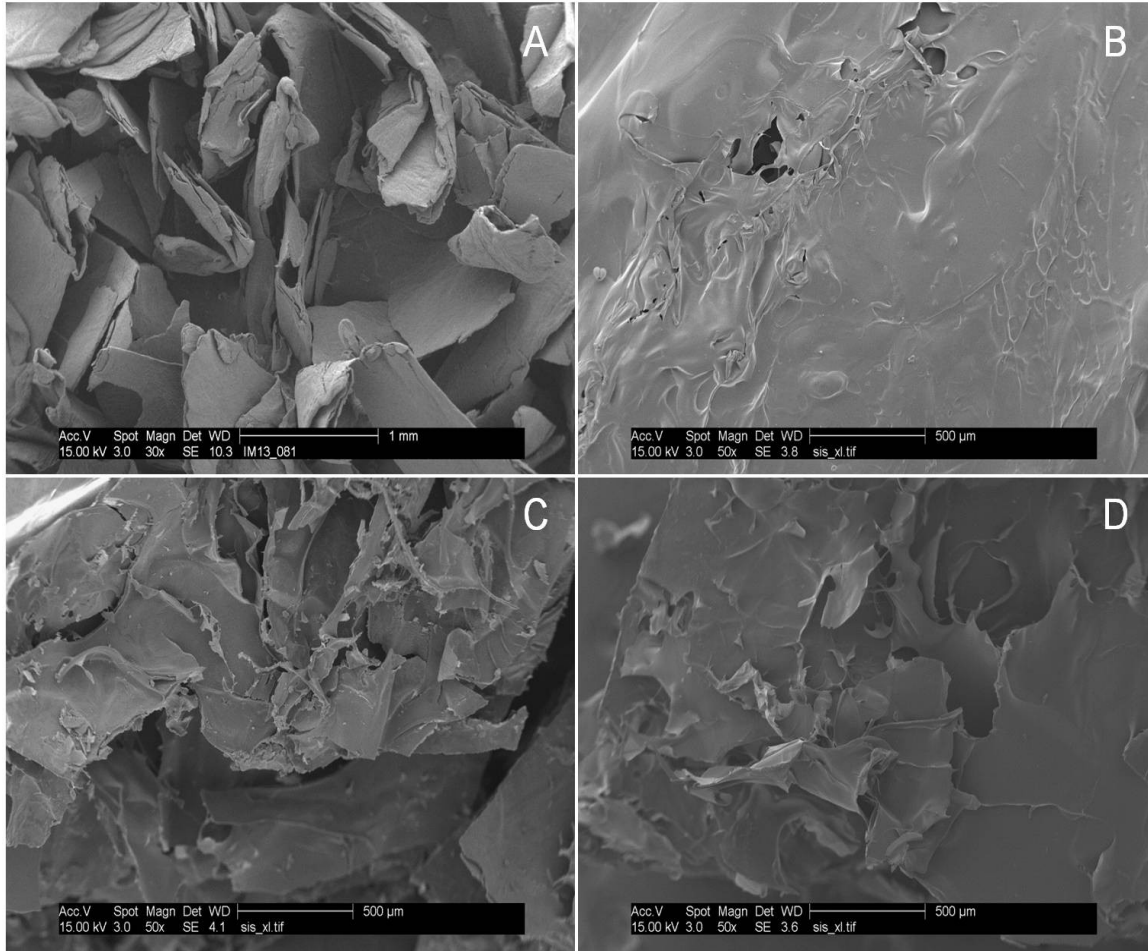


Figure 4. Scanning electron microscopy representative images of chitosan powder at 30× magnification (A) as well as the surface structure of the laminar sheets (at 50× magnification) that comprise the neutral (B), pH 5.6 buffered (C), and pH 4.6 buffered (D) chitosan sponges.

Direct contact biocompatibility. When normalized to the polyurethane sponge control (Figure 5), each type of chitosan sponge caused significant decreases in biocompatibility after one day of direct contact treatment ($p \leq 0.041$). However, after the three day treatment end point, there were no significant differences between the sponge groups and the control. Additionally, there was no cellular malformation, degeneration, sloughing, or lysis and no reduction of the cell layer at the specimen perimeter upon microscopic examination at either time point.

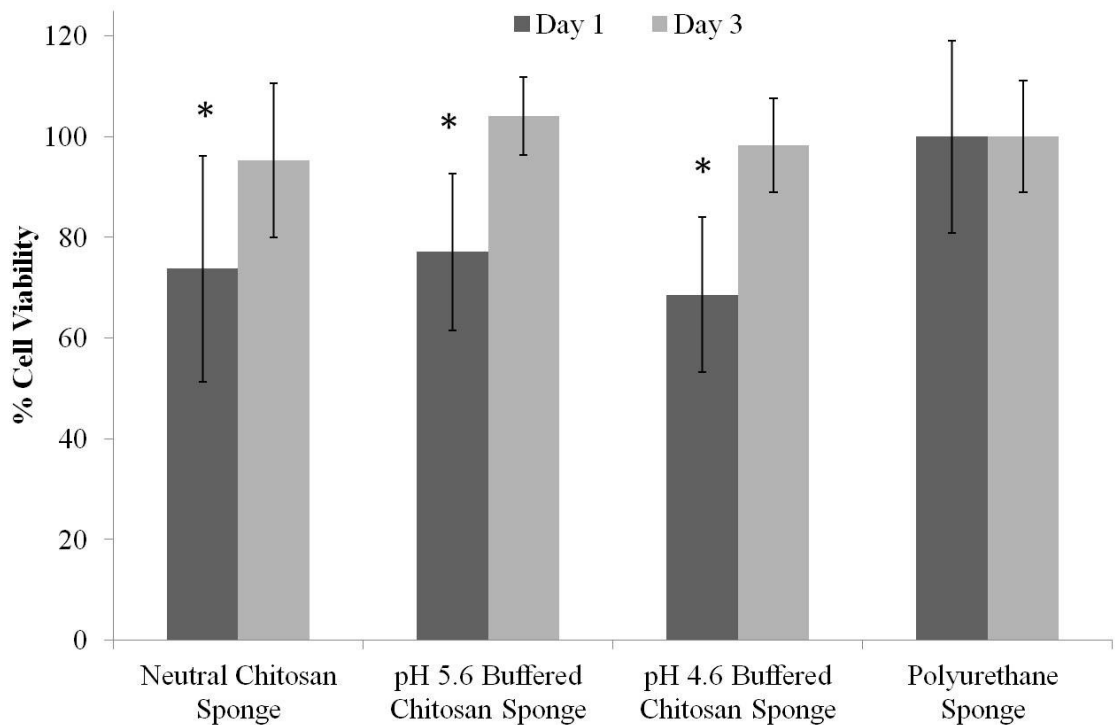


Figure 5. The percent cell viability (normalized to polyurethane sponge control) after normal human dermal fibroblast direct contact cell viability testing of neutral, pH 5.6 buffered and pH 4.6 buffered chitosan, and polyurethane sponges after 1 and 3 days, analyzed using Cell Titer-Glo Luminescent Cell Viability Assay. (n = 5, * represents $p < 0.05$ versus polyurethane sponge control)

***In vivo* degradation.** Representative images from the *in vivo* degradation study are shown in Figure 6, where Figure 6A shows an implanted sponge in a rat and Figure 6B shows a bisected tissue block before histological processing. Histological evaluation of the tissue revealed some implants to be completely degraded, (Figure 6C) while others remained more intact (Figure 6D-F).

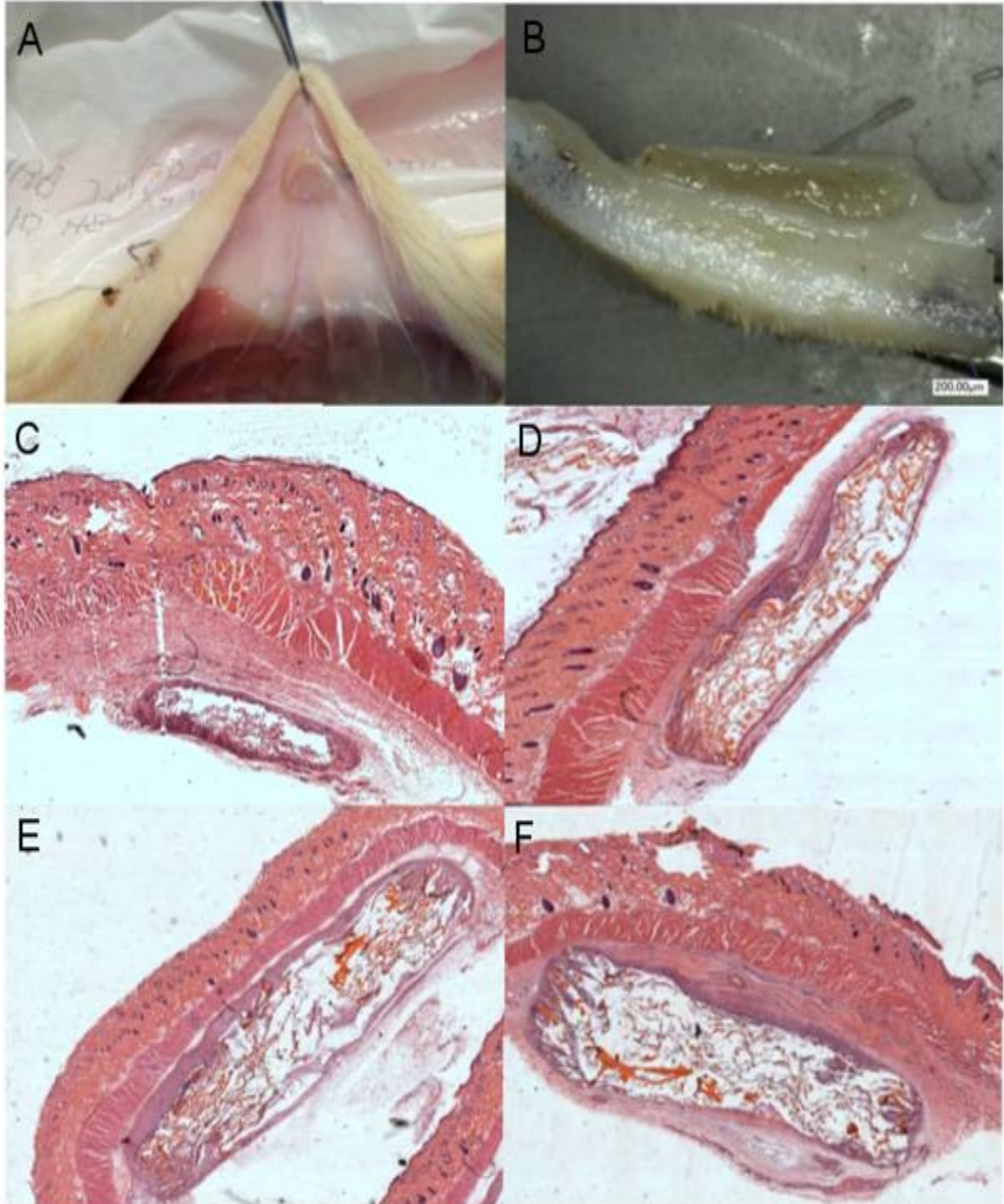


Figure 6. This image set depicts the surgery site and sponge retrieval (A), a bisected tissue section prepared for histological analysis (B), as well as representative H&E stained tissue sections of the control gelatin (C), neutral chitosan (D), pH 5.6 buffered chitosan (E) and pH 4.6 buffered chitosan sponge (F) surgery sites.

The quantitative evaluation of the tissue histology for the percentage of implant area per defect area is shown in Figure 7. After 4 and 10 days of sponge implantation in the back muscle pouches of rats, none of the experimental groups, with regard to time and sponge type, exhibited significant differences in percent of implant area per defect area ($p = 0.0856$). Although not statistically different, all three types of chitosan sponge had 5.1-5.6% and 0.3-1.6% lower average percentage of implant in the defect after 4 and 10 days than the control gelatin sponges. Both qualitative and quantitative evaluation of the fibrous tissue present around the implants revealed a wide variability in fibrous tissue response between surgical sites. After 10 days of implantation, the pH 5.6 buffered sponges exhibited a 37.08% increase in fibrous tissue present in the defect (figure 8) over the control gelatin sponges ($p = 0.003$).

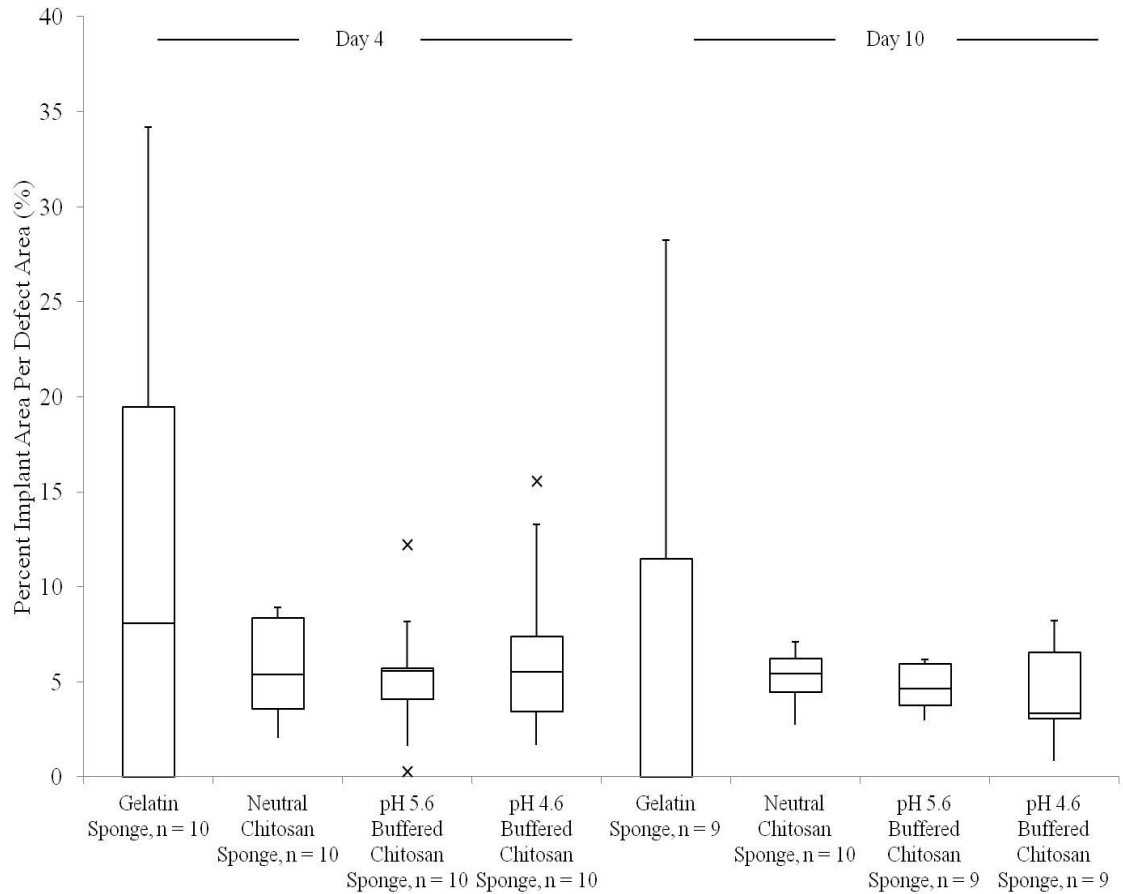


Figure 7. A histological analysis boxplot of the percent of gelatin, neutral chitosan, pH 5.6 buffered chitosan and pH 4.6 buffered chitosan sponge implants remaining in the defect area, 4 and 10 days after surgery. (x represents a data point outside of the standard deviation)

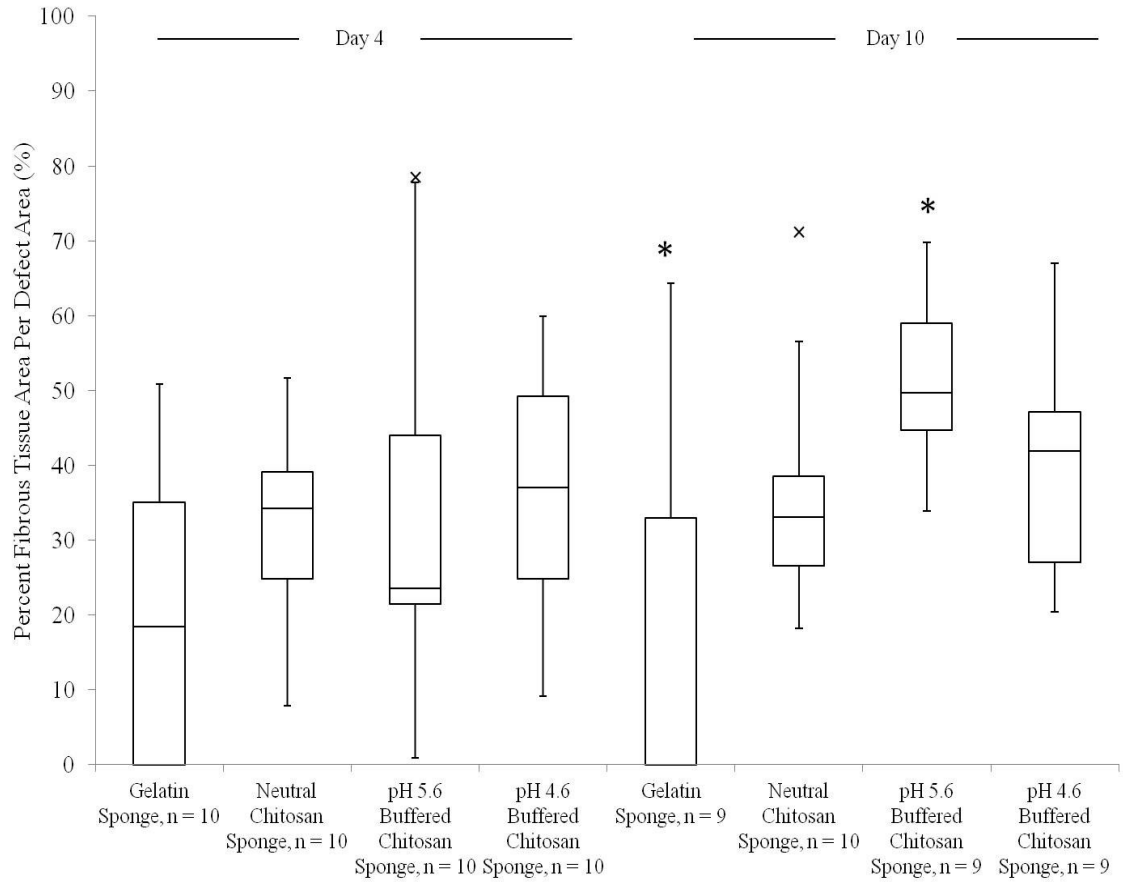


Figure 8. A histological analysis boxplot of the percent of fibrous tissue present in the defect area for gelatin, neutral chitosan, pH 5.6 buffered chitosan and pH 4.6 buffered chitosan sponge implants, 4 and 10 days after surgery. (* represents $p < 0.05$ versus each other, x represents a data point outside of the standard deviation)

The only chitosan sponge type which demonstrated complete degradation *in vivo* was the pH 4.6 buffered chitosan sponge ($n = 1$) after the satellite time point of 21 days implantation (Table 2). The pH 4.6 buffered chitosan sponge was present after 28 days of implantation in a different satellite animal, with 17.28% implant in the defect. There was no percent implant data for the pH 4.6 and 5.6 buffered chitosan sponges at days 14, 14 and 21, respectively as they may have been lost in histological processing. Based on similar photographs and tissue histology, the gelatin sponge is believed to have completely degraded after 28 days of implantation.

Table 2. Quantitative and qualitative analysis of satellite animal rat tissue histology after 14, 21, and 28 days of sponge implantation ,

<i>Sponge</i>	<i>Time (days)</i>	<i>% Implant Area/ Defect Area</i>	<i>% Fibrous Tissue/ Defect Area</i>	<i>Average Tissue Response</i>	<i>Sponge Present in Tissue Block</i>
Gelatin	14	13.36	33.06	1.7 ± 0.6	Yes
	21	24	53.03	1.9 ± 0.1	Yes
	28	0	0	0.3 ± 0.6	No
Neutral Chitosan Sponge	14	8.81	13.22	1.7 ± 0.8	Yes
	21	5.88	30.78	3.4 ± 0.7	Yes
	28	10.02	54.65	1.9 ± 0.4	Yes
pH 5.6 Buffered Chitosan Sponge	14	0	0	1.3 ± 0.6	Yes
	21	0	0	1.4 ± 0.4	Yes
	28	4.59	24.75	4.3 ± 0.5	Yes
pH 4.6 Buffered Chitosan Sponge	14	0	0	1.4 ± 0.5	Yes
	21	0	0	1.2 ± 1.0	No
	28	17.28	36.82	3.8 ± 0.2	Yes

Data is reported as mean ± standard deviation (n = 1) and tissue response is averaged from three blinded reviewers.

After 4 days, tissue inflammatory response from the pH 5.6 and pH 4.6 buffered chitosan sponges was significantly higher than the tissue response from gelatin sponges ($p = 0.029$ and $p < 0.001$, Figure 9). After 10 days of implantation, tissue response was an average of 1.98 to 2.11 grades lower from gelatin sponges than from all three types of chitosan sponges ($p < 0.001$). Cellular response was not significantly different between chitosan sponges, either neutral or buffered, at either time point. However, a highly variable response was observed for all three histophotometry measures: percentage implant, fibrous tissue, and tissue response grade.

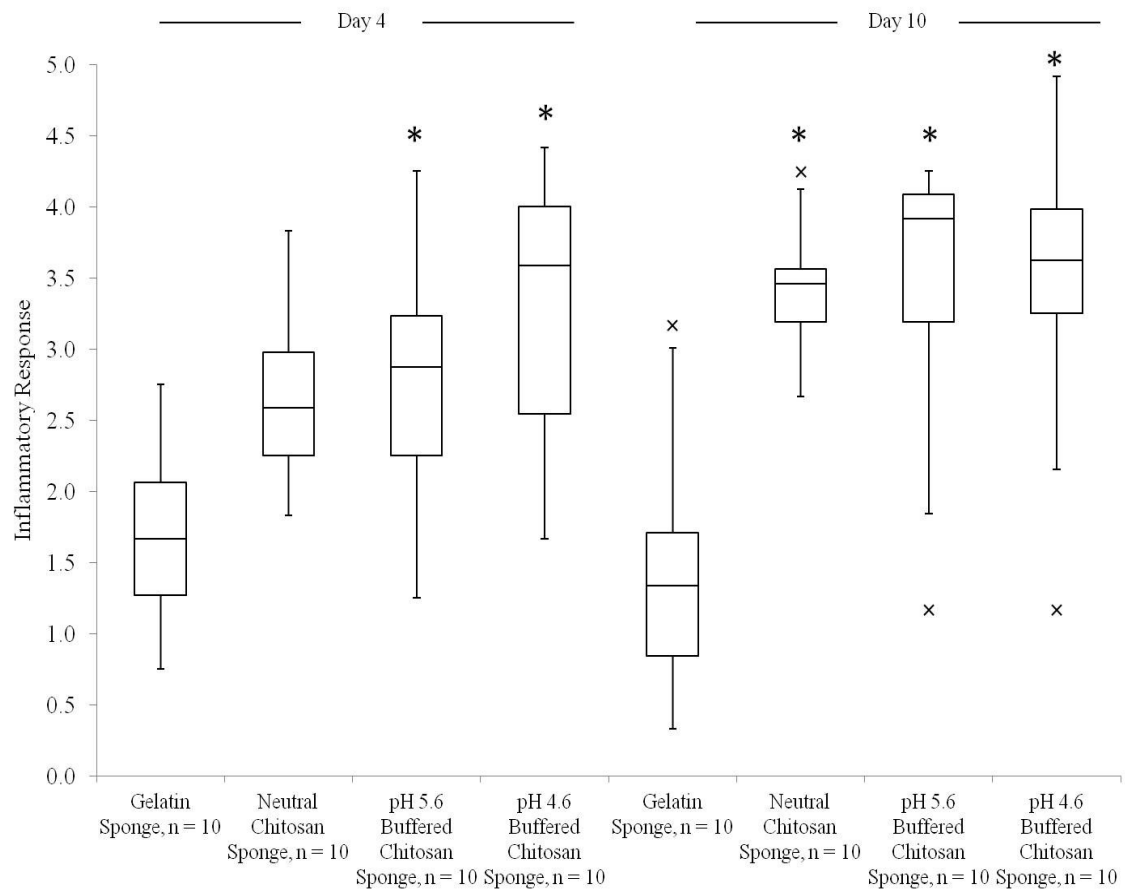


Figure 9. A histological analysis boxplot of the graded inflammatory response to the gelatin, neutral chitosan, pH 5.6 buffered chitosan and pH 4.6 buffered chitosan sponge implants, 4 and 10 days after surgery. Individual histological sections were scored (using increments of 0.25) where 0 indicated a missing or minimal implant and minimal response, 1–2 indicated mild leukocyte density, 2–3 indicated a slightly elevated response around the implant, 3–4 indicated a moderate cell response, and 4–5 indicated a high cell density in and around the implant. (* represents $p < 0.05$ versus each other at each time point, x represents a data point outside of the standard deviation)

Discussion

Our results show that the incorporation of a sodium acetate buffer into a chitosan sponge manufacturing process does significantly affect sponge material properties, especially increasing *in vitro* degradation; however, it does not affect *in vitro*

biocompatibility or *in vivo* degradation in rat intramuscular tissue. Evidence that the buffer affects *in vitro* sponge degradation is that both buffered sponge formulations degraded significantly in mass, with 18 and 42% of the pH 4.6 and pH 5.6 buffered chitosan sponges remaining after ten days, respectively, compared to the neutral sponge, with 100% sponge remaining. The buffering process at pH 4.6 reduced the sponge's molecular weight by 0.5%, compared to the neutralized sponge. Although not significant, this decrease is important because the literature indicates that *in vivo* degradation is directly proportional to its molecular weight.^{24,25} While a decrease in molecular weight was found in the chitosan sponges from the powder, the pH 5.6 buffered sponge exhibited a surprising increase in molecular weight from the neutral sponges.

Chitosan's DDA and crystallinity have both been previously shown to be inversely proportional to chitosan's degradation *in vitro*.^{34,35} Similar to other reported findings,²⁹ crystallinity analysis of the neutral and buffered sponges indicated that our manufacturing, specifically the lyophilization process, decreased crystallinity from the initial chitosan powder.

Thermal analysis of the chitosan powder and sponges indicated that the chitosan lyophilization and neutralization procedure decreased exothermic peak temperatures, corresponding to amine decomposition and a decrease in crystallinity.²³ The exothermic peak temperature decreased by 23.4°C and 30.2°C upon the addition of the buffering step which may correspond to a decrease in molecular weight from chitosan powder, a relationship shown in other investigations,^{30,36} similar to our findings of decreased sponge molecular weight for the pH 4.6 buffered chitosan sponge and decreased crystallinity for both buffered sponges.

Our chemical analysis confirmed the various standard absorbance peaks of chitosan were present in the sponges,²⁶ along with the presence of acetate functional groups in the buffered sponges as seen in other similar investigations.^{27,28} Although another researcher has reported the appearance of a carboxylic acid peak from chitosan at approximately 1750 cm⁻¹ Nunthanid et al did not see this carboxylic acid peak in either chitosan flakes or chitosan acetate which corroborates our findings.²⁷

Morphological differences were seen in surface SEM images of the neutral and buffered chitosan sponges. The apparent increase in surface roughness of both buffered chitosan sponges, as compared to the neutral sponge, may be the physical manifestation of changes in the chitosan's molecular weight and crystallinity, and therefore may also be related to an increase in *in vitro* degradation. Other studies of composite acid films similarly produced increased surface roughness with increased acid incorporation in chitosan films.⁴⁰ Both buffered sponges exhibited similar morphology, indicating little effect of the buffer's pH on surface morphology. The similarities in chitosan sponge edge and corner morphology of the neutral and buffered chitosan sponges indicate that all of the sponges have a similar internal layering of chitosan layers, an example of which may be seen in a previous publication.²⁵

A review of the literature indicates that higher DDAs and molecular weight both improve cytocompatibility and cell attachment.²⁹ All of the chitosan sponges exhibited similar molecular weights and hence similar *in vitro* cell response. While cellular compatibility levels in the literature fluctuate in direct contact assays largely due to the positive control selection and exposure time, our results show similar fluctuations over

time, where cell viability increased from one to three days, to those found for other chitosan materials and applications.^{18,30}

Chitosan is reported to be biocompatible and biodegradable²⁹, however there have been few studies performed using chitosan with only minimal modifications such as the buffer procedure, administered by routes other than orally, for assessing biodegradation and biocompatibility. In those studies that have been reported, chitosan *in vivo* degradation is described as being dependent on molecular weight,⁴³ and becomes localized in the liver after intravenous injections.⁴⁴ In other studies, chitosan has been reported as having minimal degradation after subcutaneous implantation,⁴⁵ or rapid degradation after use as a wound dressing.²³ These disparate findings led us to develop this screening animal model as an evaluation method for our chitosan sponge device. There was a wide variation in results, which lead to neither the neutral nor buffered chitosan sponges showing significant differences in percentage of implant in defect from the gelatin sponges, which served as a positive control of degradation. While there was wide variability in the percent implant in defect of the gelatin sponges, more of the gelatin sponges completely degraded than the chitosan sponges, confirming that sponge degradation could be determined with this animal model.

Chitosan sponges exhibited statistically similar inflammatory tissue responses, but there was an increase in inflammatory response in the pH 4.6 buffered sponges at day 4, as compared to the pH 5.6 buffered chitosan sponges. However, this inflammatory response difference narrowed at day 10 of implantation. The pH 4.6 buffered sponges could be more acidic and would explain the increased inflammatory response than the pH 5.6 buffered sponges in the rat muscle tissue. This result is similar to the moderate

inflammatory response observed in an *in vivo* study with Sprague-Dawley rats of chitosan coated, via silane-glutaraldehyde linkage, to titanium with histological images seemingly comparable to inflammatory responses as seen caused by the chitosan sponges.⁴⁶

Although there were no significant differences in percent implant in the defect between the chitosan sponges after 10 days, which was a surprising finding in comparison to the time course of the *in vitro* study, a few key differences could be seen in the satellite animals (days 14, 21, and 28). Because the pH 4.6 buffered chitosan sponges completely degraded after 21 days of implantation, this time point seems to be a more realistic estimate of the time course of complete *in vivo* degradation. However, the presence of the pH 4.6 buffered chitosan sponge after 28 days of implantation indicates that in future extended *in vivo* studies, some of these buffered sponges might still remain after 21 days. This degradation time may not be ideal because the chitosan sponges typically release most of the loaded antibiotics early.²²

The available chitosan literature does not report many details on *in vivo* chitosan degradation, and the *in vivo* degradation and elimination mechanism is still not well understood. In the literature, there is molecular weight dependence for timely *in vivo* degradation and elimination, while an increase in DDA and molecular weight may provide for better biocompatibility.^{34,47,48} Our results indicate that the modified chitosan sponge is biocompatible and is degrading in this screening model. From the chitosan literature, the determination and achieving a desired *in vivo* degradation rate will require balancing between the chitosan's molecular weight, DDA, crystallinity, and the applied manufacturing methods. Future work is needed and planned to define the *in vivo* degradation profile of current chitosan sponge devices over an extended period of time so

that the further development of the chitosan sponge may provide an alternative option for the adjunctive therapy of contaminated musculoskeletal wounds.

References

1. Andersson GBJ, Bouchard J, Bozic KJ. The Burden of Musculoskeletal Diseases in the United States. Rosemont, IL: American Academy of Orthopaedic Surgeons; 2008.
2. Owens BD, Kragh JF, Jr., Macaitis J, Svoboda SJ, Wenke JC. Characterization of extremity wounds in Operation Iraqi Freedom and Operation Enduring Freedom. *J Orthop Trauma* 2007;21(4):254-7.
3. Davis JS. Management of bone and joint infections due to *Staphylococcus aureus*. *Intern Med J* 2005;35 Suppl 2:S79-96.
4. Brady RA, Leid JG, Calhoun JH, Costerton JW, Shirtliff ME. Osteomyelitis and the role of biofilms in chronic infection. *FEMS Immunol Med Microbiol* 2008;52(1):13-22.
5. Chihara S, Segreti J. Osteomyelitis. *Dis Mon* 2010;56(1):5-31.
6. Tice AD, Hoaglund PA, Shoultz DA. Risk factors and treatment outcomes in osteomyelitis. *J Antimicrob Chemother* 2003;51(5):1261-8.
7. Dombrowski JC, Winston LG. Clinical failures of appropriately-treated methicillin-resistant *Staphylococcus aureus* infections. *J Infect* 2008;57(2):110-5.
8. Murray C, Hsu J, Solomkin J, Keeling J, Andersen R, Ficke J, Calhoun J. Prevention and management of infections associated with combat-related extremity injuries. *J Trauma* 2008;64(3 Suppl):S239-51.
9. Bint AJ, Burt I. Adverse antibiotic drug interactions. *Drugs* 1980;20(1):57-68.
10. Westphal JF, Vetter D, Brogard JM. Hepatic side-effects of antibiotics. *J Antimicrob Chemother* 1994;33(3):387-401.
11. Yorgason JG, Fayad JN, Kalinec F. Understanding drug ototoxicity: molecular insights for prevention and clinical management. *Expert Opin Drug Saf* 2006;5(3):383-99.
12. Diefenbeck M, Muckley T, Hofmann GO. Prophylaxis and treatment of implant-related infections by local application of antibiotics. *Injury* 2006;37:S95-S104.
13. Kendall RW, Duncan CP, Smith JA, Ngui-Yen JH. Persistence of bacteria on antibiotic loaded acrylic depots: A reason for caution. *Clin Orthop* 1996;329:273-280.

14. Tunney M, Ramage G, Patrick S, Nixon J, Murphy P, Gorman S. Antimicrobial susceptibility of bacteria isolated from orthopedic implants following revision hip surgery. *Antimicrob Agents Chemother* 1998;42(11):3002-5.
15. McLaren AC. Alternative materials to acrylic bone cement for delivery of depot antibiotics in orthopaedic infections. *Clin Orthop Relat Res* 2004(427):101-6.
16. Stone PW, Larson E, Kawar LN. A systematic audit of economic evidence linking nosocomial infections and infection control interventions: 1990-2000. *Am J Infect Control* 2002;30(3):145-52.
17. Ostermann PA, Seligson D, Henry SL. Local Antibiotic Therapy for Severe Open Fractures. *J Bone Joint Surg* 1995;77-B:93-97.
18. Turner TU, Gitelis S, Sumner D, Haggard W, Parr J. Antibiotic delivery from calcium sulfate as a synthetic bone graft substitutes in a rabbit tibial defect model. *Trans Orthop Res Soc* 1998(23):597.
19. Thomas DB, Brooks DE, Bice TG, DeJong ES, Lonergan KT, Wenke JC. Tobramycin-impregnated calcium sulfate prevents infection in contaminated wounds. *Clin Orthop Relat Res* 2005;441:366-71.
20. Jackson SR, Richelsoph KC, Courtney HS, Wenke JC, Branstetter JG, Bumgardner JD, Haggard WO. Preliminary In Vitro Evaluation of an Adjunctive Therapy for Extremity Wound Infection Reduction: Rapidly Resorbing Local Antibiotic Delivery. *Journal of Orthopaedic Research* 2008;7:903-908.
21. Robinson D, Alk D, Sandbank J, Farber R, Halperin N. Inflammatory reactions associated with a calcium sulfate bone substitute. *Ann Transplant* 1999;4(3-4):91-7.
22. Noel SP, Courtney HS, Bumgardner JD, Haggard WO. Chitosan sponges to locally deliver amikacin and vancomycin: a pilot in vitro evaluation. *Clin Orthop Relat Res* 2010;468(8):2074-80.
23. Stinner D, Noel S, Haggard W, Watson J, Wenke J. Local antibiotic delivery using tailorable chitosan sponges: the future of infection control? *J Orthop Trauma* 2010;24(9):592-7.
24. Ren D, Yi H, Wang W, Ma X. The enzymatic degradation and swelling properties of chitosan matrices with different degrees of N-acetylation. *Carbohydr Res* 2005;340(15):2403-10.
25. Smith JK, Moshref AR, Jennings JA, Courtney HS, Haggard WO. Chitosan sponges for local synergistic infection therapy: a pilot study. *Clin Orthop Relat Res* 2013;471(10):3158-64.

26. Parker AC, Jennings JA, Bumgardner JD, Courtney HS, Lindner E, Haggard WO. Preliminary investigation of crosslinked chitosan sponges for tailorable drug delivery and infection control. *J Biomed Mater Res B Appl Biomater* 2013;101(1):110-23.
27. Reves BT, Bumgardner JD, Haggard WO. Fabrication of crosslinked carboxymethylchitosan microspheres and their incorporation into composite scaffolds for enhanced bone regeneration. *Journal of Biomedical Materials Research Part B-Applied Biomaterials* 2013;101B(4):630-639.
28. Smith JK, Bumgardner JD, Courtney HS, Smeltzer MS, Haggard WO. Antibiotic-loaded chitosan film for infection prevention: A preliminary in vitro characterization. *J Biomed Mater Res B Appl Biomater* 2010;94(1):203-11.
29. Norowski PA, Mishra S, Adatrow PC, Haggard WO, Bumgardner JD. Suture pullout strength and in vitro fibroblast and RAW 264.7 monocyte biocompatibility of genipin crosslinked nanofibrous chitosan mats for guided tissue regeneration. *J Biomed Mater Res A* 2012;100(11):2890-6.
30. Mecwan MM, Rapalo GE, Mishra SR, Haggard WO, Bumgardner JD. Effect of molecular weight of chitosan degraded by microwave irradiation on lyophilized scaffold for bone tissue engineering applications. *J Biomed Mater Res A* 2011.
31. Kittur FS, Harish Prashanth KV, Udaya Sankar K, Tharanathan RN. Characterization of chitin, chitosan and their carboxymethyl derivatives by differential scanning calorimetry. *Carbohydrate Polymers* 2002;2002(49):185-193.
32. Guinesi LS, Cavalheiro ETG. The use of DSC curves to determine the acetylation degree of chitin/chitosan samples. *Thermochimica Acta* 2006(444):128-133.
33. Zhang H, Neau SH. In vitro degradation of chitosan by bacterial enzymes from rat cecal and colonic contents. *Biomaterials* 2002;23(13):2761-6.
34. Tomihata K, Ikada Y. In vitro and in vivo degradation of films of chitin and its deacetylated derivatives. *Biomaterials* 1997;18(7):567-75.
35. Hirano S, Tsuchida H, Nagao N. N-acetylation in chitosan and the rate of its enzymic hydrolysis. *Biomaterials* 1989;10(8):574-6.
36. Kurita K, Kaji Y, Mori T, Nishiyama Y. Enzymatic degradation of [beta]-chitin: susceptibility and the influence of deacetylation. *Carbohydr. Polym.*;2000(42):19-21.
37. Yuan Y, Chesnutt BM, Wright L, Haggard WO, Bumgardner JD. Mechanical property, degradation rate, and bone cell growth of chitosan coated titanium influenced by degree of deacetylation of chitosan. *J Biomed Mater Res B Appl Biomater* 2008;86(1):245-52.

38. Brugnerotto J, Lizardi J, Goycoolea FM, Argüelles-Monal W, Desbrières J, Rinaudo M. An infrared investigation in relation with chitin and chitosan characterization. *Polymer* 2001;42(8):3569-3580.
39. Nunthanid J, Laungтана-Anan A, Sriamornsak P, Limmatvapirat S, Puttipipatkachorn S, Lim LY, Khor E. Characterization of chitosan acetate as a binder for sustained release tablets. *Journal of Controlled Release* 2004;99(1):15-26.
40. Osman Z, Arof AK. FTIR studies of chitosan acetate based polymer electrolytes. *Electrochimica Acta* 2003;48(8):993-999.
41. Kim S, Liu Y, Gaber MW, Bumgardner JD, Haggard WO, Yang Y. Development of chitosan-ellagic acid films as a local drug delivery system to induce apoptotic death of human melanoma cells. *J Biomed Mater Res B Appl Biomater* 2009;90(1):145-55.
42. Dash M, Chiellini F, Ottenbrite RM, Chiellini E. Chitosan-A versatile semi-synthetic polymer in biomedical applications. *Progress in Polymer Science* 2011;36(8):981-1014.
43. Silva SS, Motta A, Rodrigues MT, Pinheiro AF, Gomes ME, Mano JF, Reis RL, Migliaresi C. Novel genipin-cross-linked chitosan/silk fibroin sponges for cartilage engineering strategies. *Biomacromolecules* 2008;9(10):2764-74.
44. Richardson S, Kolbe H, Duncan R. Potential of low molecular mass chitosan as a DNA delivery system: biocompatibility, body distribution and ability to complex and protect DNA. *Int J Pharm* 1999;178(2):231-43.
45. Guo Z, Chen R, Xing R, Liu S, Yu H, Wang P, Li C, Li P. Novel derivatives of chitosan and their antifungal activities in vitro. *Carbohydr Res* 2006(341):351-4.
46. Ma L, Gao C, Mao Z, Zhou J, Shen J, Hu X, Han C. Collagen/chitosan porous scaffolds with improved biostability for skin tissue engineering. *Biomaterials* 2003;24(26):4833-41.
47. Norowski PA, Courtney HS, Babu J, Haggard WO, Bumgardner JD. Chitosan coatings deliver antimicrobials from titanium implants: a preliminary study. *Implant Dent* 2011;20(1):56-67.
48. Kean T, Thanou M. Biodegradation, biodistribution and toxicity of chitosan. *Advanced Drug Delivery Reviews* 2010;62(1):3-11.

CHAPTER 3

PRELIMINARY EVALUATION OF CHITOSAN AND POLYETHYLENE GLYCOL BLENDED SPONGES FOR THE *IN VITRO* LOCAL DELIVERY OF AMPHOTERICIN B AND *IN VIVO* DEGRADATION IN A RAT INTRAMUSCULAR MODEL

Introduction

Infection associated with musculoskeletal extremity injuries has a significant impact on patient morbidity and mortality and can be a devastating complication. Open extremity injuries are especially susceptible to multiple pathogenic, and sometimes drug resistant, bacteria or fungi.¹ Invasive fungal infections have recently become especially troublesome for both military and civilian populations, with high mortality rates and high healthcare costs.²⁻⁴ The British Military has recently reported higher rates of fungal wound infections in casualties from the Helmand Province in Afghanistan.⁵ In a 2011 Trauma Infectious Disease Outcome Study, 36 cases of invasive fungal infections (IFI) were found in Operation Enduring Freedom soldiers with blast injuries in Afghanistan from June 2009 to December 2010, and 78% of these wounded soldiers with IFI required lower extremity amputations.⁶ An outbreak of cutaneous mucormycosis was also recently reported in victims from the 2011 tornado in Joplin, Missouri.^{7,8} *Apophysomyces trapeziformis* was identified in all 13 infected patients, 10 patients required admission to intensive care, and 5 of these patients died.^{7,8} Finally, invasive *Candida* infections are the third most common cause of hospital-acquired bloodstream infections.⁹

The current standard of care for invasive fungal infections is systemic antifungal delivery, and antifungals utilized for invasive fungal infection management include triazoles, polyenes (amphotericin B), echinocandins, and flucytosine.¹⁰ Although the Infectious Disease Society of America advocates the use of voriconazole over traditional

amphotericin B as the primary treatment of *Aspergillus* infections, both azole resistant *Aspergillus* and *Candida* have emerged (as well as echinocandin resistant *Candida*).¹¹ Amphotericin B is one of the most commonly used antifungals in clinical practice and fungal resistance to the antifungal has not emerged over 50 years.¹¹ However, systemic toxicity can be a concern with amphotericin B, so local delivery of amphotericin B is highly desirable.¹²

While antibiotics have been studied extensively in local delivery, antifungals have not been successfully locally delivered from as many degradable delivery systems because of their hydrophobicity for loading and distribution. Amphotericin B has been incorporated into a few local delivery systems, including polymethylmethacrylate (PMMA) bone cement¹²⁻¹⁴, a hydroxyapatite and chitosan composite¹⁵, a Pluronic® based copolymer gel¹⁶, and dextran hydrogels^{17,18}. Although PMMA is commonly used for local antibiotic delivery, there is conflicting data on its release of amphotericin B.¹²⁻¹⁴ Goss and researchers found an absence of amphotericin B release from bone cement, while Kweon et al. reported 0.05-0.45% release of the antifungal and Marra and researchers found amphotericin B concentrations to be 3.2 µg/mL in surgical wound fluid.¹²⁻¹⁴ Additionally, all of these local antifungal delivery systems are pre-loaded with antifungal. A local degradable delivery system that is capable of rapid point of care loading would allow the clinician to select the appropriate antimicrobial (or antimicrobials) and dosage, based on each individual patient's needs.

Previous research conducted at the University of Memphis has yielded a topical, porous, degradable chitosan sponge that provides an adaptable antibiotic delivery system in which tailored dosing and degradation can be achieved.¹⁻⁵ This system can be loaded

with antibiotics immediately prior to use, allowing for clinician selected antibiotic loading, as well as combination loading.¹⁻⁵ Additional previous research has also shown that using polyethylene glycol (PEG) as a solvent system for a hydrophobic fatty acid, cis-2-decenoic acid, allows for point of care loading of the fatty acid into the chitosan sponges.⁵ Polyethylene glycol is a water soluble polymer that exhibits protein resistance and low toxicity and immunogenicity.⁶ PEG has been used to modify chitosan films, fibers, and hydrogels, and chitosan can be blended or copolymerized with PEG.⁶⁻⁹ Polyethylene glycol has also been utilized as a solvent system, either as liposomes or nanoparticles, for amphotericin B in systemic delivery.¹⁰⁻¹³

We hypothesized that creating chitosan/PEG blended sponges would result in increased *in vitro* amphotericin B release, cytocompatibility, and *in vitro* and *in vivo* sponge degradation, as compared to control chitosan sponges. The first aim of this study was to evaluate the effect of adding PEG to the chitosan sponges on spectroscopic, morphologic, thermal, and crystalline material properties, as well as *in vitro* degradation, antifungal release, eluate fungal activity, and cytocompatibility. The second aim of the study was to evaluate the *in vivo* degradation and biocompatibility of chitosan/PEG sponges and control chitosan sponges in a rat dorsal muscle pouch model, using qualitative and quantitative histological assessment of the implant sites.

Materials and Methods

Fabrication. Chitosan was purchased from Chinitor AS (Tromsøy, Norway) with a average molecular weight of 250.6 kDA and 82.46 ± 1.679 degree of deacetylation (DDA). Polyethylene glycol (PEG) was obtained from Sigma Aldrich at two different

molecular weights, 6,000 g/mol and 8,000 g/mol. Acetic acid and sodium hydroxide (NaOH) were both purchased from Fisher Scientific (Pittsburgh, PA).

To make chitosan and PEG sponges, 0.5% (w/v) of PEG (6,000 or 8,000 g/mol) was dissolved in a 1% (v/v) acetic acid in water solution. After PEG dissolution, 0.5% (w/v) of chitosan was dissolved in the same solution. Chitosan sponges were manufactured by dissolving 1% (w/v) chitosan in the 1% acetic acid solution. Solutions were mixed on a stirplate for approximately one hour, and then 25 mL of the solution was poured into 42 mL aluminum pans. The sponges were frozen for at least one hour at -80°C and then lyophilized (lyo) in a LabConco (Kansas City, MO) FreeZone 2.5 Liter Benchtop Freeze Dry System.

After the first lyophilization, the 1% chitosan sponges were neutralized in 0.6 M NaOH, by soaking the sponges in the base solution for approximately 1-2 minutes and then washing the sponges in large amounts of water until a neutral pH was reached. The concentrations of NaOH solutions were determined through previous formulation testing. Some of the chitosan/PEG sponges were neutralized in 0.25 M NaOH (the 2 lyophilization groups), while other chitosan/PEG sponges were not neutralized at all (the 1 lyophilization groups). After neutralization, the sponges were frozen again at -80°C and lyophilized one last time. All sponges were sterilized via low dose gamma irradiation at a 25-40 kGy dosage.

FTIR. Functional group chemistry differences between the sponges were evaluated using attenuated total reflectance Fourier transform infrared spectroscopy (ATR-FTIR). A ThermoScientific (Waltham, MA) Nicolet iS10 FTIR spectrometer with a diamond ATR crystal was used to acquire the absorbance spectra ($n = 3$), using 64 scans with a

resolution of 4 cm^{-1} . The spectra were averaged and analyzed with the Thermo Scientific OMNIC™ Software Suite.

XRD. X-ray diffraction (XRD) was used to define the crystal structure of the chitosan and chitosan/PEG sponges. A Bruker AXS (Maddison, WI) Advanced D8 X-ray diffractometer was utilized to obtain X-ray diffraction patterns with a $K\alpha$ Cu radiation source at 40 kV and 40 mA. XRD data was obtained over a 2θ range from 5° to 40° with a time/step of 0.2 seconds and a step size of 0.05° .

Thermal Analysis. Differential scanning calorimetry (DSC) was used to evaluate differences in endothermic and exothermic peaks of the chitosan powder, PEG 6000, PEG 8000, 1% chitosan sponges, and chitosan/PEG sponges. A Netzsch (Selb, Germany) 200 PC differential scanning calorimeter was used to scan the samples ($n = 3$) from 40 to 400°C at $20^\circ\text{C}/\text{min}$.

Morphology. Surface morphology of the chitosan and chitosan/PEG sponges was assessed with a FEI/Philips XL30 Environmental Scanning Electron Microscope (SEM) at 15 kV using samples sputter-coated with 30 nm of Au/Pd. SEM images ($n = 3$) were qualitatively evaluated for differences between sponges such as surface texture and porosity.

***In Vitro* Degradation.** To analyze the enzymatic *in vitro* sponge degradation, sponges were dried thoroughly and weighed. The sponges were placed in 125 mL Nalgene (Rochester, NY) containers, along with 35 mL of 1 mg/mL 2 x crystallized chicken egg white lysozyme, purchased from MP Biomedicals (Santa Ana, CA). The sponges in their lysozyme solutions were placed on a shaker in an incubator at 37°C . The lysozyme solution was completely refreshed every two days. After 2, 4, 8, and 10 days of

degradation, sponge samples were removed from the lysozyme solution (n = 3), soaked briefly in deionized water to stop any enzymatic degradation, dried thoroughly in a vacuum oven at 60°C for two days, and then reweighed. This study was a destructive study, so every time point represents a different sponge sample.

The percent sponge remaining over time was calculated according to equation 1,

$$\text{Percent remaining (\%)} = \left(\frac{\text{Sponge weight at x days}}{\text{Initial dry sponge weight}} \right) \times 100 \quad (1)$$

Indirect Molecular Weight Measurement (Viscosity). To analyze the effect of *in vitro* degradation indirectly on sponge molecular weight, the viscosity of sponges dissolved in sodium acetate and acetic acid was measured. It was not possible to directly measure molecular weight measurement of the chitosan and PEG blends though gel permeation chromatography (GPC) because of different dn/dc values for chitosan and PEG.

Chitosan and chitosan/PEG sponges from the *in vitro* degradation 10 day time point (n = 3) were dissolved in a solution of 0.1 M sodium acetate and 0.2 M acetic acid.

Chitosan and chitosan/PEG sponges that were not included in the degradation study were also dissolved in the sodium acetate and acetic acid buffer (n = 3) and were considered a zero day time point. A Brookfield Programmable DV-II + Viscometer with a CPE-40 cone spindle and circulating water bath at 25°C was used to measure the viscosity of sponge solutions at 50 rpm.

Antifungal Elution. To determine if the chitosan/PEG sponges would deliver antifungals locally *in vitro*, a 1 mg/mL solution of amphotericin B (Fisher Scientific) was created in sterile Ultrapure water. The amphotericin B solution was shaken immediately prior to

loading, and 10 mL of the antifungal solution was added to the sponges (n = 3). After approximately one minute, the amphotericin B solution not absorbed by the sponge was removed and measured. Twenty milliliters of sterile 1 x phosphate buffered saline (PBS) was added to the sponges in Nalgene containers and they were then placed on a shaker in an incubator at 37° C. After 1, 3, 6, 24, 48, and 72 hours of elution, four 1 mL samples were removed from the sponge solution and the PBS was completely refreshed.

The concentration of amphotericin B in the eluates was measured via ultraviolet visible spectroscopy. To prepare the insoluble amphotericin B samples, the eluates were added 1:1 to dimethylsulfoxide (DMSO), purchased from Fisher Scientific. Highly concentrated amphotericin B solutions, including the original 1 mg/mL solution, were diluted in DMSO multiple times. Amphotericin B samples were read via absorbance at 389 nm in a Biotek (Winooski, VT) Synergy H1 plate reader and concentrations were calculated using an amphotericin B standard curve.

Antifungal Activity. To determine if the amphotericin B released from the sponges remained active against fungi, the amphotericin B eluate samples were lyophilized in foil for one day. The samples were then dissolved in 50 µL of PBS and used to inoculate blank discs. Standard concentrations of amphotericin B from 0 to 2.5 µg in 0.25 µg increments were also used to inoculate blank discs. A 0.5 McFarland standard of *Candida albicans* in sterile PBS was prepared and a cotton swab was used to streak a Mueller Hinton agar plate in three different directions. An inoculated disc was added to each plate and the plates were incubated overnight at 37°C. The zone of inhibition (ZOI) was measured for each amphotericin B sample and a standard curve was determined. Zone of

inhibition for each sample was also measured and compared to the standard curve to determine sample concentration.

***In Vitro* Biocompatibility.** The *in vitro* biocompatibility of both the chitosan/PEG sponges and the antifungal eluates was tested on normal human dermal fibroblasts (NHDFs), purchased from Lonza (Walkersville, MD). A protocol modified from ASTM F813-07 “Standard Practice for Direct Contact Cell Culture Evaluation of Materials for Medical Devices” was followed in order to assess the direct contact biocompatibility between the chitosan sponge variations.¹⁴ Cells (passages 4 through 7) were seeded at 3.66×10^4 cells/mL (day one treatment) or 1.43×10^5 cells/mL (day three treatment) and allowed to proliferate to near confluence on 12-well polystyrene tissue culture plates in Dulbecco’s Modified Eagle’s Medium (DMEM) supplemented with 10% fetal bovine serum (FBS) and penicillin (100 units/mL), streptomycin (100 mg/mL), and amphotericin B (0.25 μ g/mL), all purchased from Fisher Scientific, under standard cell culture conditions (37°C and 5% CO₂ atmosphere). Cell culture medium was aspirated and refreshed with 1 mL of fresh medium, while chitosan, chitosan/PEG, and control polyurethane sponges were soaked in pre-warmed, sterile 1 x PBS for approximately 20 minutes. A single 8 mm diameter test specimen (n = 5) was then gently placed in a well in direct contact with the cell monolayer. Cultures were incubated for either one or three days before biocompatibility was assessed with the Cell Titer-Glo® Luminescent Cell Viability assay, purchased from Promega (Madison, WI). The luminescent signal, which corresponded to the amount of adenosine triphosphate and the number of viable cells through a standard dilution of known concentrations of cells, was recorded at 590 nm

using a BioTek (Winooski, VT) Synergy H1 (day one treatment) or a BioTek FLx-800 Fluorescence Microplate Reader (day three treatment).

In Vivo Degradation. *In vivo* degradation and biocompatibility of the chitosan and chitosan/PEG sponges was assessed in 13 three to four month old male Sprague-Dawley rats. This *in vivo* study was approved by the institutional review board at the University of Memphis (IACUC protocol #0728) and followed the IACUC guidelines. Rats were anesthetized with 2% isoflurane in an environmental chamber and were maintained under 4-5% isoflurane while being prepared for sterile surgery. Two 1.5 cm incisions were made through the skin on each side of the midline (4 incisions total) and a 1.25 cm pouch was created in the latissimus dorsi muscle in each incision. One cylindrical implant, 9.5 mm in diameter and 5 mm in thickness, was implanted bilaterally in each muscle pouch. Test groups included chitosan sponge, chitosan/PEG 6000 1 lyophilization (lyo), chitosan/PEG 6000 2 lyo, and chitosan/PEG 8000 1 lyo sponges. Each rat received one of each implant, randomized among four incision sites. The muscle incision was sutured and the skin was closed with one to three staples. Carprofen was administered prior to surgery and for two days post-operatively. Five rats were sacrificed at the 4 and 10 day time points (n = 5), and satellite animals were sacrificed on the 14, 21 and 28 day time points (n = 1). The degradation data from the satellite animals served as a preliminary indication for longer degradation and for selecting degradation time points for future *in vivo* studies. After sacrifice, the implanted region and surrounding tissue were excised, placed in 10% formalin buffered phosphate (FBS) for two days, and then bisected across the implant for quantitative and qualitative histological evaluation (paraffin-embedded and H&E stained). Surgical defect areas of the stained tissue sections were measured as the

remaining sponge plus surrounding fibrous tissue using a Nikon inverted microscope Eclipse TE300 and BIOQUANT® OSTEO II image analysis software. The area of sponge and fibrous tissue were measured separately, divided by defect area, and converted to a percentage. Qualitative histological evaluation was conducted by three blinded reviewers based on cellular response. Histology was scored on a scale of 0 to 5 (low to high) in increments of 0.25, using a modified version of the Knodell Histological Activity Index (HAI).¹⁵ Cellular response scores were 0 for no tissue for evaluation, 1 for very mild leukocytic density, 2 for slightly more elevated cellular response, 3 for moderate cellular response, 4 for high cell density in and around implant site, and 5 for extremely high cellular response.

Statistical Analysis. Viscometry data was analyzed using one-way Analysis of Variance (ANOVA) with Holm Sidak post hoc analysis. Thermal analysis was analyzed by one-way ANOVA with Holm Sidak post hoc analysis, except for the endothermic peak temperatures and areas, which were analyzed using Kruskal-Wallis one-way ANOVA on ranks with Tukey's post hoc analysis. Antifungal elution, activity and cytocompatibility data were analyzed using two-way ANOVA with Holm Sidak post hoc analysis. Two-way ANOVA was utilized to analyze the percent fibrous tissue in the defect and the tissue response in the *in vivo* rat study. The percentage of implant in the defect in the rat study was analyzed using Kruskal-Wallis one-way ANOVA with Dunn post hoc analysis. Statistical significance level was set at $\alpha = 0.05$.

Results

FTIR. Results from the FTIR analysis of the chitosan/PEG blended sponges and control chitosan sponges are provided in Figure 1A, while Figure 1B shows the FTIR spectra of

chitosan powder, PEG 6000, and PEG 8000. Characteristic peaks were seen in the 1% chitosan sponges at 3290 (O-H stretching), 1643 (amide I C=O stretching), and 1557 (amide II N-H) cm^{-1} .^{7,8,16} Characteristic C-O bending peaks were seen in PEG 6000 and 8000 at 1093, and peaks from the crystalline region of PEG were exhibited at 1278, 960, and 840 cm^{-1} .^{7,8}

All blended sponges exhibited the characteristic chitosan peaks at 3357-3360 cm^{-1} , and all peaks were shifted to higher wavenumbers compared to the 1% chitosan sponges. Characteristic chitosan peaks at approximately 1643 and 1557 cm^{-1} were also seen in all blended sponges. All sponges and PEG also exhibited peaks at approximately 1145-1149 cm^{-1} (C-O stretching), where the peaks in the spectra of both 1 lyophilization blended sponges, PEG 6000, and PEG 8000 were at lower wavenumber than the 1% chitosan sponge and 2 lyophilization blended sponges.¹⁶ Both the chitosan/PEG 6000 1 lyo and 8000 1 lyo sponges exhibited the peaks seen in PEG at 1279 and 1099 cm^{-1} , but neither blended sponges with 2 lyophilizations nor the chitosan sponges exhibited these peaks. All of the blended sponges, except for the chitosan/PEG 6000 2 lyo sponge, showed the peak from PEG at 960-962 cm^{-1} . All sponges exhibited the peak at 840-843 cm^{-1} , but both blended sponges with 1 lyophilization and PEG had peaks with higher absorbance than the 2 lyophilization blended and 1% chitosan sponges.

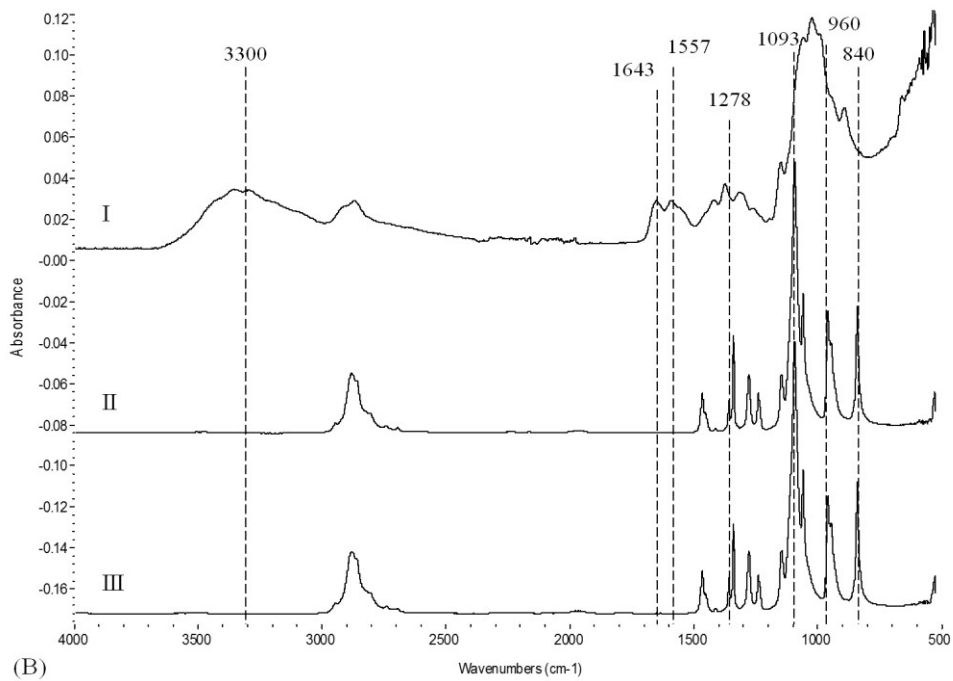
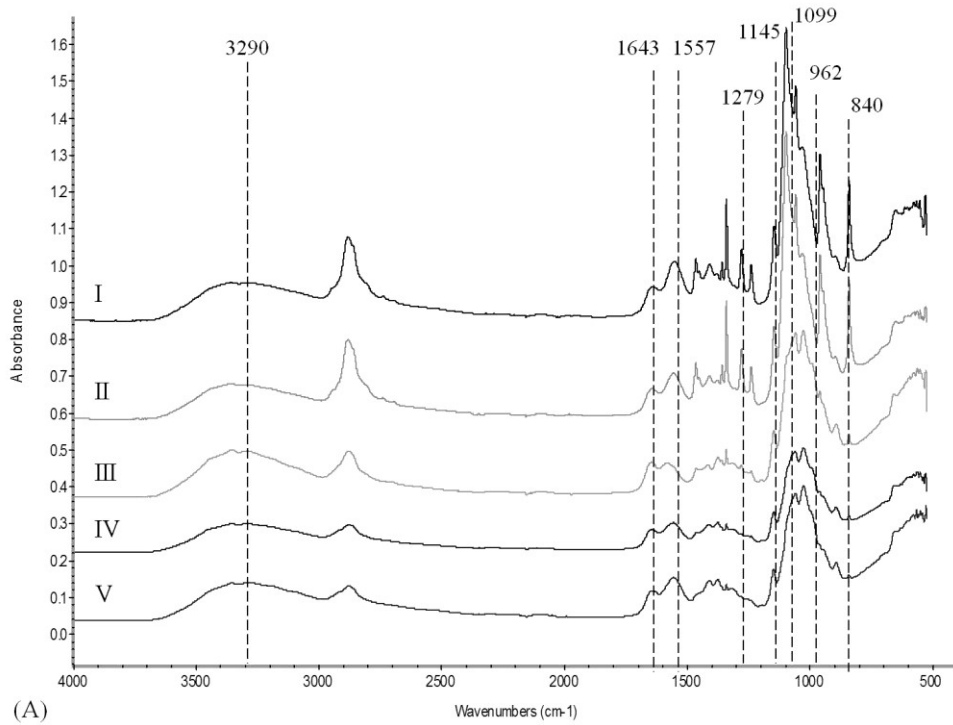


Figure 1. Stacked and averaged ($n = 3$) ATR-FTIR absorbance spectra for (A) I. chitosan/PEG 6000 1 lyo, II. chitosan/PEG 8000 1 lyo, III. chitosan/PEG 8000 2 lyo, IV. chitosan/PEG 6000 2 lyo, and V. 1% chitosan sponges, and (B) I. chitosan powder, II. PEG 6000, and III. PEG 8000.

XRD. X-ray diffraction results (Figure 2A) reveal a difference between the chitosan powder and all sponge types. The chitosan powder exhibited the typical crystalline peak at approximately 20° , but this peak disappeared upon manufacturing the powder into sponges, both in the control chitosan sponges or the chitosan/PEG blended sponges. Additionally, the peak at approximately 12° in the chitosan powder decreases upon sponge manufacturing, and the 1% chitosan, chitosan/PEG 6000 2 lyo, and chitosan/PEG 8000 1 lyo sponges displayed the smaller peaks. A very small peak can be seen in the chitosan/PEG 6000 1 lyo sponge at 24° , which is a contribution from the crystalline peak of PEG 6000 (seen in Figure 2B).

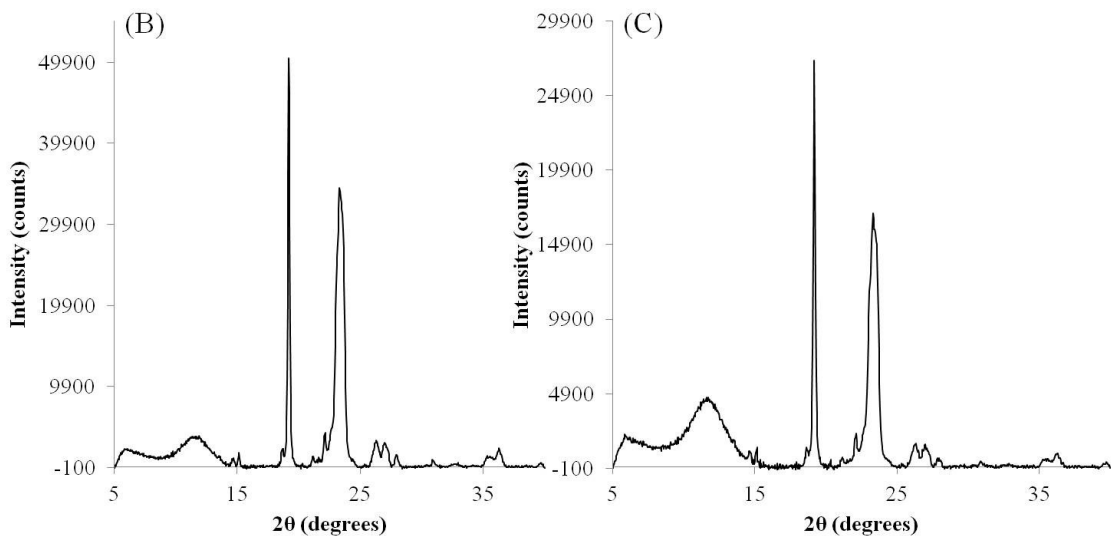
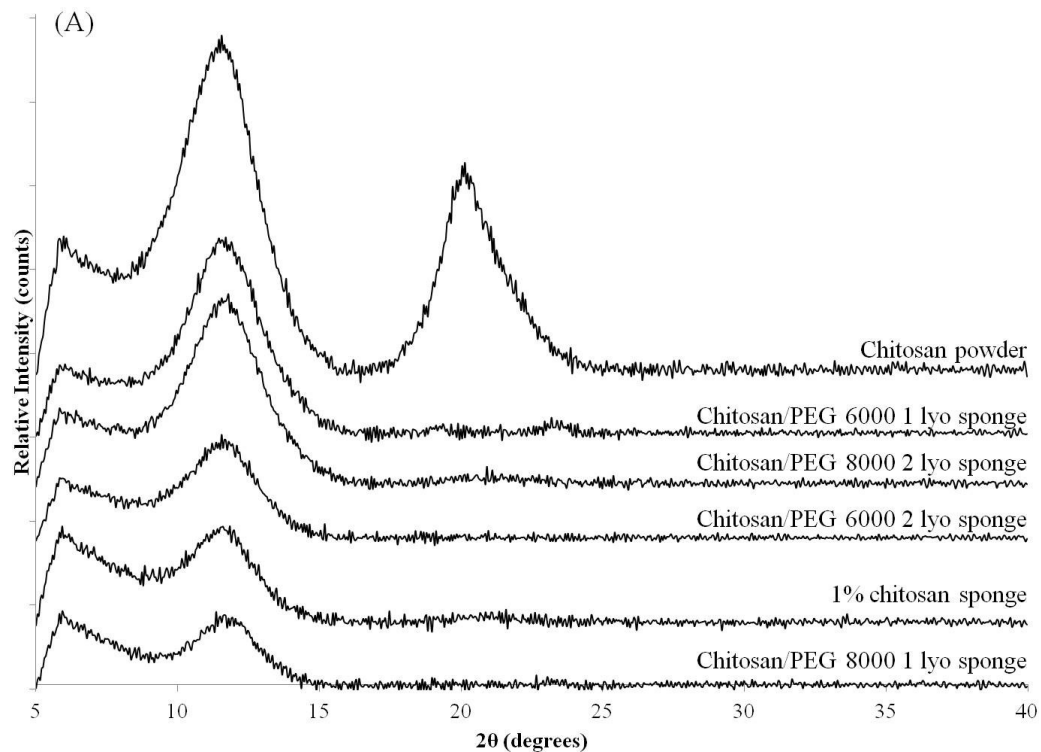


Figure 2. (A) Stacked x-ray diffraction (XRD) spectra in the 2θ range from 5° to 40° of (top to bottom) the chitosan powder, chitosan/PEG 6000 1 lyo sponge, chitosan/PEG 8000 2 lyo sponge, chitosan/PEG 6000 2 lyo sponge, 1% chitosan sponge, and chitosan/PEG 8000 1 lyo sponge, and XRD spectra in the 2θ range from 5° to 40° of (B) PEG 6000, and (C) PEG 8000.

DSC. The DSC data for the chitosan/PEG and chitosan sponges, and chitosan, PEG 6000, and PEG 8000 powder is provided in Table 1.

Table 1. Differential scanning calorimetry results of chitosan/PEG and chitosan sponges, as well as chitosan, PEG 6000, and PEG 8000 powder.

Sample	Endothermic Peak			Exothermic Peak		
	Temperature (°C)	Height (mW/mg)	Area (J/g)	Temperature (°C)	Height (mW/mg)	Area (J/g)
Chit/PEG 6000 1 Lyo	56.0 ± 1.0 ^{§γ}	1.6 ± 0.2	-70 ± 4.4	313.7 ± 0.9 ^{*†}	0.9 ± 0.02 ^{*†}	93.5 ± 11.8 ^{*†}
Chit/PEG 6000 2 Lyo	110.8 ± 4.8	1.1 ± 0.1	-191.8 ± 28.9	319.5 ± 1.1	2.3 ± 0.3	169.7 ± 22.0
Chit/PEG 8000 1 Lyo	58.6 ± 0.6	1.6 ± 0.1	-79.2 ± 6.3	315.4 ± 2.0 ^{*†}	1.0 ± 0.1 ^{**†}	94.8 ± 7.7 ^{*†}
Chit/ PEG 8000 2 Lyo	122.9 ± 9.2 ^γ	1.1 ± 0.1	-200.7 ± 9.5	319.1 ± 0.2	2.3 ± 0.2	168.1 ± 2.9
1% Chitosan Sponge	126.7 ± 7.8 [§]	1.1 ± 0.04	-210.5 ± 12.0	319.2 ± 1.1	2.1 ± 0.1	160.1 ± 5.4
Chitosan powder	111.6 ± 4.9	1.0 ± 0.1	-181 ± 28.3	326.0 ± 0.1 [‡]	3.3 ± 0.1 [‡]	178.7 ± 8.6
PEG 6000	68.1 ± 0.5	6.1 ± 0.4	-201.6 ± 9.5 ^{*†}	N/A	N/A	N/A
PEG 8000	67.9 ± 0.4	6.6 ± 0.6	203.2 ± 6.9 ^{*†}	N/A	N/A	N/A

[§] and ^γ indicate p < 0.05 vs. each other, ^{*} represents p < 0.05 versus all others except [†], [‡] indicates p < 0.05 versus all others

Analysis of the thermal data revealed that endothermic and exothermic peaks appeared at 56-126°C and 313-319°C in the sponges and powder samples. The endothermic peak can be attributed to water loss, while the exothermic peak corresponds to the decomposition of amine units.¹⁷⁻¹⁹ Because the PEG 6000 and 8000 powder samples do not have amine units, both are lacking the exothermic peak. The chitosan powder had the highest exothermic peak temperature, but after processing the chitosan

into a 1% chitosan sponge, the exothermic peak temperature decreased by 6.8°C ($p < 0.001$). The chitosan/PEG 2 lyo sponges also exhibited similar exothermic peak temperatures to the 1% chitosan sponge. However, the chitosan/PEG 6000 and 8000 1 lyo sponges exhibited 5.44°C and 3.77°C lower exothermic peak temperatures than the 1% chitosan sponge ($p < 0.001$ and $p = 0.008$). Additionally, the height and area of the exothermic peaks in the chitosan/PEG 1 lyo sponges also decreased significantly from the chitosan/PEG 2 lyo and 1% chitosan sponges. The chitosan/PEG 1 lyo sponges also exhibited lower endothermic peak temperatures and areas than the chitosan/PEG 2 lyo sponges, 1% chitosan sponges, and chitosan powder.

SEM. The morphology of the cross-sections of the 1% chitosan sponges and chitosan/PEG blended sponges can be seen in Figure 3A-E, while the surface structure of the 1% chitosan sponges and chitosan/PEG blended sponges can be seen in Figure 3F-J. The cross-sections of all sponges do not appear to be significantly different. However, the surface of the 1% chitosan sponge appears to have the greatest surface roughness, with the chitosan/PEG 6000 1 lyo and chitosan/PEG 8000 1 lyo sponges exhibiting a slight decrease in surface roughness. In the chitosan/PEG 8000 2 lyo sponge, only a few visible pores can be seen, while none can be seen in the chitosan/PEG 8000 1 lyo sponge.

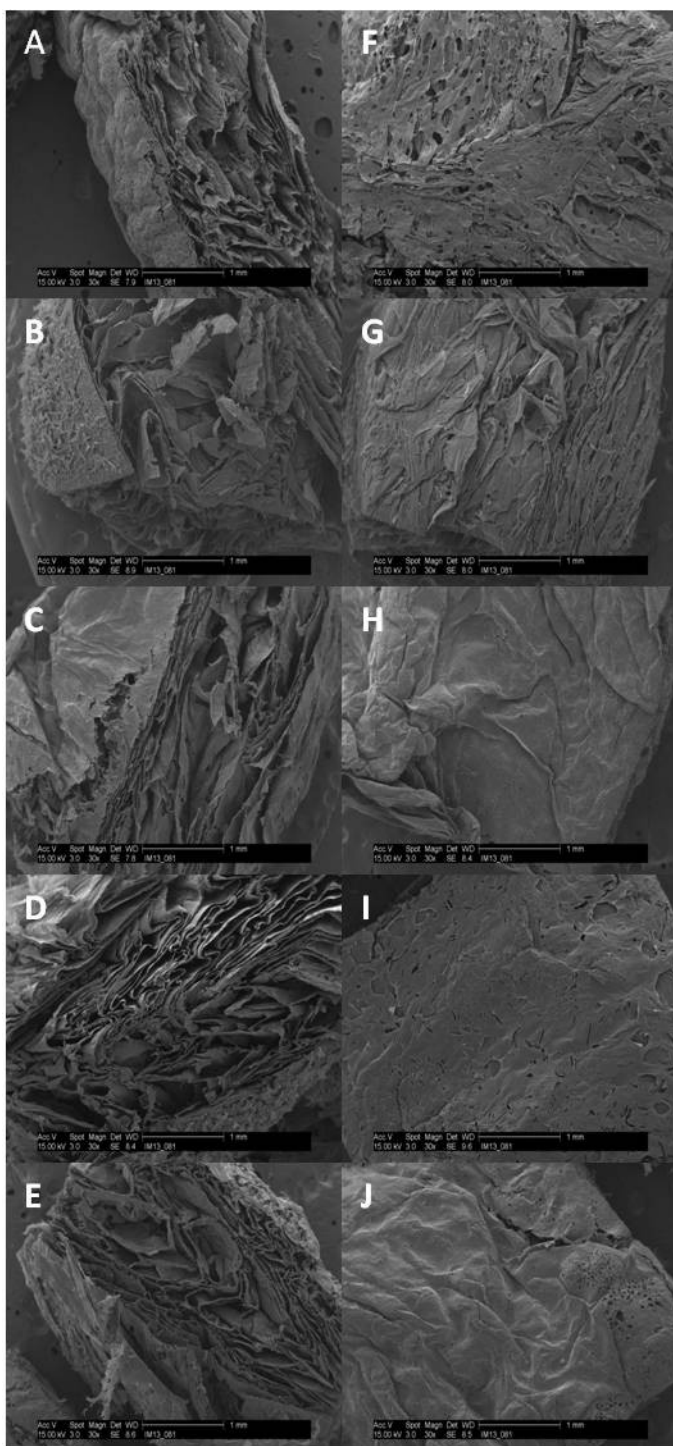


Figure 3. Representative scanning electron microscopy of sponge cross sections at 30 \times magnification: (A) 1% chitosan, (B) chitosan/PEG 6000 1 lyo, (C) chitosan/PEG 6000 2 lyo, (D) chitosan/PEG 8000 1 lyo, and (E) chitosan/PEG 8000 2 lyo sponges, as well as sponge surface structure at 30 \times magnification of (F) 1% chitosan, (G) chitosan/PEG 6000 1 lyo, (H) chitosan/PEG 6000 2 lyo, (I) chitosan/PEG 8000 1 lyo, and (J) chitosan/PEG 8000 2 lyo sponges.

***In vitro* degradation and viscosity.** Results from the *in vitro* degradation study of the chitosan/PEG blended sponges and control chitosan sponges are provided in Figures 4A and 4B. The chitosan/PEG 6000 1 lyo, chitosan/PEG 6000 2 lyo, and chitosan/PEG 8000 1 lyo sponges exhibited significant differences in degradation, 58.99, 31.11, and 94.18% respectively, than the control chitosan sponge, as well as 49.37, 21.59, and 84.66% less sponge remaining than the chitosan/PEG 8000 2 lyo sponge (Figure 4A). There was no significant decrease in remaining sponge over time for any of the chitosan/PEG sponges.

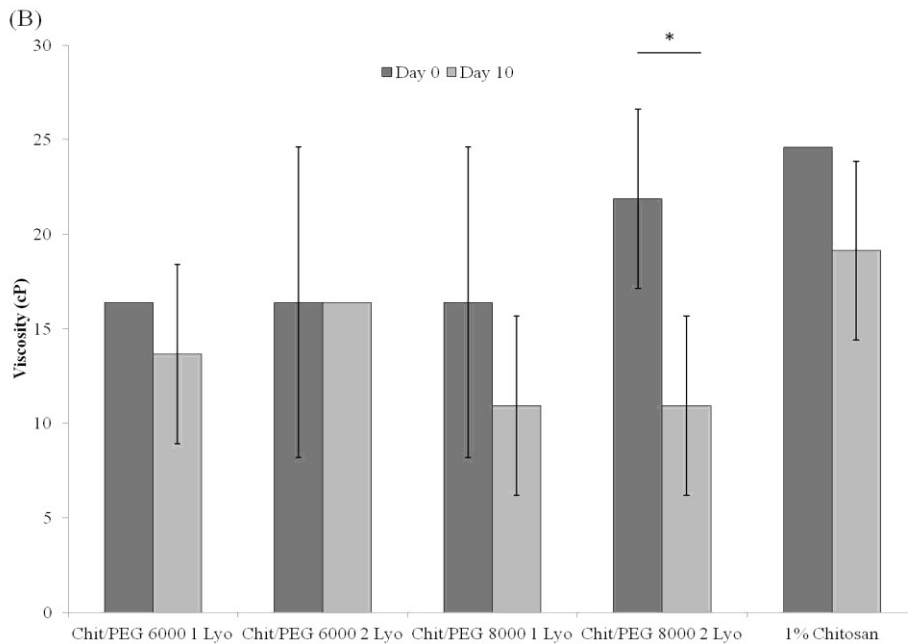
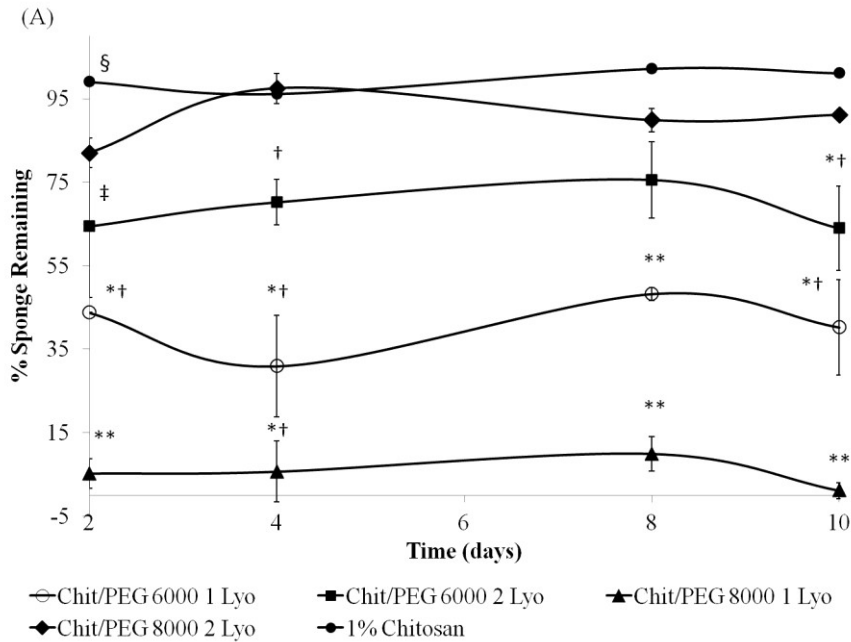


Figure 4.(A) Percent sponge remaining (mean \pm standard deviation) of chitosan/PEG 6000 1 lyo (○), chitosan/PEG 6000 2 lyo (■), chitosan/PEG 8000 1 lyo (▲), chitosan/PEG 8000 2 lyo (◆), and 1% chitosan (●) sponges after 2, 4, 8, or 10 days of *in vitro* enzymatic-mediated degradation (n = 3), where at each time point, * indicates $p < 0.05$ versus 1% chitosan, † denotes $p < 0.05$ versus chitosan/PEG 8000 2 lyo, ** indicates $p < 0.05$ versus all, and ‡ represents $p < 0.05$ versus all except §. (B) Brookfield viscosity measurements of sponges dissolved in 0.1 M sodium acetate and 0.2 M acetic acid before degradation (day 0) and after enzymatic-mediated degradation (day 10), where * denotes $p < 0.05$ pairwise.

Viscosity measurements were used in order to indirectly evaluate possible molecular weight changes of the blended polymer sponges after degradation; direct molecular weight measurements were not possible through GPC. All of the sponges, except for the chitosan/PEG 6000 2 lyo sponges, exhibited a decrease in viscosity from day 0 to day 10 of degradation (Figure 4B), although only the chitosan/PEG 8000 2 lyo sponge exhibited a statistically significant difference ($p = 0.014$).

***In Vitro* Amphotericin B Elution.** The *in vitro* amphotericin B release from the chitosan/PEG and chitosan sponges is reported in Figure 5. The average concentrations of amphotericin B released from all sponges after 1 and 3 hours were all above the minimum inhibitory concentration (MIC) for *Candida albicans*, but not for all later time points. The chitosan/PEG 6000 1 lyo sponge was the only sponge formulation to release amphotericin B at levels above the *C. albicans* MIC throughout the entire 72 hour elution. The chitosan/PEG 6000 and 8000 2 lyo sponges released average amphotericin B concentrations above the MIC at 72 hours, but not for all earlier time points. After 1 hour of elution, the chitosan/PEG 6000 1 lyo sponge released 20.41, 11.88, 19.34, and 23.60 more $\mu\text{g/mL}$ of amphotericin B than the chitosan/PEG 6000 2 lyo, chitosan/PEG 8000 1 lyo, chitosan/PEG 8000 2 lyo, and 1% chitosan sponges, respectively. The chitosan/PEG 8000 1 lyo sponge also released 8.53, 7.46, and 7.91 more $\mu\text{g/mL}$ of antifungal after 1 hour than the chitosan/PEG 6000 2 lyo, chitosan/PEG 8000 2 lyo, and 1% chitosan sponges, respectively. The cumulative percent release of loaded amphotericin B after 72 hours was determined to be 12.4 ± 3.8 , 5.3 ± 3.6 , 5.2 ± 0.3 , 5.4 ± 2.1 , and $7.7 \pm 2.2\%$ for the chitosan/PEG 6000 1 lyo, 6000 2 lyo, 8000 2 lyo, and 1%

chitosan sponges, respectively. While the chitosan/PEG 1 lyo, and 1% chitosan sponges exhibited significant differences in antifungal elution over time, the chitosan/PEG 2 lyo sponges did not release significantly different concentrations of amphotericin B over time.

Antifungal Activity. Results from the antifungal activity zone of inhibition assay can be seen in Figure 6, reported as amphotericin B concentration in $\mu\text{g/mL}$. All of the selected amphotericin B eluates tested in the assay had sufficient corresponding activity on *Candida albicans*, except for the eluates from the 1% chitosan sponges. Some of the amphotericin B eluates released from the 1% chitosan sponges that were measured at levels above the *C. albicans* MIC did not inhibit growth of *C. albicans* in the ZOI assay. In the ZOI assay, the eluates from the chitosan/PEG 6000 1 lyo and 8000 1 lyo sponges had the highest *C. albicans* zone of inhibition and corresponding amphotericin B concentration, and were both significantly different from the 1% chitosan sponges after 6 ($p = 0.004$ and $p = 0.006$) and 48 hours ($p = 0.006$) of elution.

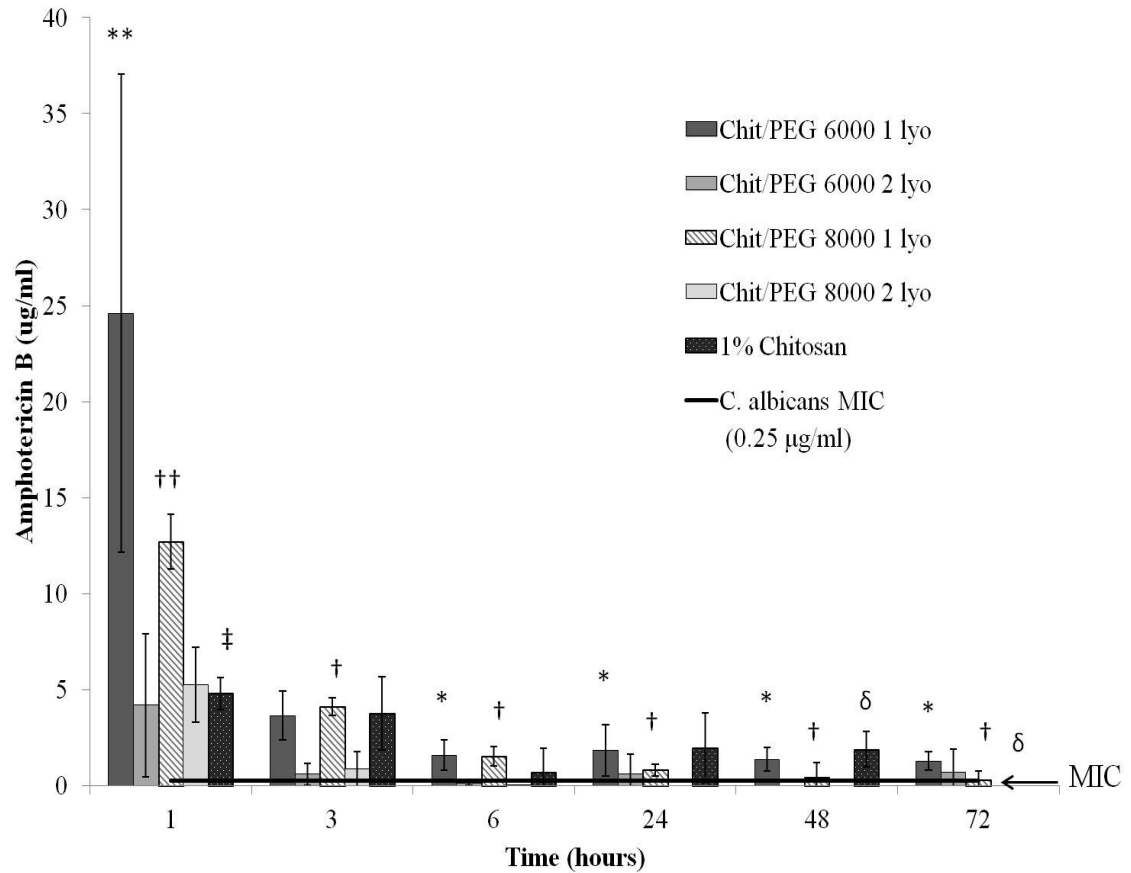


Figure 5. Amphotericin B released *in vitro* in $\mu\text{g/ml}$ (mean \pm standard deviation) from sponges over time and the minimum inhibitory concentration of amphotericin B for *Candida albicans*, where * represents $p < 0.001$ versus chit/PEG 6000 1 lyo 1 hour time point, † denotes $p < 0.003$ versus chit/PEG 8000 1 lyo 1 hour time point, δ indicates $p < 0.05$ versus 1% chitosan 1 hour time point, ** represents $p < 0.001$ versus all sponge groups within the time point, and †† denotes $p < 0.007$ versus all sponge groups within the time point except for ‡.

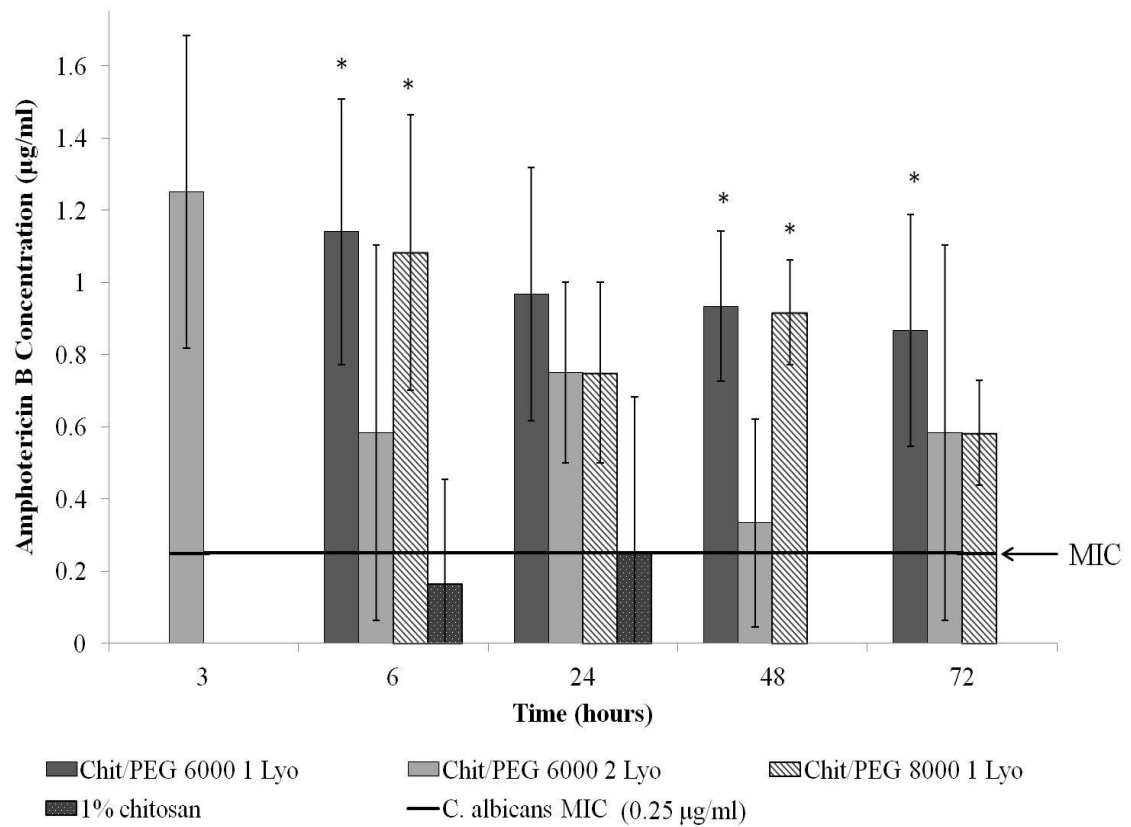


Figure 6. Results from antifungal activity zone of inhibition assay using selected amphotericin B eluted from chitosan/PEG and 1% chitosan sponges, where * indicates $p < 0.05$ versus control 1% chitosan sponge.

Cytocompatibility. As seen in Figure 7, each type of sponge caused significant decreases in cytocompatibility from the control polyurethane sponge, where the control was considered 100% cell viability, after one day of direct contact treatment ($p < 0.014$).

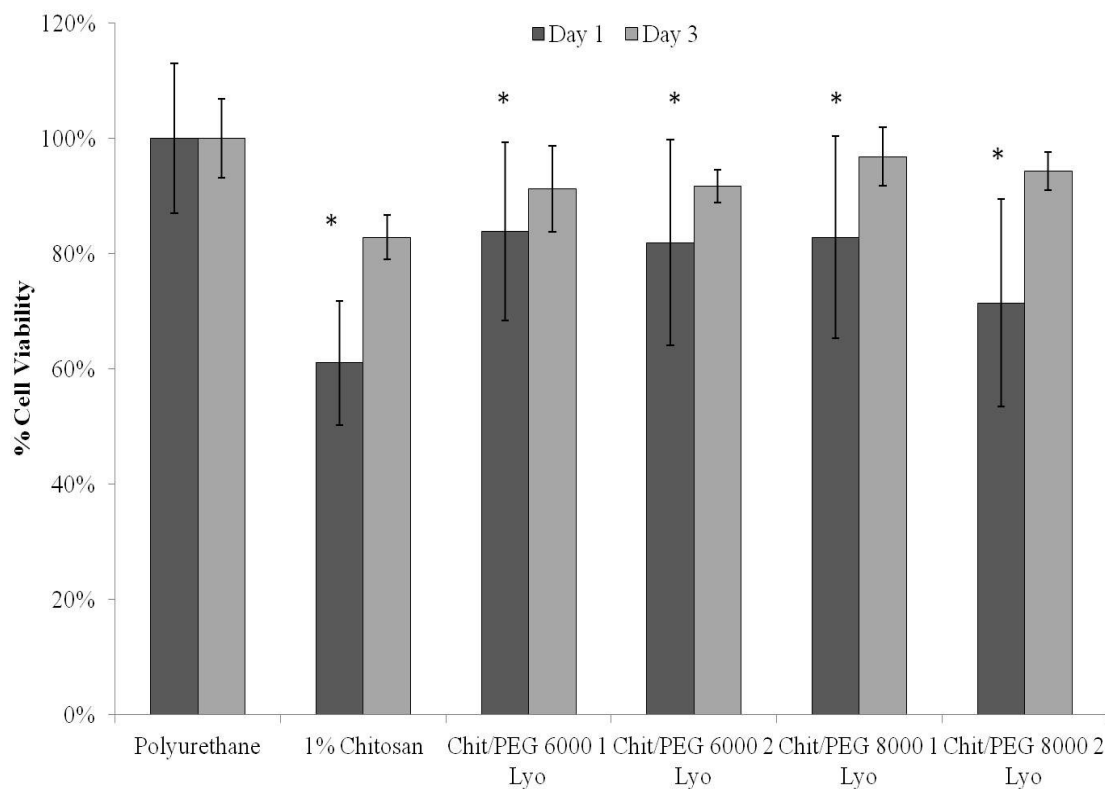


Figure 7. Direct contact biocompatibility normalized to polyurethane sponge control, represented in mean percent cell viability \pm standard deviation, of normal human dermal fibroblasts after exposure to polyurethane, chitosan/PEG, and 1% chitosan sponges for one and three days, analyzed using Cell Titer-Glo® luminescent assay (* indicates $p < 0.05$ versus polyurethane sponge control)

After 1 day, the 1% chitosan sponge and chitosan/PEG 8000 2 lyo sponges exhibited the largest decreases in percent cell viability, with 39 and 28.57% reduction in cell viability from the polyurethane control, respectively. Upon microscopic examination after one day of treatment, both the 1% chitosan and chitosan/PEG 8000 2 lyo sponges exhibited slight cellular malformation changes in some fibroblasts, while the other blended sponges did not cause any visible changes to the cells from the control. However, after three days of treatment, there were no significant differences between any of the sponges and the polyurethane sponge control. After three days of treatment, the cellular

morphology that was visible after day one for some of the sponges was no longer present. Additionally, these cytocompatibility evaluations found no sloughing, lysis, or reduction of the cell layer at either time point.

In Vivo Degradation and Biocompatibility. Data from the quantitative and qualitative evaluation of the rat tissue histology is shown in Figures 8-10. The percentage of implant area per defect area after 4 and 10 days of implantation is shown in Figure 8, but none of the experimental groups, with regard to time, exhibited significant differences ($p = 0.449$). The control 1% chitosan sponges and chitosan/PEG 6000 1 lyo sponges did exhibit significant differences in percent implant after 4 days of implantation ($p = 0.001$). None of the sponges degraded completely after 10 days. Quantitative and qualitative evaluation of fibrous tissue present around the sponges revealed a wide variability between surgical sites (Figure 9). Additionally, there were no statistically significant differences in percent fibrous tissue area per defect area between any of the sponges, with regard to sponge or time ($p = 0.130$ and $p = 0.723$).

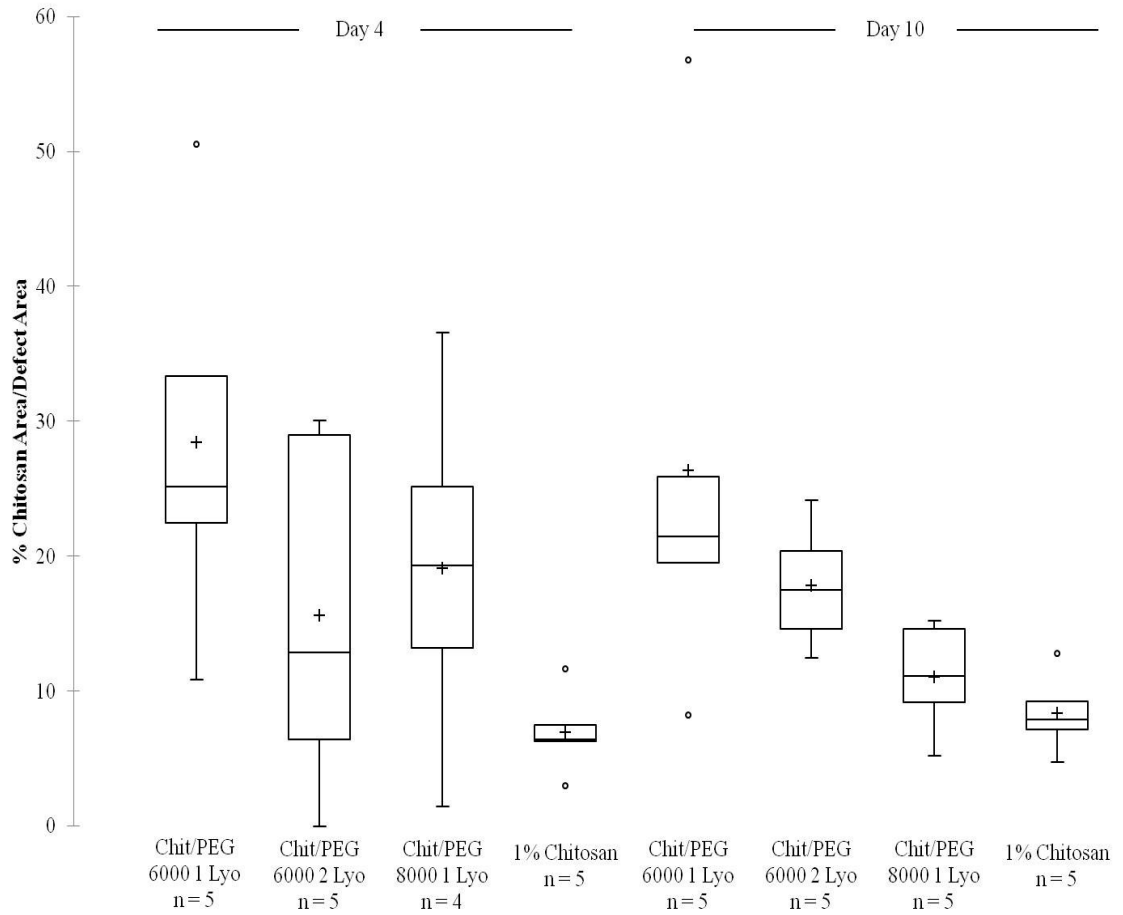


Figure 8. Histological analysis boxplot of the percentage of sponge implants present in the defect area, 4 and 10 days after surgery (+ and o represents the mean and a data point outside of the standard deviation, respectively)

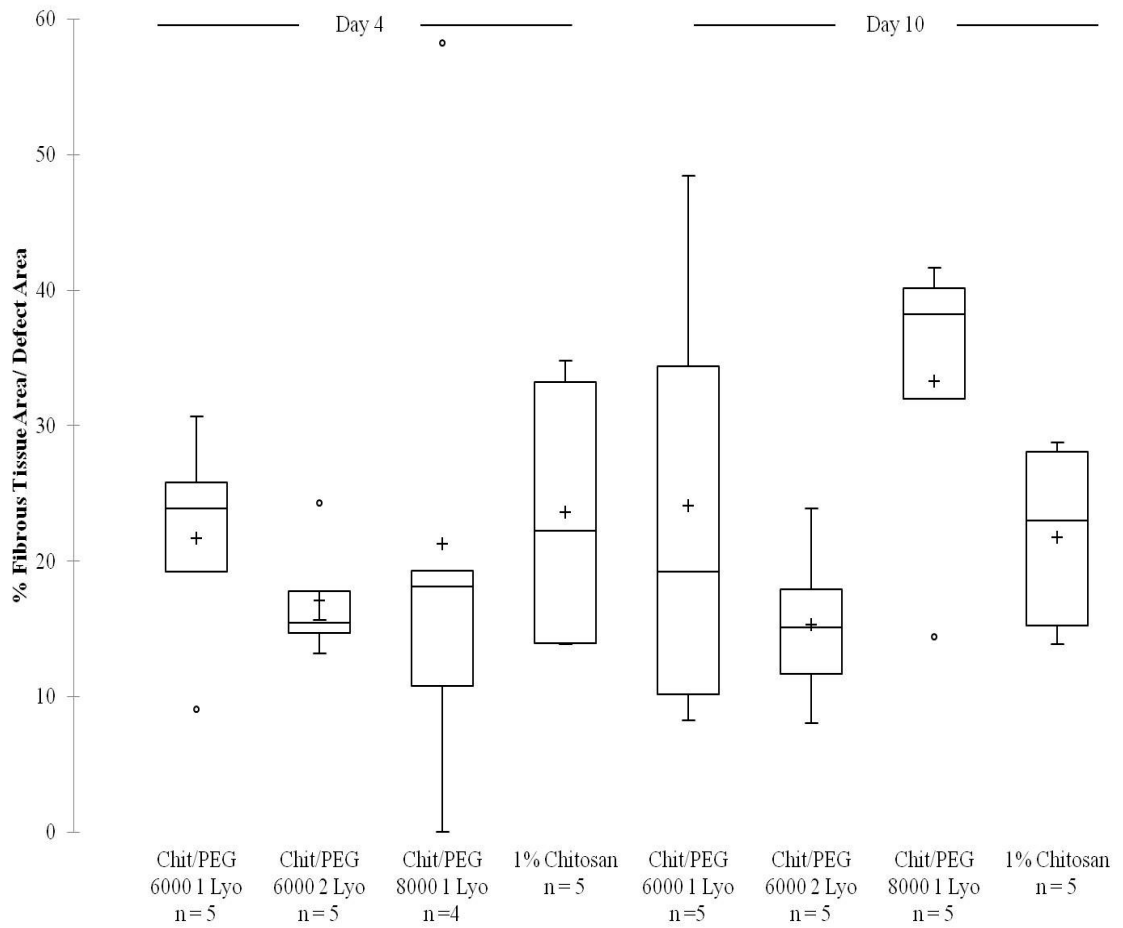


Figure 9. Histological analysis boxplot of the percentage of fibrous tissue present in the defect area (+ and o represents the mean and a data point outside of the standard deviation, respectively)

After 4 days of implantation, the chitosan/PEG 8000 1 lyo sponge exhibited the lowest average tissue response of the blended sponges (Figure 10), although not statistically different ($p = 0.336$). Similar to the implant percentage results, the chitosan/PEG 6000 1 lyo sponge displayed the highest average tissue response of all the sponges. After 10 days of implantation, the average tissue response increased by 5, 4, 5, and 72% for the 1% chitosan, chitosan/PEG 6000 1 lyo, chitosan/PEG 6000 2 lyo, and chitosan/PEG 8000 1 lyo sponges, respectively.

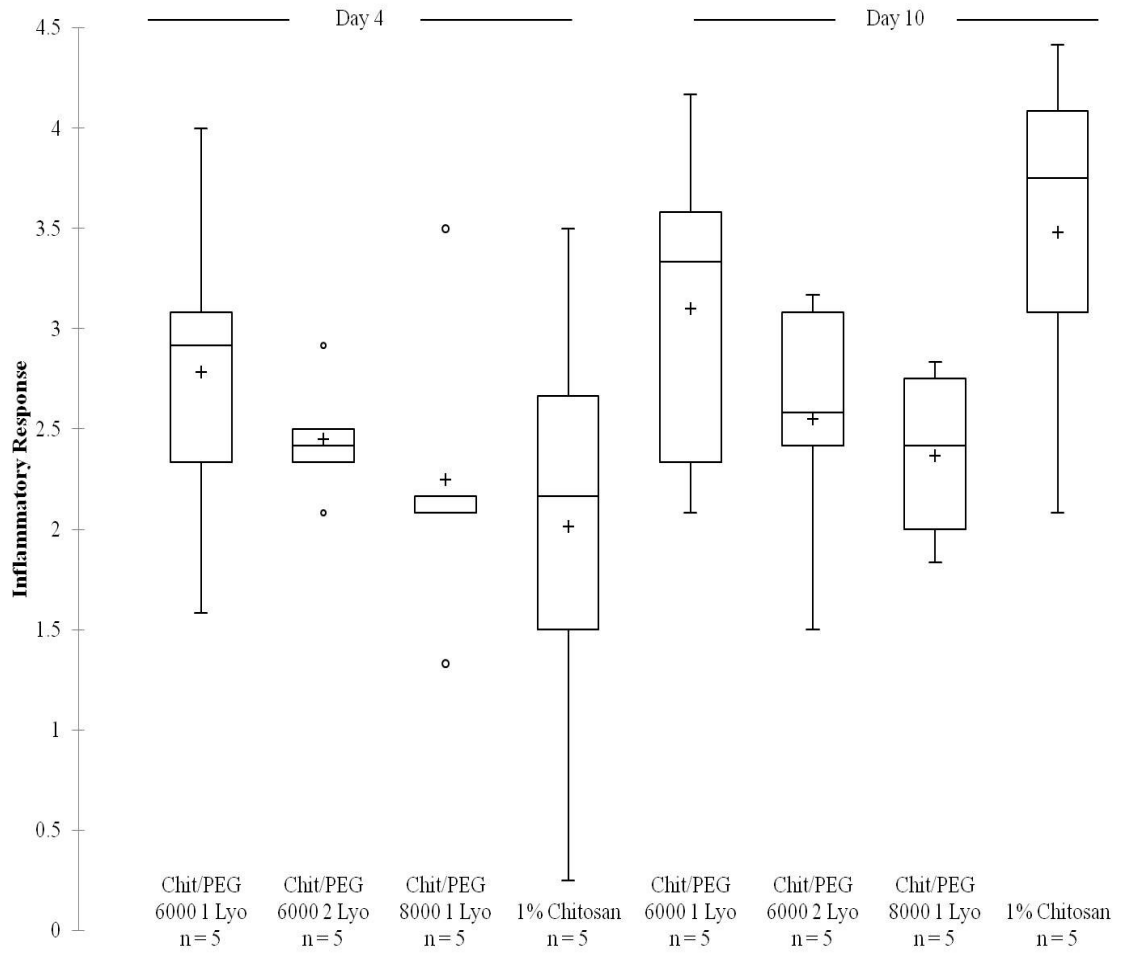


Figure 10. Histological analysis boxplot of the average graded inflammatory response from three blinded reviewers (+ and o represents the mean and a data point outside of the standard deviation, respectively)

In the satellite animals, none of the chitosan/PEG blended sponges nor the chitosan sponges degraded completely after 14, 21, or 28 days (Table 2). However, the chitosan/PEG sponges exhibited decreases in percent implant from 10 days to 28 days, and the chitosan/PEG 6000 2 lyo sponge demonstrated the largest decrease in implant percentage with an 88.77% reduction in percent implant from 10 to 28 days of implantation. While there is no data for the percentage of chitosan/PEG 6000 1 lyo sponge in defect after 14 days, the sponge was present in the original tissue block, so it is believed to have been lost in histological processing.

Table 2. Quantitative and qualitative analysis of satellite animal rat tissue histology after 14, 21, and 28 days of sponge implantation

<i>Sponge</i>	<i>Time (days)</i>	<i>% Implant Area/ Defect Area</i>	<i>% Fibrous Tissue/ Defect Area</i>	<i>Average Tissue Response</i>	<i>Sponge Present in Tissue Block</i>
Chitosan/PEG 6000 1 Lyo Sponge	14	0	0	1.33 ± 0.14	Yes
	21	27.55	27.55	2.5 ± 0.5	Yes
	28	9.58	9.58	2.08 ± 1.01	Yes
Chitosan/PEG 6000 2 Lyo Sponge	14	14.25	17.53	3.08 ± 0.88	Yes
	21	5.78	15.51	2.75 ± 0.90	Yes
	28	1.76	5.01	1.67 ± 1.61	Yes
Chitosan/PEG 8000 1 Lyo Sponge	14	8.52	10.33	3.33 ± 0.58	Yes
	21	14.72	24.96	3.5 ± 0.25	Yes
	28	8.13	12.05	1.83 ± 1.04	Yes
1% Chitosan Sponge	14	4.02	27.9	4 ± 0.25	Yes
	21	7.08	28.19	3.75 ± 0.43	Yes
	28	21.58	23.6	2 ± 0.5	Yes

Data is reported as mean ± standard deviation (n = 1) and tissue response is averaged from three blinded reviewers.

Discussion

These experimental results demonstrate that blending chitosan with polyethylene glycol in sponge form does significantly affect sponge material properties, amphotericin B elution, antifungal activity, and *in vivo* degradation in rat intramuscular tissue. However, blending does not affect *in vitro* cytocompatibility or *in vivo* biocompatibility in rat tissue. The presence of characteristic PEG peaks at 1279, 1099, 960, and 842 cm^{-1} in both 1 lyo chitosan/PEG blended sponges confirm the presence of PEG in the sponges. Although these peaks are not present in the 2 lyophilization blended sponges, the peak shift to lower wavelength at 842 cm^{-1} in the 2 lyophilization sponges, as compared to 843 cm^{-1} in the 1% chitosan sponge, indicates the possibility of residual PEG and possible interaction between chitosan and PEG. The chitosan/PEG 8000 2 lyo blended sponge also exhibited the characteristic PEG peak at 962 cm^{-1} , which indicates this blended sponge may have more PEG present in the sponge than the 6000 2 lyo sponge, which did not exhibit the peak. The FTIR spectra of the blended sponges in this study did not demonstrate a disappearance or shift of the amide I band to lower wavelength, as reported in previous research.^{7,8} However, all blended sponges, except for the 6000 2 lyo sponge, exhibited decreased absorbance of the amide I peak at 1643 cm^{-1} . The chitosan/PEG 1 lyo sponge also demonstrated both a shift of the amide II N-H peak at 1557 cm^{-1} to lower wavelength and increased absorbance compared to the chitosan sponge, which has also been confirmed by previous studies.^{7,8}

Analysis of the XRD spectra revealed that the chitosan powder exhibited a hydrated crystalline peak at $2\theta = 10^\circ$ and a sharp hydrated crystalline peak at $2\theta = 20^\circ$, indicating the presence of anhydrous chitosan crystal structure.²⁰ After chitosan

dissolution and lyophilization, the crystalline peak at 20° disappeared and the 10° peak decreased and became broader, suggesting a large loss in helical crystalline forms.²¹ Additionally, the increase of the peak and its sharpness at $2\theta = 7^\circ$ in the sponges from the powder indicates there could be some reordering of the polymer chains. Because of the increased 10° peak in both the chitosan/PEG 6000 1 lyo and 8000 2 lyo sponges and the presence of the small PEG crystalline peak at approximately 24° in the chitosan/PEG 6000 1 lyo sponge, both of these blended sponges appeared to exhibit increased crystallinity from the other blended and control chitosan sponges. The chitosan/PEG 6000 2 lyo and 8000 1 lyo sponges only showed a slightly reduced 10° peak from the chitosan sponge, which is similar to previously reported research on chitosan/PEG blended fibers⁷ and films¹⁶. Similar to this study, Wang et al. also found chitosan/PEG blended fibers to be absent of PEG crystalline peaks in XRD spectra.⁷

Thermal analysis of the chitosan powder, sponges, and chitosan/PEG blended sponges indicated that the chitosan double lyophilization and neutralization procedure decreased exothermic peak temperatures, which corresponded to amine decomposition.¹⁹ Additionally, the one lyophilization procedure for some of the chitosan/PEG sponges decreased the exothermic peak temperatures even further, by up to 5.5°C from the chitosan powder, and decreased the exothermic peak height and area as well. This shift of the exothermic peak to lower temperatures in the 1 lyo sponges is similar to previously reported findings that, with increasing PEG content in chitosan and PEG blended films, the exothermic peak temperature shifted to lower temperatures.¹⁶ Additionally, the decreased endothermic peak temperatures (56.03 and 58.57°C) in the chitosan/PEG 1 lyo sponges can be attributed to the melting temperature of PEG 6000 and 8000,

approximately 68°C. The shift to even lower endothermic peak temperatures can be explained by increased lattice defects due to partial miscibility of the noncrystalline phase.^{16,22}

Morphological differences were seen in surface SEM images, but not cross-section images, of the chitosan/PEG and chitosan sponges. The smoother appearance of the chitosan and PEG blended sponges, as compared to the 1% chitosan sponges, may indicate the compatibility of two polymers in a blend. The chitosan/PEG sponges' morphologies agrees with previously reported research that chitosan/PEG blended films⁶ and fibers⁷ exhibited smooth and nonporous surfaces⁶ and smooth and homogenous cross sections⁷, respectively.

In vitro degradation is one of the sponge material properties affected by the addition of PEG, molecular weight of PEG, and number of lyophilizations. The addition of PEG 6000 to the chitosan sponges, as well as the use of only 1 lyophilization, caused the chitosan/PEG 6000 1 and 2 lyo and chitosan/PEG 8000 1 lyo sponges to degrade significantly in mass, with 1-75% sponge remaining over ten days, compared to 82.04-97.46% and 99-100% sponge remaining in the chitosan/PEG 8000 2 lyo and control chitosan sponges. As expected, the degradation of the blended chitosan/PEG sponges in this study is higher than the degradation that Tanuma et al. reported for PEG crosslinked chitosan films, 7% weight loss after 8 days of lysozyme mediated degradation.²³ While molecular weight could not be directly measured through GPC methods, the sponges' slight decrease in viscosity after ten days of degradation demonstrates there might be a slight decrease in sponge molecular weight after degradation; however, the viscosity of the blended sponges did not decrease as much as the 55% reduction in specific viscosity

of PEG grafted chitosan solutions in 7.5 mg/mL lysozyme reported in a previous study.²⁴ Although the chitosan/PEG 6000 and 8000 1 lyo sponges exhibited the lowest percent sponge remaining in the *in vitro* degradation study, the smoother surfaces of the blended sponges visualized by SEM, as compared to the chitosan sponge, indicates that surface roughness may not be related to increased *in vitro* degradation.

Differences in amphotericin B elution were seen in the sponges upon adding PEG to the chitosan sponges and using only one lyophilization. The chitosan/PEG 6000 1 lyo sponge released $12.43 \pm 3.81\%$ of loaded amphotericin B after 72 hours, while the chitosan/PEG 6000 2 lyo sponge released $5.27 \pm 3.55\%$ of loaded amphotericin B over the same time frame. While the chitosan/PEG 8000 1 lyo sponge only released $5.22 \pm 0.31\%$ of loaded antifungal over 72 hours, the sponge released significantly more amphotericin B after one hour of elution than the other blended sponges. Although the sponges are still retaining amphotericin B, all of the sponges released more antifungal *in vitro* than what has been previously reported for amphotericin B loaded bone cement, 0.45 and 0.05% with and without a poragen²⁵ or 0.03% release²⁶ of loaded amphotericin B. As expected, the percent cumulative release from the post-loaded chitosan/PEG blended sponges was less than the 60% amphotericin B release after 2 days from a preloaded Pluronic® based multi-block copolymer gel.²⁷

Although the control chitosan sponges released more amphotericin B than some of the blended sponges with $7.68 \pm 2.20\%$ cumulative release, many of these antifungal eluates did not maintain sufficient activity against *C. albicans*. Whereas, all the tested amphotericin B elution samples from the chitosan/PEG 6000 and 8000 1 lyo sponges and all but three elution samples from the chitosan/PEG 6000 2 lyo sponges remained active

against *C. albicans*. The active amphotericin B eluates from the chitosan/PEG sponges are similar to previously reported active amphotericin B eluates from PMMA bone cement.²⁸ The antifungal activity ZOI assay results in this current study provide an indication that the addition of PEG to the chitosan sponges is an improvement for antifungal elution and activity over the unblended chitosan sponges.

As expected, the chitosan/PEG blended sponges did not elicit any significant cytotoxic effects on normal human dermal fibroblasts. Previous research has shown that adding PEG to chitosan films enhanced protein adsorption and cell adhesion, growth, and proliferation.⁶ The chitosan/PEG 8000 2 lyo sponge's slight decrease in cell viability after one day of treatment indicates there may be more similarities between the chitosan/PEG 8000 2 lyo sponge and control chitosan sponge than the other blended sponges. The differences in cytocompatibility found over time for all sponges in this study are also similar to previous results reported for other chitosan applications.^{3,29}

While adding PEG to the chitosan sponges resulted in increased *in vitro* degradation, the chitosan/PEG sponges did not exhibit increased *in vivo* degradation in the rat intramuscular model compared to the chitosan sponges. However, similar to the *in vitro* degradation results, the chitosan/PEG 8000 1 lyo sponge demonstrated the lowest percent implant in the defect after ten days of implantation. Conversely, the increased *in vivo* degradation in the chitosan/PEG 6000 2 lyo sponge over the chitosan/6000 1 lyo sponge, whereas the opposite was shown *in vitro*, demonstrates the difficulty of translating from *in vitro* studies to *in vivo*. Although chitosan has been reported to be biodegradable and biocompatible, wide data variations exist in the literature; for example, one study reported chitosan to have minimal degradation after subcutaneous

implantation, while other researchers showed a chitosan wound dressing to have rapid degradation.^{2,30,31} There was also wide variation in results in this study which led to none of the blended sponges showing significant decreases, either in percent implant and percent fibrous tissue, from the control chitosan sponges.

Chitosan/PEG and chitosan sponges exhibited statistically similar inflammatory tissue responses, but the chitosan/PEG 6000 1 lyo sponge demonstrated increased inflammatory response after 4 days of implantation and slightly higher average tissue response after 10 days. These results demonstrate that, in addition to reduced *in vivo* sponge degradation, the chitosan/PEG 6000 1 lyo sponge exhibits a more acute inflammatory response than the other two blended sponges; these findings have lead us to eliminate this blended sponge formulation from future research. The average inflammatory response for the control chitosan sponges was also higher than all of the chitosan/PEG blended sponges after 10 days of implantation. However, the inflammatory responses from all of the sponges are still lower than the tissue response from the sutures and are similar to reported moderate inflammatory responses from chitosan coated titanium pins implanted in Sprague-Dawley rats.³²

Although none of the sponges degraded within 28 days, all of the blended sponges appeared to be degrading over time and a few important differences can still be seen in the satellite animal data. After 28 days, the chitosan/PEG 6000 2 lyo sponge was surprisingly the most degraded of the sponge types, and was almost completely degraded. Even though these results are just in one animal for each sponge, the data still provides an indication of *in vivo* degradation trends.

There has not been much research on local antifungal delivery systems, and many of the local delivery systems that exist release too little antifungal or are not designed to degrade. In previous research, biocompatible polyethylene glycol (PEG) has been utilized to deliver the hydrophobic antifungal, amphotericin B. Our results indicate that blending chitosan and PEG into sponges creates biocompatible and degradable sponges capable of point of care amphotericin B loading and *in vitro* release that perform better than our previously developed chitosan sponges. Future work is needed to extend the *in vivo* study to better define the time of *in vivo* degradation. Other studies are also planned to study the loading and release of both antifungals and antibiotics, separately and combined, from the blended sponges so that the further development of the chitosan/PEG blended sponges may provide a truly customizable adjunctive therapy for bacterial and fungal contaminated musculoskeletal wounds.

References

1. Noel SP, Courtney HS, Bumgardner JD, Haggard WO. Chitosan sponges to locally deliver amikacin and vancomycin: a pilot *in vitro* evaluation. *Clin Orthop Relat Res* 2010;468(8):2074-80.
2. Stinner D, Noel S, Haggard W, Watson J, Wenke J. Local antibiotic delivery using tailorable chitosan sponges: the future of infection control? *J Orthop Trauma* 2010;24(9):592-7.
3. Parker AC, Jennings JA, Bumgardner JD, Courtney HS, Lindner E, Haggard WO. Preliminary investigation of crosslinked chitosan sponges for tailorable drug delivery and infection control. *J Biomed Mater Res B Appl Biomater* 2013;101(1):110-23.
4. Smith JK, Moshref AR, Jennings JA, Courtney HS, Haggard WO. Chitosan sponges for local synergistic infection therapy: a pilot study. *Clin Orthop Relat Res* 2013;471(10):3158-64.
5. Jennings JA, Courtney HS, Haggard WO. Cis-2-decenoic acid inhibits *S. aureus* growth and biofilm *in vitro*: a pilot study. *Clin Orthop Relat Res* 2012;470(10):2663-70.

6. Zhang M, Li XH, Gong YD, Zhao NM, Zhang XF. Properties and biocompatibility of chitosan films modified by blending with PEG. *Biomaterials* 2002;23(13):2641-8.
7. Wang Q, Zhang N, Hu X, Yang J, Du Y. Chitosan/polyethylene glycol blend fibers and their properties for drug controlled release. *Journal of Biomedical Materials Research Part A* 2008;85(4):881-7.
8. Kolhe P, Kannan RM. Improvement in ductility of chitosan through blending and copolymerization with PEG: FTIR investigation of molecular interactions. *Biomacromolecules* 2003;4(1):173-180.
9. Zhao L, Zhu L, Liu F, Liu C, Shan D, Wang Q, Zhang C, Li J, Liu J, Qu X and others. pH triggered injectable amphiphilic hydrogel containing doxorubicin and paclitaxel. *Int J Pharm* 2011;410(1-2):83-91.
10. Moribe K, Maruyama K, Iwatsuru M. Molecular localization and state of amphotericin B in PEG liposomes. *Int J Pharm* 1999;193(1):97-106.
11. Moribe K, Maruyama K. Pharmaceutical design of the liposomal antimicrobial agents for infectious disease. *Curr Pharm Des* 2002;8(6):441-54.
12. Darole PS, Hegde DD, Nair HA. Formulation and evaluation of microemulsion based delivery system for amphotericin B. *AAPS PharmSciTech* 2008;9(1):122-8.
13. Tiyaboonchai W, Limpeanchob N. Formulation and characterization of amphotericin B-chitosan-dextran sulfate nanoparticles. *International Journal of Pharmaceutics* 2007;329(1-2):142-9.
14. ASTM International. F813-07 2007.
15. Knodell RG, Ishak KG, Black WC, Chen TS, Craig R, Kaplowitz N, Kiernan TW, Wollman J. Formulation and application of a numerical scoring system for assessing histological activity in asymptomatic chronic active hepatitis. *Hepatology* 1981;1(5):431-5.
16. He L, Xue R, Yang D, Liu Y, Song R. Effects of Blending Chitosan with PEG on Surface Morphology, Crystallization and Thermal Properties. *Chinese Journal of Polymer Science* 2009;27(4):501-510.
17. Mecwan MM, Rapalo GE, Mishra SR, Haggard WO, Bumgardner JD. Effect of molecular weight of chitosan degraded by microwave irradiation on lyophilized scaffold for bone tissue engineering applications. *J Biomed Mater Res A* 2011.
18. Kittur FS, Harish Prashanth KV, Udaya Sankar K, Tharanathan RN. Characterization of chitin, chitosan and their carboxymethyl derivatives by differential scanning calorimetry. *Carbohydrate Polymers* 2002;2002(49):185-193.

19. Guinesi LS, Cavalheiro ETG. The use of DSC curves to determine the acetylation degree of chitin/chitosan samples. *Thermochimica Acta* 2006(444):128-133.
20. Ogawa K. Effect of Heating an Aqueous Suspension of Chitosan on the Crystallinity and Polymorphs. *Agric. Biol. Chem* 1991;55(9):2375-2379.
21. Zhang Y, Xue C, Xue Y, Gao R, Zhang X. Determination of the degree of deacetylation of chitin and chitosan by X-ray powder diffraction. *Carbohydr Res* 2005;340(11):1914-7.
22. Wan Y, Wu H, Yu A, Wen D. Biodegradable polylactide/chitosan blend membranes. *Biomacromolecules* 2006;7(4):1362-72.
23. Tanuma H, Saito T, Nishikawa K, Dong T, Yazawa K, Inoue Y. Preparation and characterization of PEG-cross-linked chitosan hydrogel films with controllable swelling and enzymatic degradation behavior. *Carbohydrate Polymers* 2010;80(1):260-265.
24. Hu YQ, Jiang HL, Xu CN, Wang YJ, Zhu KJ. Preparation and characterization of poly(ethylene glycol)-g-chitosan with water- and organosolubility. *Carbohydrate Polymers* 2005;61(4):472-479.
25. Kweon C, McLaren AC, Leon C, McLemore R. Amphotericin B delivery from bone cement increases with porosity but strength decreases. *Clin Orthop Relat Res* 2011;469(11):3002-7.
26. Goss B, Lutton C, Weinrauch P, Jabur M, Gillett G, Crawford R. Elution and mechanical properties of antifungal bone cement. *J Arthroplasty* 2007;22(6):902-8.
27. Kim YT, Shin BK, Garripelli VK, Kim JK, Davaa E, Jo S, Park JS. A thermosensitive vaginal gel formulation with HPgammaCD for the pH-dependent release and solubilization of amphotericin B. *Eur J Pharm Sci* 2010;41(2):399-406.
28. Cunningham B, McLaren AC, Pauken C, McLemore R. Liposomal formulation increases local delivery of amphotericin from bone cement: a pilot study. *Clin Orthop Relat Res* 2012;470(10):2671-6.
29. Silva SS, Motta A, Rodrigues MT, Pinheiro AF, Gomes ME, Mano JF, Reis RL, Migliaresi C. Novel genipin-cross-linked chitosan/silk fibroin sponges for cartilage engineering strategies. *Biomacromolecules* 2008;9(10):2764-74.
30. Dash M, Chiellini F, Ottenbrite RM, Chiellini E. Chitosan-A versatile semi-synthetic polymer in biomedical applications. *Progress in Polymer Science* 2011;36(8):981-1014.

31. Ma L, Gao C, Mao Z, Zhou J, Shen J, Hu X, Han C. Collagen/chitosan porous scaffolds with improved biostability for skin tissue engineering. *Biomaterials* 2003;24(26):4833-41.
32. Norowski PA, Courtney HS, Babu J, Haggard WO, Bumgardner JD. Chitosan coatings deliver antimicrobials from titanium implants: a preliminary study. *Implant Dent* 2011;20(1):56-67.

CHAPTER 4

CHARACTERIZATION OF LOCAL DELIVERY WITH AMPHOTERICIN B AND VANCOMYCIN FROM MODIFIED CHITOSAN SPONGES AND FUNCTIONAL BIOFILM PREVENTION EVALUATION

Introduction

Musculoskeletal trauma is one of the most prevalent types of injuries in the United States; more than three out of five of the unintentional injuries occurring annually in the U.S. are musculoskeletal injuries.^{1,2} Musculoskeletal extremity injuries are especially susceptible to multiple pathogenic, and sometimes drug resistant bacteria and fungi, such as methicillin resistant *Staphylococcus aureus* (MRSA), *Pseudomonas aeruginosa*, *Acinetobacter baumannii*, *Escherichia coli*, *Aspergillus* spp., and *Candida albicans*.^{2,3} These infection complications can increase morbidity and/or mortality, as well as increase hospitalization costs and stays.⁴ Although bacteria typically cause the majority of musculoskeletal infections, invasive fungal infections (IFI) have recently caused significant problems for both the British and United States military; the U.S. reported that 78% of the IFI infected U.S. soldiers injured in Afghanistan from 2009 to 2010 required lower limb amputations.⁵ However, these fungal infections are problematic for civilians as well as for the military; for example, invasive *Candida* infections are the third most common cause of hospital acquired infections.⁶

In addition to the presence of multidrug resistant bacteria or fungi, the presence of necrotic tissue, debris, and fixation devices or implants creates a favorable environment for the development of biofilms and corresponding infection.⁷ According to an estimate by the CDC, approximately 65% of bacterial infections are associated with biofilms.⁸ In biofilms, the metabolic activity of the bacteria is reduced, resulting in less susceptibility

to antimicrobials and an increased minimal inhibitory concentration (MIC).⁹ Additionally, the typical clinical presence of multiple bacterial and/ or fungal strains means that the traditional view of individual pathogen infections and single antimicrobial delivery may not be appropriate.¹⁰

Because systemic antimicrobials cannot be administered at very high concentrations to fight localized bacteria, fungi, and/or biofilms, local antibiotic delivery can be an effective route for treating wounds and minimizing infections, when used as an adjunctive therapy to systemic dosing.¹¹ Additionally, local delivery systems often have the capability for the release of multiple antimicrobials for polymicrobial infection prevention. While there are a large amount of local antibiotic delivery systems available, there have not many local antifungal delivery systems developed because of the problematic hydrophobicity of many antifungals. Amphotericin B, a common clinically used antifungal, has been studied in polymethylmethacrylate (PMMA) bone cement¹²⁻¹⁴, dextran gels^{15,16}, a Pluronic® based gel¹⁷, and a composite of hydroxyapatite and chitosan^{18,19}; however, all of these delivery systems were pre-loaded with the antifungal and the resulting data varies widely. A local antifungal delivery system capable of expeditious point of care loading in the operating room would allow a clinician to tailor the antibiotic and/or antifungal choice and dosage for the needs of each patient.

In previous studies, we developed a degradable chitosan sponge local antibiotic delivery system that is capable of tailored point of care antibiotic loading and release.^{20,21} Additionally, these sponges can be loaded with multiple antibiotics and have released antibiotics at levels high enough to prevent *S. aureus* biofilm growth *in vivo*.^{20,21} The water soluble polymer polyethylene glycol (PEG) has also been utilized as a solvent for

cis-2-decenoic acid, a hydrophobic fatty acid, for incorporation into the same chitosan sponge delivery system.²² Polyethylene glycol exhibits low toxicity and immunogenicity and has been used in liposome or nanoparticle form as a solvent system for the systemic delivery of amphotericin B.²³⁻²⁷ Researchers have also modified chitosan hydrogels, fibers, and films with PEG, as well as blending or copolymerization.^{23,28-30}

Therefore, our research purpose was to determine if blending chitosan with PEG in sponge form would generate a local delivery system capable of releasing both antibiotic and antifungal for polymicrobial wound infection prevention. The first objective of this study was to evaluate the sponges' swelling and *in vitro* amphotericin B and vancomycin release, both single and dual loaded, confirm antifungal and antibiotic activity, and determine the cytocompatibility of the eluates. The second objective of this research was to evaluate the capability of the chitosan/PEG blended sponges to prevent *S. aureus* biofilm growth *in vivo* in a preliminary infected catheter murine model.

Methods

Materials: Chitosan and polyethylene glycol (PEG) were purchased from Chitinor AS (Tromsøy, Norway) and Sigma Aldrich (St. Louis, MO), respectively. Sodium deoxycholate solubilized amphotericin B and vancomycin were obtained from Amresco (Solon, OH) and Fisher Scientific (Pittsburg, PA), respectively. All other reagents and chemicals were of analytical grade and were purchased from Fisher Scientific.

Sponge Fabrication: To fabricate blended chitosan and PEG sponges, 0.5% (w/v) of PEG, at 6,000 or 8,000 g/mol, was dissolved in a 1% (v/v) acetic acid solution. After rapid PEG dissolution, 0.5% (w/v) of chitosan (250 kDa and 82.46 ± 1.679 degree of deacetylation) was added to the same solution. Control chitosan sponges were made in

the same manner, but with 1% (w/v) chitosan in solution. Chitosan/PEG and chitosan solutions were mixed for approximately one hour and then poured into 42 mL aluminum pans at a volume of 25 mL. Solutions were frozen for a minimum of one hour at -80°C, followed by lyophilization in a LabConco (Kansas City, MO) FreeZone 2.5 Liter Benchtop Freeze Dry System.

After lyophilization, the control chitosan sponges and the chitosan/PEG sponges with 6,000 g/mol PEG were neutralized in either 0.6 or 0.25 M NaOH, respectively. Sponges were soaked in the base solutions for approximately 1-2 minutes and then washed in copious amounts of water until a neutral pH was reached. Once neutralized, the chitosan and chitosan/PEG 6000 sponges were frozen and lyophilized again. The chitosan/PEG sponges with 8,000 g/mol PEG were only lyophilized once and not neutralized. All sponge groups were sterilized with low dose gamma irradiation at a dosage of 25-40 kGy.

Swelling: Sponges were evaluated for their swelling ability by loading the pre-weighed sponges with 10 mL of 1 x phosphate buffered saline (PBS) via absorbance. After 2 minutes, the sponges were quickly blotted to remove excess surface water and then weighed immediately (n = 3). The swelling ability of the sponges was calculated using equation 1,

$$\text{Swelling Ratio} = \frac{W_w}{W_d} \quad (1)$$

where W_w is the wet sponge weight and W_d is the original dry sponge weight.

***In Vitro* Antifungal and Antibiotic Elution:** The *in vitro* local release of antifungals and/or antibiotics from the sponges was evaluated by loading the sponges with either 1 mg/ml sodium deoxycholate solubilized amphotericin B, 4 mg/ml vancomycin, or a combined solution of 4 mg/ml and 1 mg/ml solution of vancomycin and sodium deoxycholate solubilized amphotericin B. All antimicrobial solutions were created in sterile Ultrapure water, and the dual vancomycin and amphotericin B solution was made by creating separate antibiotic and antifungal solutions first and then combining the two solutions into one. All antimicrobial solutions were shaken immediately prior to use and 10 mL of each solution was added to the sponges (n = 3). After approximately one minute of absorbance, the antimicrobial solutions not absorbed by the sponges was removed and measured. Sponges were added to twenty mL of sterile 1x PBS in 125 mL Nalgene (Rochester, NY) containers and incubated at 37°C on a shaker. Elution samples were removed after 1, 3, 6, 24, 48, and 72 hours in 1 mL aliquots and the PBS was completely refreshed.

The concentration of single loaded amphotericin B released from the sponges was measured via high pressure liquid chromatography (HPLC) with a ThermoScientific BDS Hypersil C18 column. Amphotericin B was measured at 407 nm in a mobile phase of acetonitrile, methanol, and 10 mM sodium phosphate monobasic (41:10:49).³¹ Both single and dual loaded vancomycin eluates were also measured with HPLC and the same column. Vancomycin was measured at 235 nm in a mobile phase of 35% acetonitrile and 65% buffer (0.08 M disodium phosphate and 0.013 M monosodium phosphate adjusted to pH 3 with phosphoric acid).³²

The concentrations of amphotericin B released from sponges loaded with both vancomycin and amphotericin B were also measured with ultraviolet visible (UV-Vis) spectroscopy since the antifungal was not accurately detected using the previously mentioned HPLC method. According to an amphotericin B manufacturer³³, the typical detection methods used for amphotericin B detection include microbial assays, HPLC, and UV-Vis; however, these methods have not been studied with simultaneous vancomycin elution. Because some of the dual elution samples exhibited precipitates, the eluates were added 1:1 to dimethylsulfoxide (DMSO) and well mixed. The highly concentrated stock solution was diluted in DMSO multiple times. Amphotericin B eluates from dual loaded sponges were read via absorbance at 389 nm in a Biotek (Winooski, VT) Synergy H1 plate reader. Antifungal concentrations were calculated using an amphotericin B standard curve.

***In Vitro* Antifungal Activity:** To determine if the amphotericin B released from the single and dual loaded sponges maintained activity against a common fungi, a microbial zone of inhibition assay was conducted. The amphotericin B eluates were lyophilized for one day, reconstituted in 50 μ L of PBS, and used to inoculate blank discs. Standard amphotericin B concentrations, ranging from 0 to 2.5 μ g in 0.25 μ g increments, were also used to inoculate blank discs. A 0.5 McFarland standard of *Candida albicans* was prepared in sterile PBS and used to streak a Mueller-Hinton agar plate in three different directions. An inoculated disc was added to each plate and plates were incubated overnight at 37°C. The zone of inhibition was measured for each amphotericin B standard and a standard curve was generated. Zone of inhibition of amphotericin B

eluate samples were also measured and compared to the standard curve to determine sample concentration.

***In Vitro* Antibiotic Activity:** To determine if the vancomycin released from the single and dual loaded sponges maintained activity against bacteria, a bacterial turbidity assay was conducted following The Clinical and Laboratory Standards Institute standard M7-A4, “Methods for Dilution Antimicrobial Susceptibility for Bacteria that Grow Aerobically”.³⁴ Dilutions (1:10) of vancomycin eluates from single and dual loaded sponges were tested against *S. aureus* (UAMS-1). Vancomycin eluate samples were added in 200 μ L increments to 1.75 mL of sterile trypticase soy broth (TSB) and 50 μ L of *S. aureus* inoculum with approximately 2×10^6 colony forming units (CFU). Sterile 1x PBS was also used as a positive control. The inoculated elution samples were then mixed, incubated at 37°C overnight, mixed again and read via absorbance at 530 nm in a spectrophotometer.

***In Vitro* Cytocompatibility:** The *in vitro* cytocompatibility of the amphotericin B, vancomycin, and combination amphotericin B and vancomycin elution samples was tested on normal human dermal fibroblasts (NHDFs) purchased from Lonza (Walkersville, MD). Cells (passages 9 through 12) were seeded at 2.5×10^4 cells/ml in Dulbecco’s Modified Eagle’s Medium (DMEM) supplemented with 10% fetal bovine serum (FBS), penicillin (100 units/mL), streptomycin (100 mg/mL), and amphotericin B (0.25 μ g/ml) on 48 well polystyrene tissue culture plates (TCP) under standard cell culture conditions (37°C and 5% CO₂). Elution samples were pre-warmed and diluted 1:1 in fresh medium (n = 3), absent of additional antibiotics and antimycotics. After cells reached near confluence, the cell culture medium was aspirated from the plates and

refreshed with the medium and eluate dilution samples. Cells were incubated for one or three days before cytocompatibility was evaluated with the Cell Titer-Glo® Luminescent Cell Viability assay, obtained from Promega (Madison, WI). A standard dilution of known concentration of cells was also plated and assayed. The luminescent signal, which corresponded to the amount of adenosine triphosphate and the number of viable cells based on the standard curve, was recorded at 590 nm with a BioTek Synergy H1 plate reader. The number of viable cells was converted to cell viability percentage by normalization to the TCP controls in each respective plate.

***In Vivo* Mouse Study:** *In vivo* prevention of *S. aureus* biofilm growth by vancomycin loaded chitosan/PEG sponges was assessed in 20 NIH Swiss mice, following an established mouse model protocol.^{35,36} This *in vivo* study was approved by the institutional review board at the University of Arkansas for Medical Sciences (IACUC protocol #3461). Mice were anesthetized with isoflurane in an environmental chamber and anesthesia was confirmed by lack of toe pinch reflex. The mice were shaved and a 0.3 cm incision was made in the skin on each flank. A 1 cm section of polytetrafluoroethylene (PTFE) catheter was placed under the skin on each flank. At the same time, the chitosan/PEG 6000, chitosan/PEG 8000, or control chitosan sponges were loaded with either 4 mg/ml vancomycin or 1x PBS solutions (4 animals and 8 catheters per group) and were placed adjacent to the catheters. Incisions were closed with surgical glue and 1 cc of 10^4 CFUs of *S. aureus* (UAMS-1 strain) was injected into the lumen of the catheter. After 48 hours post-surgery, mice were sacrificed and catheters were surgically removed from each flank and placed in a sterile saline solution. The catheters were sonicated in PBS to remove adherent bacteria; the resulting bacteria aliquots were

then plated on tryptic soy agar and incubated at 37°C overnight in order to count the number of CFUs of *S. aureus* recovered from each catheter.

Statistical Analysis

All data, except for the percent clearance of bacteria from the mouse model, is presented as mean \pm standard deviation. One way ANOVA was used to analyze the swelling ratios of the sponges. Antifungal and antibiotic elution and antifungal activity was analyzed using three way Analysis of Variance (ANOVA) with Holm Sidak post hoc analysis. Eluate cytocompatibility data was analyzed with three way ANOVA with Holm Sidak post hoc analysis compared to the controls. Colony forming unit data from the *in vivo* mouse model was analyzed with the nonparametric Kruskal-Wallis one way ANOVA on ranks with Tukey post hoc analysis. Statistical significance level was set at $\alpha = 0.05$.

Results

Results from the swelling analysis of the blended chitosan/PEG and control chitosan sponges are provided in Table 1, along with critical details about each sponge formulation. As expected, the blended sponge with 1 lyophilization exhibited a significantly higher average swelling ratio than the chitosan sponge. The chitosan/PEG 6000 sponge with 2 lyophilizations also exhibited a higher swelling ratio than the chitosan sponge.

Table 1. Formulation variables and swelling ratios (n = 3) of blended chitosan/PEG and chitosan sponges, where * indicates p = 0.033 versus each other.

Sponge	PEG MW (g/mol)	Number of lyophilizations	NaOH concentration	Swelling Ratio
Chitosan/PEG 6000	6000	2	0.25 M	19.82 ± 5.72
Chitosan/PEG 8000	8000	1	N/A	23.21 ± 0.91*
Chitosan	N/A	2	0.6 M	12.94 ± 1.63*

The *in vitro* amphotericin B (the sodium deoxycholate form) release profiles of chitosan/PEG and chitosan sponges, loaded with amphotericin B alone or in combination with vancomycin, are shown in Figure 1. All sponges released amphotericin B, alone and in combination with the antibiotic, well above the amphotericin B minimum inhibitory concentration of *Candida albicans* over the 72 hour elution. The dual loaded sponges also released more amphotericin B than the single loaded sponges, especially after one hour of elution. Overall significant differences could be seen in the antifungal release between the chitosan/PEG 6000 single and dual loaded sponges (p = 0.003).

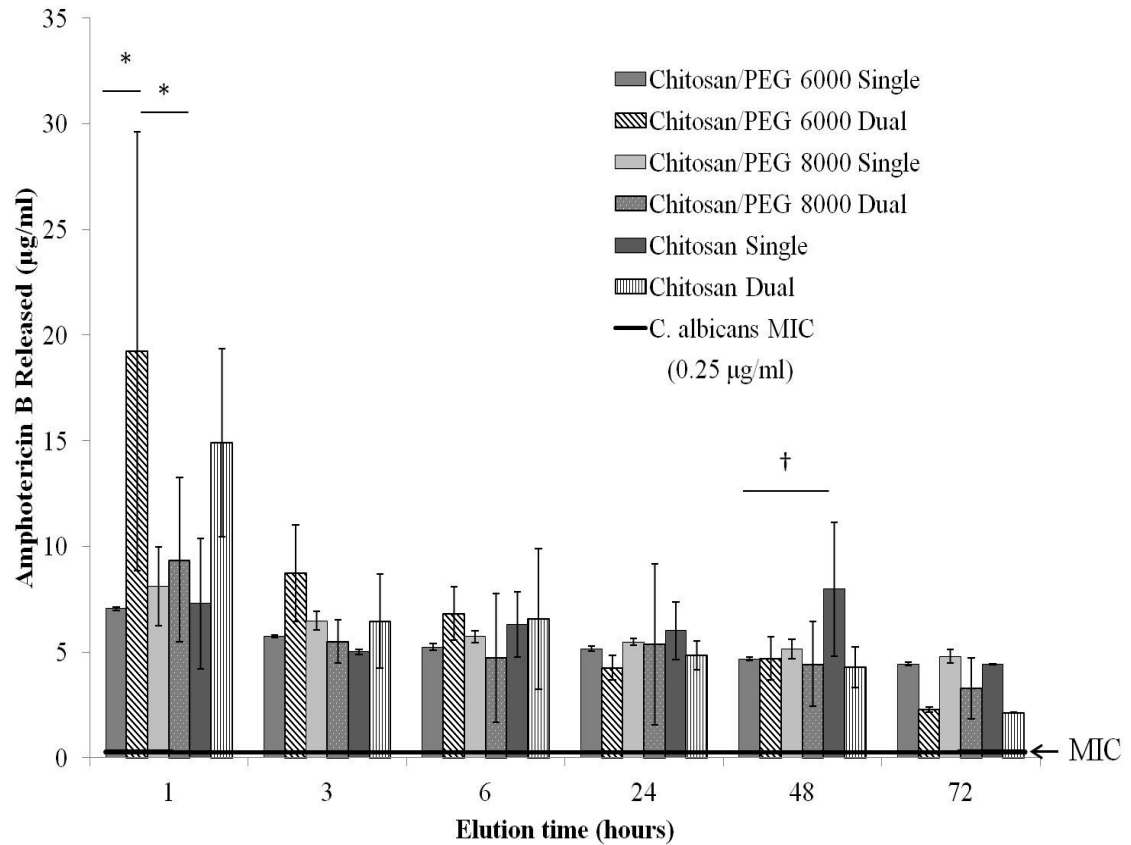


Figure 1. Sodium deoxycholate solubilized amphotericin B released *in vitro* in µg/ml (mean ± standard deviation) from single loaded and dual loaded (with vancomycin) sponges over time (n = 3), where * indicates p < 0.05 pairwise overall, and † represents p < 0.05 pairwise at the respective time point.

Unlike the antifungal elution, vancomycin release from single and dual loaded blended and chitosan sponges (Figure 2) decreased quickly after the initial burst release.

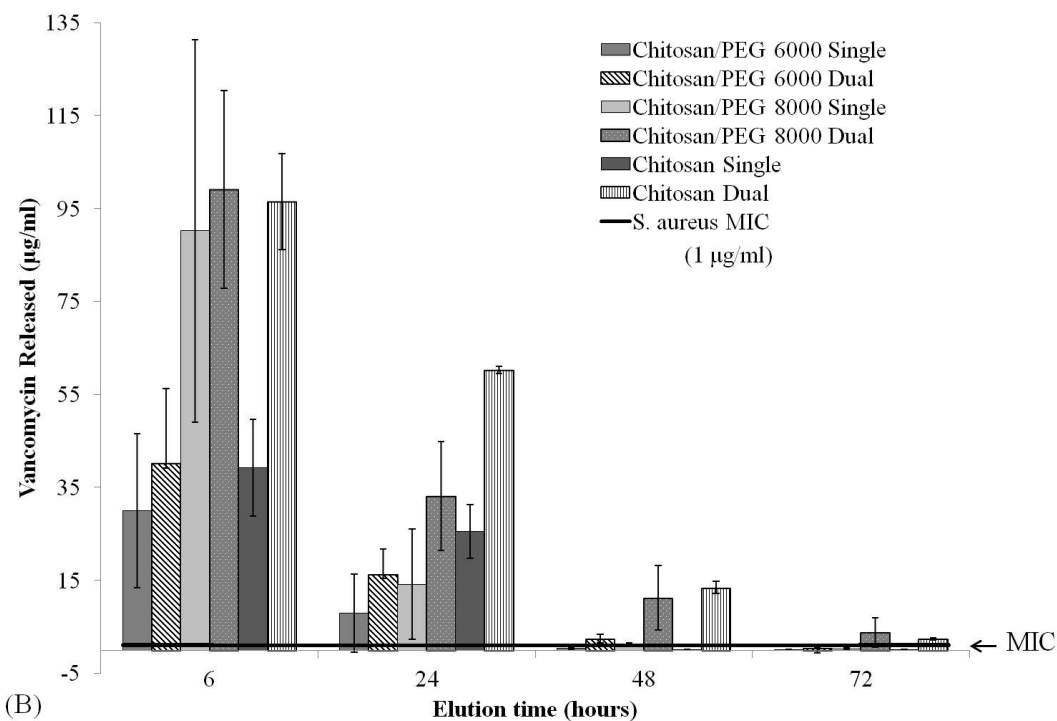
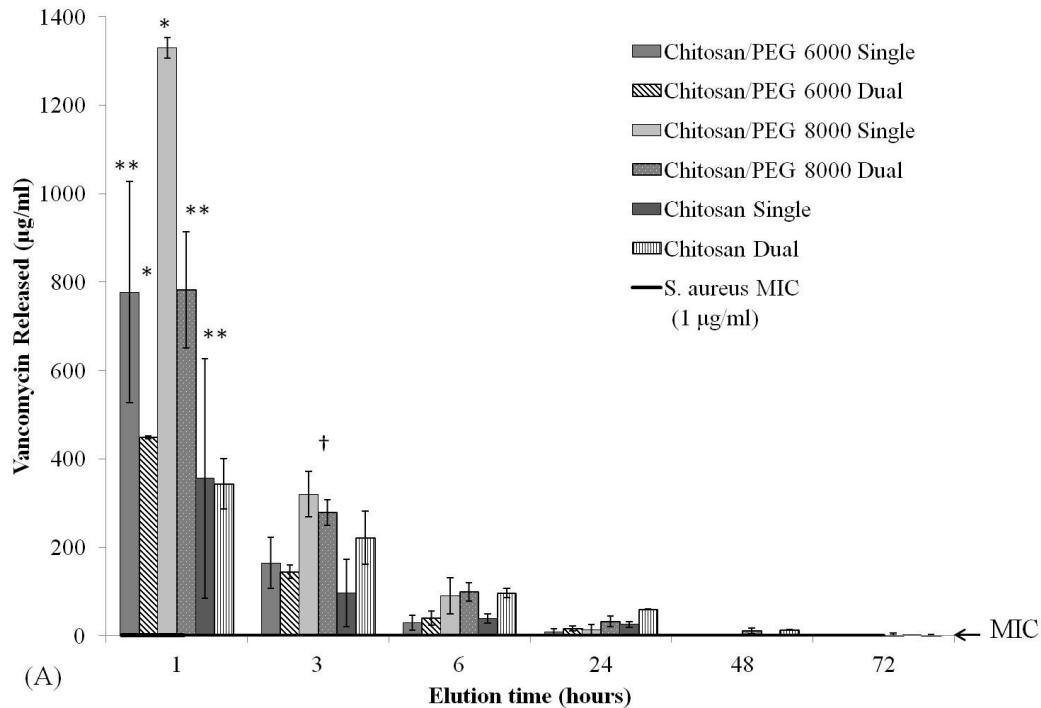


Figure 2. (A) Vancomycin released *in vitro* in $\mu\text{g/ml}$ (mean \pm standard deviation) from single loaded and dual loaded (with amphotericin B) sponges over time ($n = 3$), where at each respective time point, * indicates $p < 0.001$ versus other loading condition within sponge group, † represents $p < 0.05$ versus all other sponges, and ** denotes $p < 0.001$ versus all sponge types in loading condition, and (B) an inset graph of (A).

All sponges released vancomycin at levels above the *S. aureus* MIC through 24 hours, but only the dual loaded chitosan/PEG 8000 and chitosan sponges released vancomycin above the MIC through 72 hours of elution. The chitosan/PEG 8000 single loaded sponge also released significantly more vancomycin than the other dual loaded sponges after one hour of elution and than all other sponges after three hours. Additionally, the opposite behavior to the amphotericin B release appeared in the sponges' vancomycin release; instead of the dual loaded sponges releasing more antibiotic, the single loaded sponges release more vancomycin than the dual loaded.

Antifungal activity zone of inhibition assay results, reported as amphotericin B concentration in $\mu\text{g/ml}$, are shown in Figure 3. All selected amphotericin B eluates remained active against *C. albicans* at all time points. After three hours of elution, the same trend was found as in the antifungal elution data, where the dual loaded sponges released more active amphotericin B than the single loaded sponges. However, the chitosan/PEG 6000 dual loaded sponge did not exhibit higher average levels of active antifungal than the same single loaded sponge after one hour of elution ($p = 0.616$).

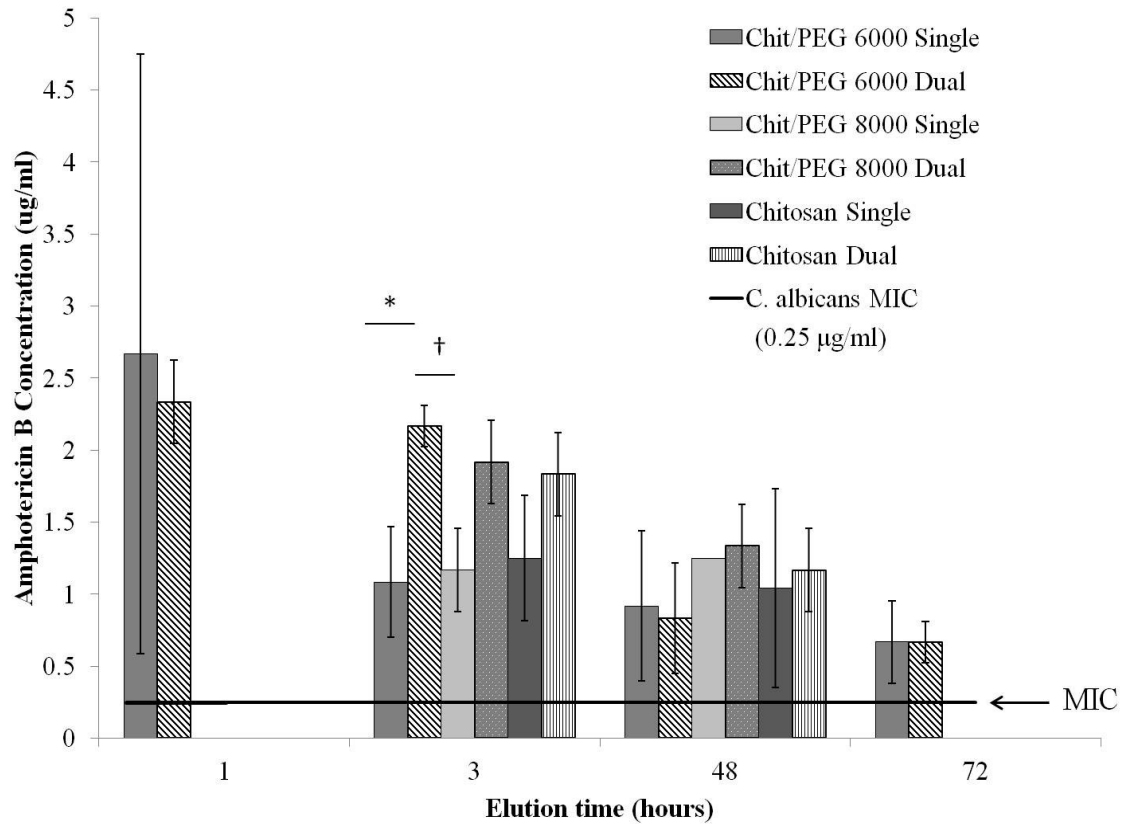


Figure 3. Results from antifungal activity zone of inhibition assay using selected amphotericin B eluted from chitosan/PEG and chitosan sponges, where * indicates $p = 0.001$ and † represents $p = 0.002$ pairwise.

The activity of vancomycin released from single and dual loaded chitosan/PEG and chitosan sponges against *Staphylococcus aureus* is reported in Table 2. All sponges released vancomycin active against the bacteria over six hours of elution, and the dual loaded chitosan sponges still inhibited bacterial growth through 24 hours. As previously reported in Figure 2, the dual loaded chitosan sponges released more amphotericin B at 24 hours of elution than the other sponge groups.

Table 2. Activity of 1:10 dilutions of vancomycin released (both single loaded and dual loaded with amphotericin B) from blended chitosan/PEG and control chitosan sponges against *S. aureus*

Loading	Sponge	Hours of Elution					
		1	3	6	24	48	72
Single	Chitosan/PEG 6000 2 lyo	-	-	-	+	+	+
Single	Chitosan/PEG 8000 1 lyo	-	-	-	+	+	+
Single	1% Chitosan	-	-	-	+	+	+
Dual	Chitosan/PEG 6000 2 lyo	-	-	-	+	+	+
Dual	Chitosan/PEG 8000 1 lyo	-	-	-	+	+	+
Dual	1% Chitosan	-	-	-	-	+	+

- and + indicate no bacterial growth or the growth of bacteria, respectively (n = 3)

As seen in Figures 4A-C, the one hour amphotericin B elution samples from single loaded chitosan/PEG sponges caused significant decreases in cytocompatibility from the control tissue culture plastic plate after one and three days of treatment. However, these same sponge eluate samples exhibited a rebound effect on the viability after one hour or three hours of elution for chitosan/PEG 6000 and 8000 sponges, respectively. An increase in cell viability occurred from one to three days of treatment for most time points, except for the one and 72 hour time points for all sponges.

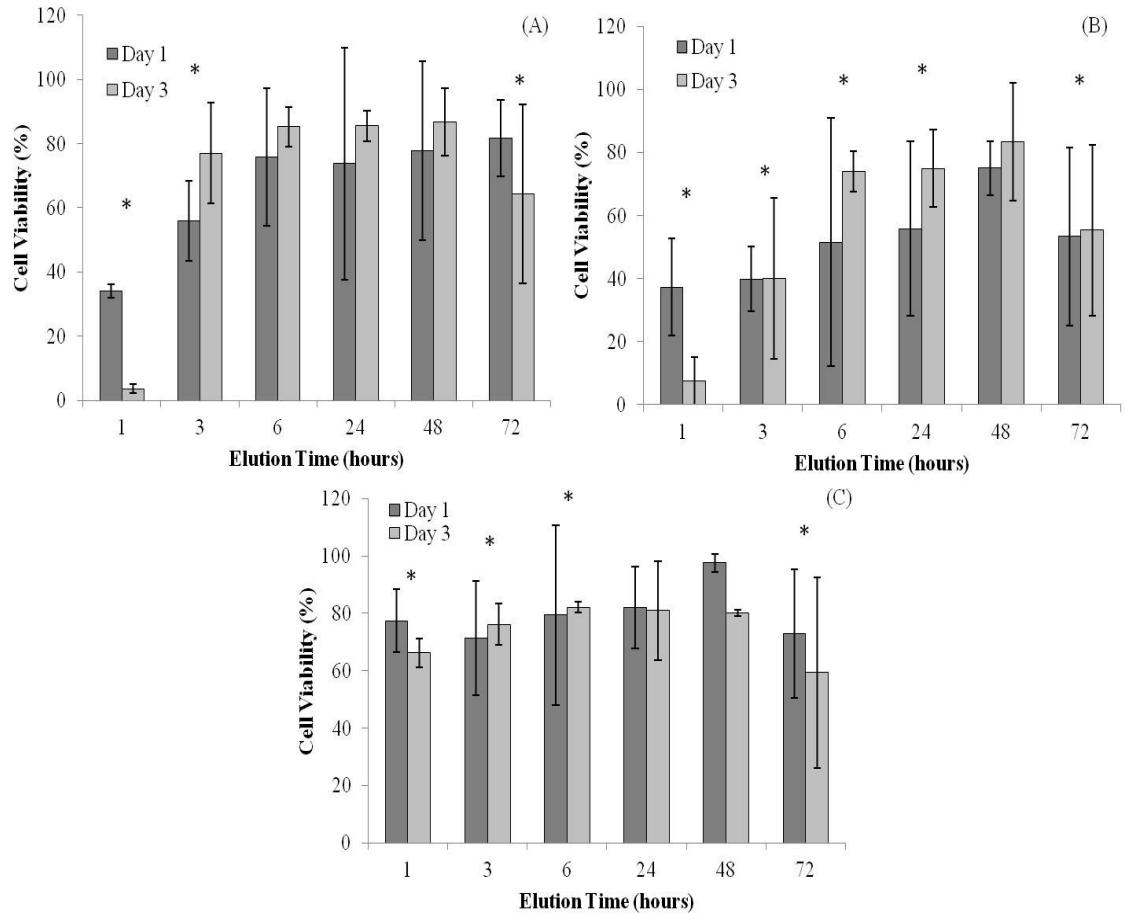


Figure 4. Cytocompatibility (mean \pm standard deviation) of single loaded amphotericin B eluates ($n = 3$) from the (A) chitosan/PEG 6000 sponge, (B) chitosan/PEG 8000 sponge, and (C) control chitosan sponge, to normal human dermal fibroblasts after one and three days. Cells were analyzed using Cell Titer-Glo[®] luminescent assay and resulting cell numbers were converted to percent cell viability by normalization to tissue culture plastic (TCP) controls. (* indicates $p < 0.05$ versus TCP controls)

As expected, vancomycin eluted from single loaded chitosan/PEG and chitosan sponges exhibited higher cell viability than the released amphotericin B (Figures 5A-C). However, while none of the elution samples exhibited significantly lower cell viability than the TCP controls after one day of treatment, all elution samples for each sponge group exhibited lower cell viability than the controls after three days of treatment.

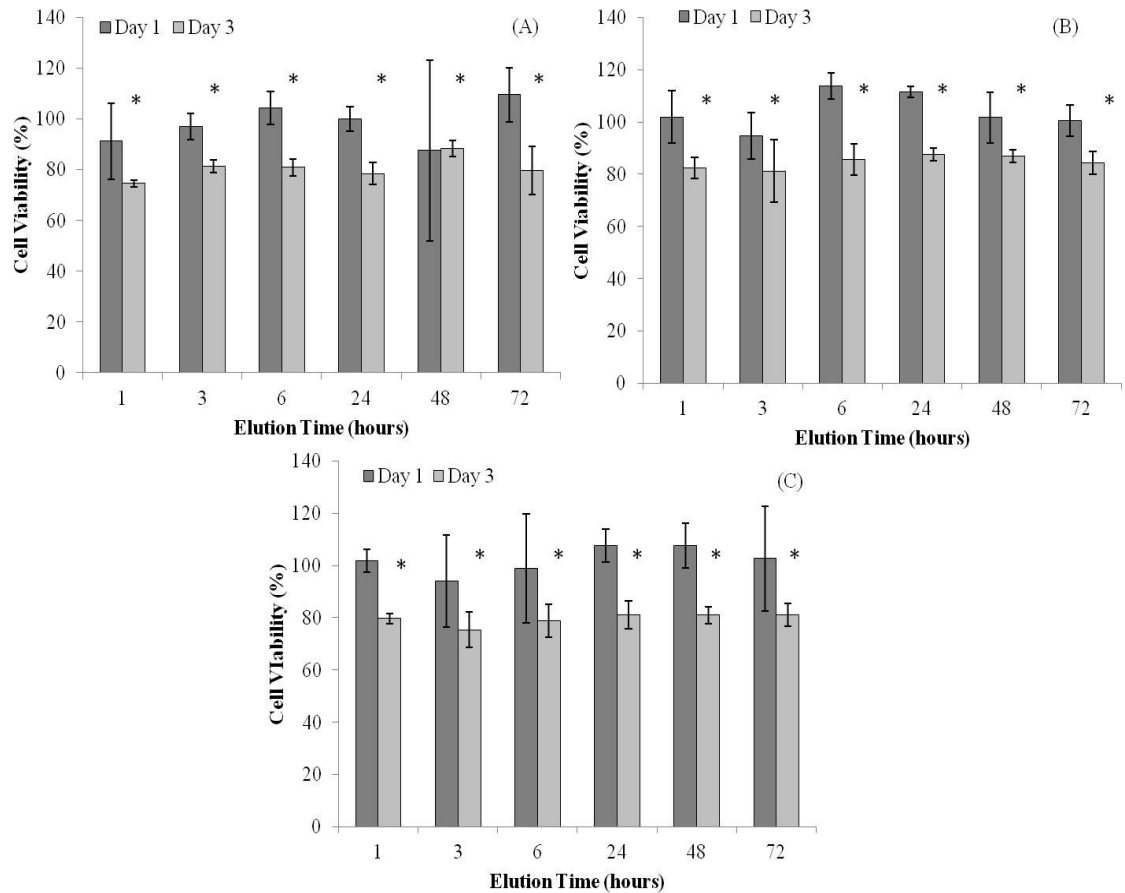


Figure 5. Cytocompatibility (mean \pm standard deviation) of single loaded vancomycin eluates ($n = 3$) from the (A) chitosan/PEG 6000 sponge, (B) chitosan/PEG 8000 sponge, and (C) control chitosan sponge, to normal human dermal fibroblasts after one and three days. Cells was analyzed using Cell Titer-Glo® luminescent assay and resulting cell numbers were converted to percent cell viability by normalization to tissue culture plastic (TCP) controls. (* indicates $p < 0.05$ versus TCP controls)

Combination vancomycin and amphotericin B eluted from all dual loaded sponge types caused high decreases in cell viability after one day of treatment (Figures 6A-C), but no statistical difference was found over time for the elution time points ($p = 0.279$). However, these same eluates exhibited higher cell viability after three days of treatment from six to 72 hours of elution from their respective one treatment day numbers. The one

and three hour elution samples from the chitosan/PEG 6000, 8000, and chitosan sponges exhibited significantly lower cell viability than the controls, and the 72 hour elution sample from chitosan/PEG 8000 sponge also cause a significant decrease in cell viability ($p < 0.001$).

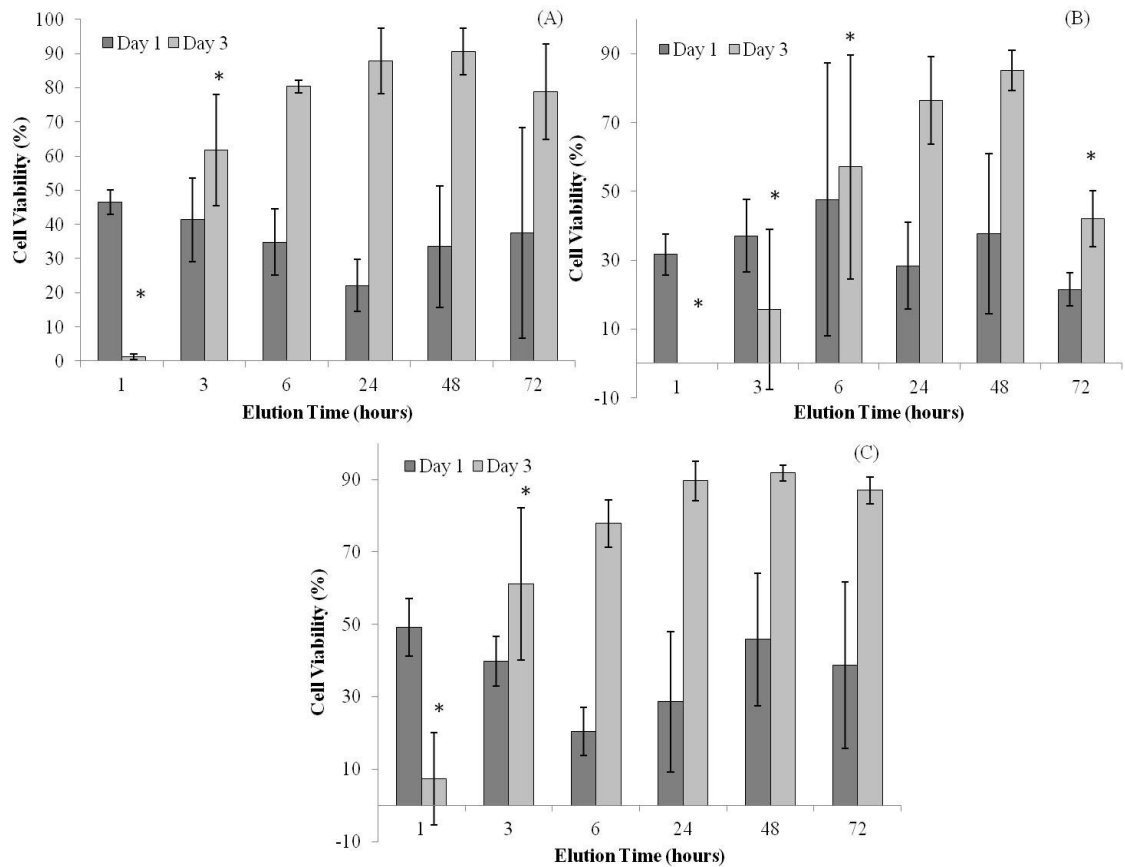


Figure 6. Cytocompatibility (mean \pm standard deviation) of dual loaded vancomycin and amphotericin B eluates ($n = 3$) from the (A) chitosan/PEG 6000 sponge, (B) chitosan/PEG 8000 sponge, and (C) control chitosan sponge, to normal human dermal fibroblasts after one and three days. Cells was analyzed using Cell Titer-Glo[®] luminescent assay and resulting cell numbers were converted to percent cell viability by normalization to tissue culture plastic (TCP) controls. (* indicates $p < 0.05$ versus TCP controls)

Results from the *in vivo* *S. aureus* biofilm prevention mouse model are provided in Figures 7A and B. As seen in Figure 7A, the vancomycin loaded chitosan/PEG 6000 sponge resulted in 100% bacteria clearance from the catheters. Six of the eight catheters used with the vancomycin loaded chitosan/PEG 8000 sponges were cleared, while only 50% of the catheters treated with the vancomycin loaded chitosan sponges were cleared. Additionally, as revealed by Figure 7B, the average colony forming units on the colonized catheters from the vancomycin loaded chitosan/PEG 8000 and chitosan sponge treatments were significantly lower than the CFUs from the PBS loaded chitosan/PEG 8000 sponge treatment ($p = 0.038$ and $p = 0.032$).

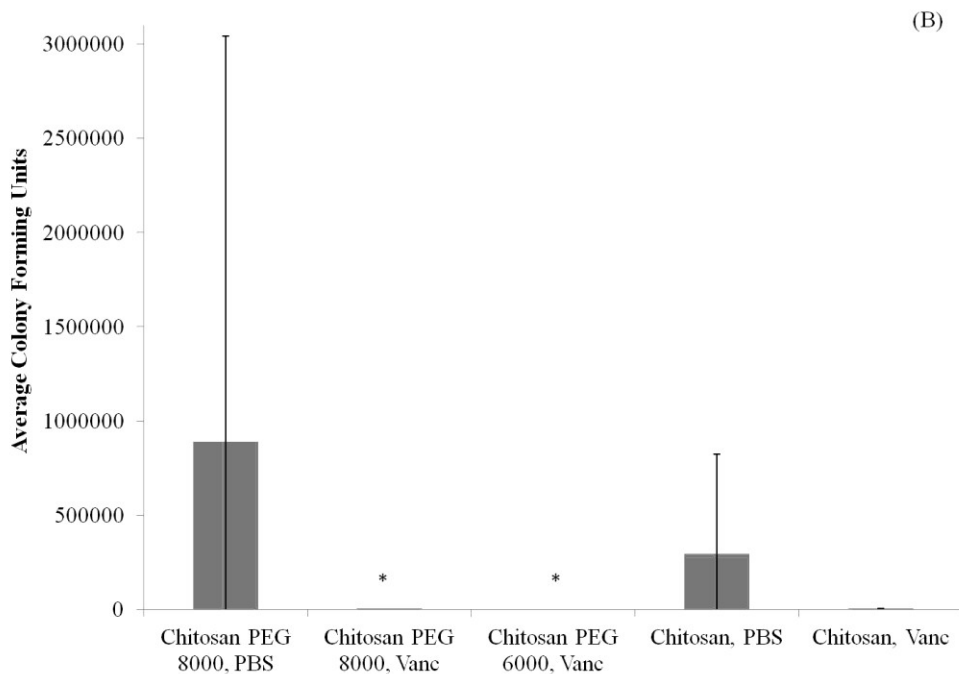
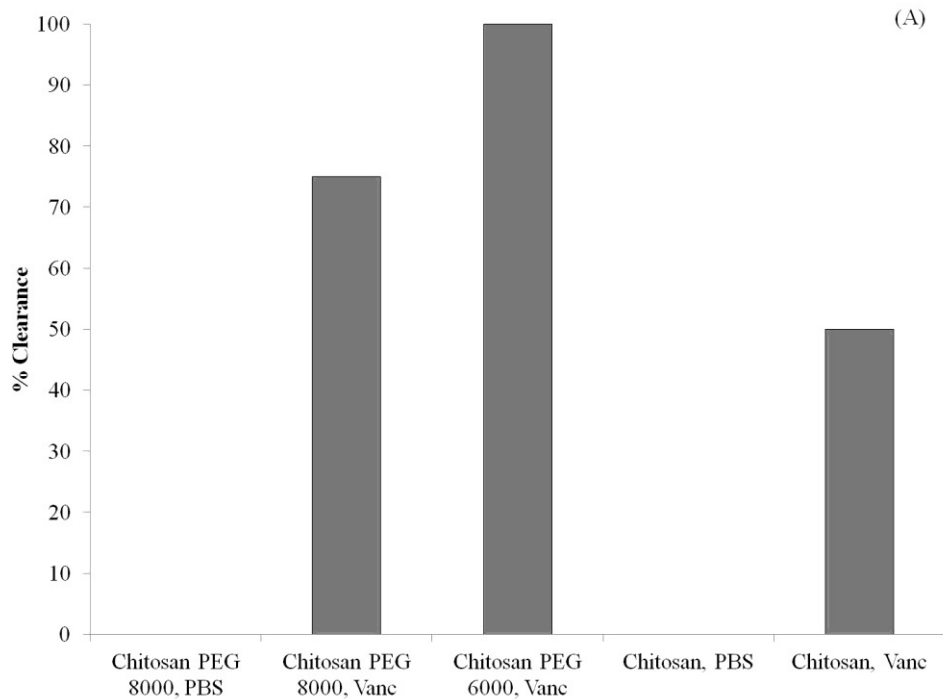


Figure 8. (A) Percentage of catheters cleared of *S. aureus* and (B) the average colony forming units (CFUs) per catheter for catheters retrieved from mice treated with chitosan/PEG 6000, chitosan/PEG 8000, and chitosan sponges (four animals and eight catheters). Sponges were loaded with either PBS or 4 mg/ml of vancomycin (Vanc) * indicates $p < 0.05$ versus PBS loaded sponges.

Discussion

Polymicrobial musculoskeletal infections, especially from invasive bacteria, fungi or biofilm pathogens, are challenging complications that often increase patient morbidity, mortality, and hospitalization costs.³⁷ The clinical need for degradable local antimicrobial delivery systems to fight localized bacteria, fungi, and/or biofilms with patient tailored antimicrobial point of care loading has resulted in the previous development of a chitosan sponge local delivery system.^{11,20,21} Our research was designed to determine if the blending of these chitosan sponges with polyethylene glycol would result in local drug delivery systems capable of antifungal and antibiotic release for the prevention of polymicrobial wound infections.

After previous sponge formulation and material characterization, the selected chitosan/PEG sponges were evaluated for their swelling, *in vitro* amphotericin B and vancomycin release, both alone and in combination, as well as activity and cytocompatibility of the resulting antimicrobial eluates.³⁸ The chitosan/PEG 6000 sponge formulations exhibited higher *in vitro* amphotericin B release when loaded with vancomycin, while the chitosan/PEG 8000 sponge exhibited the highest swelling and released more vancomycin *in vitro*, both alone and in combination with the antifungal. Antibiotic eluates from the blended sponges did not exhibit differences in activity against *S. aureus* and all the amphotericin B elution samples tested remained active against *C. albicans*. Antifungal eluates from blended sponges, both alone and in combination with vancomycin, caused significant decreases in cell viability after one and three hours of elution, compared to controls. However, cells recovered as the time of amphotericin B

elution increased, when the amphotericin B concentrations were reduced in the samples. Interestingly, vancomycin elution from the blended chitosan sponges exhibited opposite behavior *in vivo* to *in vitro* vancomycin release. In the mice, the vancomycin loaded chitosan/PEG 6000 sponge cleared 25% and 50% more of the bacteria from the catheters than the vancomycin loaded chitosan/PEG 8000 and chitosan sponge, respectively.

Comparing the blended chitosan/PEG sponges to the sparse previous literature on local antifungal delivery, there are some similarities and differences to published research on local antifungal delivery systems.^{12,13,17,39} While the blended sponges in this study still retained amphotericin B, both the chitosan/PEG 6000 and 8000 sponges released more antifungal *in vitro* in comparison to previously reports for amphotericin B loaded PMMA bone cement. Kweon et al.¹³ and Goss et al.¹² have reported bone cement to release 0.45 and 0.05%, with and without a poragen, or 0.03% of loaded amphotericin B, respectively. However, the chitosan/PEG sponges released less antifungal than the 60% cumulative amphotericin B released after two days from a preloaded Pluronic® based copolymer gel.¹⁷ Additionally, the amphotericin B eluates from the sponges in this study are similar to the reported active amphotericin B eluted from PMMA bone cement.³⁹ While antifungal released from the blended sponges reduced cell viability after one hour of elution, previous research has confirmed amphotericin B's negative effects on cells, when exposed to high concentrations.⁴⁰ Harmsen and researchers have studied amphotericin B at typical locally delivered concentrations and found amphotericin B at 100 µg/ml caused fibroblast death after 5 hours, while 5 and 10 µg/ml caused abnormal cell morphology and reduced proliferation after 7 days and 5 hours and 7 days, respectively.⁴⁰

The *in vitro* local vancomycin release from the blended sponges can also be compared to previous studies on antibiotic loaded chitosan sponges.^{20,21,41} Vancomycin release after one hour of elution, from single or dual loaded sponges, was 23-52% and 12-59% higher from the chitosan/PEG sponges than previously studied vancomycin loaded crosslinked chitosan sponges.⁴¹ However, unlike the blended sponges, these previously studied crosslinked sponges released vancomycin at levels above the *S. aureus* MIC throughout the entire 72 hours of elution.⁴¹ The chitosan/PEG 8000 sponge, loaded with vancomycin only, initially released more vancomycin *in vitro* than previously reported for chitosan sponges made with lactic and acetic acid and loaded with 5 mg/ml vancomycin; however, the blended sponge did not release high enough levels of vancomycin throughout the entire elution study to inhibit *S. aureus* growth as long as described in the previous study.²⁰

Limitations of this study include the challenging *in vitro* measurement of amphotericin B concentration when released simultaneously with vancomycin and the lack of direct comparison in the antifungal and antibiotic activity assays due to the different dilutions utilized in the studies. However, this study is one of the few published studies on the simultaneous *in vitro* loading and release of amphotericin B and a representative antibiotic, vancomycin. Additionally, the small number of animals and antibiotic concentrations studied in the pilot *in vivo* study should be increased in future animal studies. However, the initial results of the preliminary *in vivo* model provide a sufficient trend of the *in vivo* behavior of the blended chitosan sponges to prevent biofilm formation. Although additional work is needed to evaluate *in vivo* release of amphotericin B, the blended chitosan and polyethylene glycol sponges may provide a way to locally

deliver clinician selected antifungals and/or antibiotics for use as an adjunctive therapy for the prevention of polymicrobial musculoskeletal wound infections.

References

1. Andersson GBJ, Bouchard J, Bozic KJ, et al. 2008. Musculoskeletal Injuries. In: *The Burden of Musculoskeletal Diseases in the United States*. Rosemont, IL: American Academy of Orthopaedic Surgeons; p 123-162.
2. Davis JS. 2005. Management of bone and joint infections due to *Staphylococcus aureus*. *Intern Med J* 35:S79-S96.
3. Brady RA, Leid JG, Calhoun JH, Costerton JW, Shirtliff ME. 2008. Osteomyelitis and the role of biofilms in chronic infection. *FEMS Immunol Med Microbiol* 52:13-22.
4. Murray CK, Obremskey WT, Hsu JR, Andersen RC, Calhoun JH, Clasper JC, Whitman TJ, Curry TK, Fleming ME, Wenke JC, et al. 2011. Prevention of Infections Associated with Combat-Related Extremity Injuries. *The Journal of Trauma Injury, Infection and Critical Care* 71:S235-S257.
5. Tribble D. 2011. Trauma Infectious Disease Outcomes Study (TIDOS) Invasive Fungal Infection (IFI) Case Investigation.
6. CDC and Fungal Diseases Fact Sheet. 2011. In: *Prevention CfDCA*, editor.
7. Costerton JW, Lewandowski Z, Caldwell DE, Korber DR, Lappin-Scott HM. 1995. Microbial biofilms. *Annu Rev Microbiol* 49:711-745.
8. Costerton JW, Stewart PS, Greenberg EP. 1999. Bacterial biofilms: a common cause of persistent infections. *Science* 284:1318-1322.
9. Diefenbeck M, Muckley T, Hofmann GO. 2006. Prophylaxis and treatment of implant-related infections by local application of antibiotics. *Injury* 37:S95-S104.
10. Bertesteanu S, Triaridis S, Stankovic M, Lazar V, Chifiriuc MC, Vlad M, Grigore R. 2014. Polymicrobial wound infections: Pathophysiology and current therapeutic approaches. *Int J Pharm* 463:119-126.
11. Hanssen AD. 2005. Local antibiotic delivery vehicles in the treatment of musculoskeletal infection. *Clin Orthop Relat Res* 437:91-96.
12. Goss B, Lutton C, Weinrauch P, Jabur M, Gillett G, Crawford R. 2007. Elution and mechanical properties of antifungal bone cement. *J Arthroplasty* 22:902-908.

13. Kweon C, McLaren AC, Leon C, McLemore R. 2011. Amphotericin B delivery from bone cement increases with porosity but strength decreases. *Clin Orthop Relat Res* 469:3002-3007.
14. Marra F, Robbins GM, Masri BA, Duncan C, Wasan KM, Kwong EH, Jewesson PJ. 2001. Amphotericin B-loaded bone cement to treat osteomyelitis caused by *Candida albicans*. *Can J Surg* 44:383-386.
15. Hudson SP, Langer R, Fink GR, Kohane DS. 2010. Injectable in situ cross-linking hydrogels for local antifungal therapy. *Biomaterials* 31:1444-1452.
16. Zumbuehl A, Ferreira L, Kuhn D, Astashkina A, Long L, Yeo Y, Iaconis T, Ghannoum M, Fink GR, Langer R, et al. 2007. Antifungal hydrogels. *Proc Natl Acad Sci U S A* 104:12994-12998.
17. Kim YT, Shin BK, Garripelli VK, Kim JK, Davaa E, Jo S, Park JS. 2010. A thermosensitive vaginal gel formulation with HPgammaCD for the pH-dependent release and solubilization of amphotericin B. *Eur J Pharm Sci* 41:399-406.
18. Krisanapiboon A, Buranapanitkit B, Oungbho K. 2006. Biocompatibility of hydroxyapatite composite as a local drug delivery system. *J Orthop Surg (Hong Kong)* 14:315-318.
19. Buranapanitkit B, Oungbho K, Ingviya N. 2005. The efficacy of hydroxyapatite composite impregnated with amphotericin B. *Clin Orthop Relat Res* 437:236-241.
20. Noel SP, Courtney HS, Bumgardner JD, Haggard WO. 2010. Chitosan sponges to locally deliver amikacin and vancomycin: a pilot in vitro evaluation. *Clin Orthop Relat Res* 468:2074-2080.
21. Stinner D, Noel S, Haggard W, Watson J, Wenke J. 2010. Local antibiotic delivery using tailorable chitosan sponges: the future of infection control? *J Orthop Trauma* 24:592-597.
22. Jennings JA, Courtney HS, Haggard WO. 2012. Cis-2-decenoic acid inhibits *S. aureus* growth and biofilm in vitro: a pilot study. *Clin Orthop Relat Res* 470:2663-2670.
23. Zhang M, Li XH, Gong YD, Zhao NM, Zhang XF. 2002. Properties and biocompatibility of chitosan films modified by blending with PEG. *Biomaterials* 23:2641-2648.
24. Moribe K, Maruyama K, Iwatsuru M. 1999. Molecular localization and state of amphotericin B in PEG liposomes. *Int J Pharm* 193:97-106.
25. Moribe K, Maruyama K. 2002. Pharmaceutical design of the liposomal antimicrobial agents for infectious disease. *Curr Pharm Des* 8:441-454.

26. Darole PS, Hegde DD, Nair HA. 2008. Formulation and evaluation of microemulsion based delivery system for amphotericin B. *AAPS PharmSciTech* 9:122-128.
27. Tiyaboonchai W, Limpeanchob N. 2007. Formulation and characterization of amphotericin B-chitosan-dextran sulfate nanoparticles. *International Journal of Pharmaceutics* 329:142-149.
28. Wang Q, Zhang N, Hu X, Yang J, Du Y. 2008. Chitosan/polyethylene glycol blend fibers and their properties for drug controlled release. *Journal of Biomedical Materials Research Part A* 85:881-887.
29. Kolhe P, Kannan RM. 2003. Improvement in ductility of chitosan through blending and copolymerization with PEG: FTIR investigation of molecular interactions. *Biomacromolecules* 4:173-180.
30. Zhao L, Zhu L, Liu F, Liu C, Shan D, Wang Q, Zhang C, Li J, Liu J, Qu X, et al. 2011. pH triggered injectable amphiphilic hydrogel containing doxorubicin and paclitaxel. *Int J Pharm* 410:83-91.
31. Egger P, Bellmann R, Wiedermann CJ. 2001. Determination of amphotericin B, liposomal amphotericin B, and amphotericin B colloidal dispersion in plasma by high-performance liquid chromatography. *J Chromatogr B Biomed Sci Appl* 760:307-313.
32. Smith JK, Moshref AR, Jennings JA, Courtney HS, Haggard WO. 2013. Chitosan sponges for local synergistic infection therapy: a pilot study. *Clin Orthop Relat Res* 471:3158-3164.
33. Technical Support X-Gen Pharmaceuticals. 2014. Personal Communication.
34. Institute CaLS. 2009. *Methods for Dilution Antimicrobial Susceptibility for Bacteria that Grow Aerobically- Eight Edition*. Wayne, Pennsylvania: Clinical and Laboratory Standards Institute.
35. Beenken KE, Dunman PM, McAleese F, Macapagal D, Murphy E, Projan SJ, Blevins JS, Smeltzer MS. 2004. Global gene expression in *Staphylococcus aureus* biofilms. *J Bacteriol* 186:4665-4684.
36. Weiss EC, Zielinska A, Beenken KE, Spencer HJ, Daily SJ, Smeltzer MS. 2009. Impact of sarA on daptomycin susceptibility of *Staphylococcus aureus* biofilms in vivo. *Antimicrob Agents Chemother* 53:4096-4102.
37. Murray C, Hsu J, Solomkin J, Keeling J, Andersen R, Ficke J, Calhoun J. 2008. Prevention and management of infections associated with combat-related extremity injuries. *J Trauma* 64:S239-S251.

38. Parker AC, Rhodes C, Jennings JA, Hittle L, Shirtliff ME, Bumgardner J, Haggard W. 2014. Preliminary evaluation of chitosan and polyethylene glycol blended sponges for the in vitro local delivery of amphotericin B and in vivo degradation in a rat intramuscular model. To Be Submitted to JBMRB.
39. Cunningham B, McLaren AC, Pauken C, McLemore R. 2012. Liposomal formulation increases local delivery of amphotericin from bone cement: a pilot study. *Clin Orthop Relat Res* 470:2671-2676.
40. Harmsen S, McLaren AC, Pauken C, McLemore R. 2011. Amphotericin B is cytotoxic at locally delivered concentrations. *Clin Orthop Relat Res* 469:3016-3021.
41. Parker AC, Jennings JA, Bumgardner JD, Courtney HS, Lindner E, Haggard WO. 2013. Preliminary investigation of crosslinked chitosan sponges for tailorable drug delivery and infection control. *J Biomed Mater Res B Appl Biomater* 101:110-123.

CHAPTER 5

CONCLUSIONS

The results presented in this dissertation indicate that the chitosan sponge can be modified, either through buffering with sodium acetate or blending with polyethylene glycol (PEG), to create local drug delivery systems with different *in vitro* material properties and *in vivo* functionality for wound infection prevention. Chapter 2 demonstrated the capability to modify the properties of the chitosan sponge through a buffering procedure to increase degradation and still remain biocompatible. Additionally, the results indicate that one can adapt the characteristics of the sponge based on the intended application, for example, a short or long length of degradation.

The polyethylene glycol and chitosan blended sponges developed in Chapters 3 and 4 also confirmed chitosan's modification potential, but through blending with an additional polymer instead of a buffer. By adding PEG to the chitosan sponges, an increase in *in vitro* water insoluble amphotericin B release was seen, as well as increased activity of the antifungal eluates compared to the control unmodified chitosan sponges. Similar to the buffered sponges from Chapter 2, the chitosan/PEG sponges also exhibited increased *in vitro* degradation from the original chitosan sponges and remained cytocompatible (Chapter 3). Specifically, the chitosan/PEG 8000 1 lyo sponge demonstrated increased *in vitro* degradation from both buffered sponges, and the chitosan/PEG 6000 1 lyo sponge exhibited increased degradation from the pH 5.6 buffered sponge. Modifying the chitosan sponge with PEG also resulted in similar cell viability results to the buffered chitosan sponges. In the *in vivo* intramuscular rat model, the chitosan/PEG blended sponges revealed higher percentage of implant area in the

defect area than the buffered sponges. However, the PEG modified sponges exhibited less fibrous tissue overall and a decreased average graded inflammatory response after ten days of implantation than the buffered chitosan sponges. Both the buffered and PEG modified chitosan sponges exhibited reduced *in vivo* degradation compared to their *in vitro* degradation analyses.

Chapter 4 described an *in vitro* and *in vivo* evaluation of the functionality of the chitosan/PEG sponges for local antifungal and antibiotic release and infection prevention. The chitosan/PEG sponges with a PEG molecular weight of 6,000 g/mol and two lyophilizations exhibited a slight increase in *in vitro* water soluble amphotericin B release (single loaded) after one hour of elution, but the chitosan/PEG 8000 sponge with one lyophilization demonstrated increased *in vitro* vancomycin elution from either single or dual loaded sponges, compared to the other sponge groups. However, the opposite behavior was seen in the pilot *in vivo* *Staphylococcus aureus* biofilm infection prevention mouse model, where the vancomycin loaded chitosan/PEG 6000 and 8000 sponges cleared 100% and 75% of the bacteria from the implanted catheters, respectively. Both antibiotic loaded PEG modified sponges exhibited improvements in biofilm prevention over the control unmodified chitosan sponges, loaded with vancomycin or PBS. These *in vitro* and *in vivo* results indicate the potential use of the antifungal and/or antibiotic loaded chitosan/PEG sponge local delivery system for use as an adjunctive therapy to prevent bacterial and fungal wound infections. However, as recommended in Chapter 6, additional research is needed to confirm *in vivo* chitosan/PEG sponge functionality for prevention of fungal infections.

In conclusion, these results provide strong support of the stated hypothesis: that modified chitosan sponges, with a buffer or polyethylene glycol, will function as degradable local antimicrobial delivery systems for use as an adjunctive therapy to prevent infection establishment in musculoskeletal wounds. The PEG modified chitosan sponges were specifically shown to function as a local delivery system for both hydrophilic antibiotics and hydrophobic antifungals, loaded alone or in combination. While additional work is needed to confirm the *in vivo* degradation of both types of modified sponges, the significant *in vitro* degradation indicates the potential for eventual degradation. With additional research, both of these modified chitosan sponges could meet the clinical need of reliable, low-cost polymicrobial infection prevention that can be used as an adjunctive topical therapy to surgical debridement and irrigation and systemic antibiotic regimens.

CHAPTER 6

RECOMMENDATIONS FOR FUTURE WORK

Additional research evaluations should be conducted on the chitosan/PEG sponge in order to develop a more thorough understanding of the sponge's properties and its functionality for local antifungal delivery and infection prevention. More *in vitro* elution studies and activity research with other antifungals, such as voriconazole, or other hydrophobic compounds could extend the possible applications of the modified chitosan sponge. The chitosan/PEG sponges should also be evaluated for *in vitro* antibiotic delivery with antibiotics other than vancomycin and tested against bacteria other than *Staphylococcus aureus*.

In order to increase degradation, PEG with a lower molecular weight could be blended with chitosan because previous research has shown a link between molecular weight and degradation.^{44,59} Additionally, an extended *in vivo* degradation study for both the PEG modified and buffered chitosan sponges would provide a more accurate length of time for complete degradation. In order to assess the *in vivo* functionality of the modified sponges for fungal infection prevention, it is also recommended that amphotericin B loaded chitosan/PEG sponges be evaluated in an *in vivo* fungal infection model. Finally, both the buffered and chitosan/PEG sponges should be studied in an *in vivo* large animal model, with traumatic musculoskeletal wounds more applicable to clinical cases.

REFERENCES

1. Andersson GBJ, Bouchard J, Bozic KJ. The Burden of Musculoskeletal Diseases in the United States. Rosemont, IL: American Academy of Orthopaedic Surgeons; 2008.
2. Murray CK, Obremskey WT, Hsu JR, Andersen RC, Calhoun JH, Clasper JC, Whitman TJ, Curry TK, Fleming ME, Wenke JC and others. Prevention of Infections Associated with Combat-Related Extremity Injuries. *The Journal of Trauma Injury, Infection and Critical Care* 2011;71(2):S235-257.
3. Boxma H, Broekhuizen T, Patka P, Oosting H. Randomised controlled trial of single-dose antibiotic prophylaxis in surgical treatment of closed fractures: the Dutch Trauma Trial. *Lancet* 1996;347(9009):1133-7.
4. Petersen K, Riddle MS, Danko JR, Blazes DL, Hayden R, Tasker SA, Dunne JR. Trauma-related infections in battlefield casualties from Iraq. *Ann Surg* 2007;245(5):803-11.
5. Arnold K, Cutting RT. Causes of death in United States Military personnel hospitalized in Vietnam. *Mil Med* 1978;143(3):161-4.
6. Davis JS. Management of bone and joint infections due to *Staphylococcus aureus*. *Intern Med J* 2005;35 Suppl 2:S79-96.
7. Brady RA, Leid JG, Calhoun JH, Costerton JW, Shirtliff ME. Osteomyelitis and the role of biofilms in chronic infection. *FEMS Immunol Med Microbiol* 2008;52(1):13-22.
8. Costerton JW, Lewandowski Z, Caldwell DE, Korber DR, Lappin-Scott HM. Microbial biofilms. *Annu Rev Microbiol* 1995;49:711-45.
9. Costerton JW, Stewart PS, Greenberg EP. Bacterial biofilms: a common cause of persistent infections. *Science* 1999;284(5418):1318-22.
10. Diefenbeck M, Muckley T, Hofmann GO. Prophylaxis and treatment of implant-related infections by local application of antibiotics. *Injury* 2006;37:S95-S104.
11. Nickel JC, Ruseska I, Wright JB, Costerton JW. Tobramycin resistance of *Pseudomonas aeruginosa* cells growing as a biofilm on urinary catheter material. *Antimicrob Agents Chemother* 1985;27(4):619-24.
12. Pfaller MA, Diekema DJ. Epidemiology of Invasive Candidiasis: a Persistent Public Health Problem. *Clinical Microbiology Reviews* 2007;20(1):133-163.
13. Horn F, Heinekamp T, Kniemeyer O, Pollm?cher J, Valiante V, Brakhage AA. Systems biology of fungal infection. *Frontiers in Microbiology* 2012;3.

14. Eardley WG, Brown KV, Bonner TJ, Green AD, Clasper JC. Infection in conflict wounded. *Philos Trans R Soc Lond B Biol Sci* 2011;366(1562):204-18.
15. Tribble D. Trauma Infectious Disease Outcomes Study (TIDOS) Invasive Fungal Infection (IFI) Case Investigation. 2011.
16. Neblett Fanfair R, Benedict K, Bos J, Bennett SD, Lo YC, Adebajo T, Etienne K, Deak E, Derado G, Shieh WJ and others. Necrotizing cutaneous mucormycosis after a tornado in Joplin, Missouri, in 2011. *N Engl J Med* 2012;367(23):2214-25.
17. 15 October News. *Clinical Infectious Diseases* 2011;53(8):i-ii.
18. Kim A, Nicolau DP, Kuti JL. Hospital costs and outcomes among intravenous antifungal therapies for patients with invasive aspergillosis in the United States. *Mycoses* 2011;54(5):e301-12.
19. Brissaud O, Guichoux J, Harambat J, Tandonnet O, Zaoutis T. Invasive fungal disease in PICU: epidemiology and risk factors. *Ann Intensive Care* 2012;2(1):6.
20. CDC and Fungal Diseases Fact Sheet. In: *Prevention CfDCa*, editor; 2011.
21. Park H, Copeland C, Henry S, Barbul A. Complex Wounds and Their Management. *Surg Clin North Am* 2010;90:1181-1194.
22. Hanssen AD. Local antibiotic delivery vehicles in the treatment of musculoskeletal infection. *Clin Orthop Relat Res* 2005(437):91-6.
23. Lazzarini L, Mader JT, Calhoun JH. Osteomyelitis in long bones. *J Bone Joint Surg Am* 2004;86-A:2305-2318.
24. Nandi SK, Mukherjee P, Roy S, Kundu B, De DK, Basu D. Local antibiotic delivery systems for the treatment of osteomyelitis- A review. *Materials Science and Engineering C* 2009;29:2478-2485.
25. Ostermann PA, Seligson D, Henry SL. Local Antibiotic Therapy for Severe Open Fractures. *J Bone Joint Surg* 1995;77-B:93-97.
26. Thomas DB, Brooks DE, Bice TG, DeJong ES, Lonergan KT, Wenke JC. Tobramycin-impregnated calcium sulfate prevents infection in contaminated wounds. *Clin Orthop Relat Res* 2005;441:366-71.
27. Jackson SR, Richelsoph KC, Courtney HS, Wenke JC, Branstetter JG, Bumgardner JD, Haggard WO. Preliminary In Vitro Evaluation of an Adjunctive Therapy for Extremity Wound Infection Reduction: Rapidly Resorbing Local Antibiotic Delivery. *Journal of Orthopaedic Research* 2008;7:903-908.
28. Borrelli JJ, Prickett W, Ricci W. Treatment of nonunions and osseous defects with bone graft and calcium sulfate. *Clin Orthop Relat Res* 2003(411):245-54.

29. Robinson D, Alk D, Sandbank J, Farber R, Halperin N. Inflammatory reactions associated with a calcium sulfate bone substitute. *Ann Transplant* 1999;4(3-4):91-7.
30. Swieringa AJ, Goosen JH, Jansman FG, Tulp NJ. In vivo pharmacokinetics of a gentamicin-loaded collagen sponge in acute periprosthetic infection: serum values in 19 patients. *Acta Orthop* 2008;79(5):637-42.
31. Kweon C, McLaren AC, Leon C, McLemore R. Amphotericin B delivery from bone cement increases with porosity but strength decreases. *Clin Orthop Relat Res* 2011;469(11):3002-7.
32. Krisanapiboon A, Buranapanitkit B, Oungbho K. Biocompatibility of hydroxyapatite composite as a local drug delivery system. *J Orthop Surg (Hong Kong)* 2006;14(3):315-8.
33. Kim YT, Shin BK, Garripelli VK, Kim JK, Davaa E, Jo S, Park JS. A thermosensitive vaginal gel formulation with HPgammaCD for the pH-dependent release and solubilization of amphotericin B. *Eur J Pharm Sci* 2010;41(2):399-406.
34. Hudson SP, Langer R, Fink GR, Kohane DS. Injectable in situ cross-linking hydrogels for local antifungal therapy. *Biomaterials* 2010;31(6):1444-52.
35. Zumbuehl A, Ferreira L, Kuhn D, Astashkina A, Long L, Yeo Y, Iaconis T, Ghannoum M, Fink GR, Langer R and others. Antifungal hydrogels. *Proc Natl Acad Sci U S A* 2007;104(32):12994-8.
36. Henriksen I, Green KL, Smart JD, Smistad G, Karlsen J. Bioadhesion of hydrated chitosans: An in vitro and in vivo study. *International Journal of Pharmaceutics* 1996;145(1-2):231-240.
37. Xu J, McCarthy SP, Gross RA, Kaplan DL. Chitosan film acylation and effects on biodegradability. *Macromolecules* 1996;29(10):3436-3440.
38. Khor E, Lim LY. Implantable applications of chitin and chitosan. *Biomaterials* 2003;24(13):2339-2349.
39. Nunthanid J, Laungtana-Anan A, Sriamornsak P, Limmatvapirat S, Puttipipatkachorn S, Lim LY, Khor E. Characterization of chitosan acetate as a binder for sustained release tablets. *Journal of Controlled Release* 2004;99(1):15-26.
40. Abdou ES, Nagy KSA, Elsabee MZ. Extraction and characterization of chitin and chitosan from local sources. *Bioresource Technology* 2008;99(5):1359-1367.
41. Nunthanid J, Puttipipatkachorn S, Yamamoto K, Peck G. Physical properties and molecular behavior of chitosan films. *Drug Dev Ind Pharm* 2001;27(2):143-57.

42. Bhattarai N, Gunn J, Zhang M. Chitosan-based hydrogels for controlled, localized drug delivery. *Advanced Drug Delivery Reviews* 2010;62(1):83-99.
43. Nair LS, Laurencin CT. Biodegradable polymers as biomaterials. *Progress in Polymer Science* 2007;32(8-9):762-798.
44. Tomihata K, Ikada Y. In vitro and in vivo degradation of films of chitin and its deacetylated derivatives. *Biomaterials* 1997;18(7):567-75.
45. Cardenas G, Anaya P, von Plessing C, Rojas C, Sepulveda J. Chitosan composite films. Biomedical applications. *J Mater Sci Mater Med* 2008;19(6):2397-405.
46. Noel S, Courtney H, Bumgardner J, Haggard W. Chitosan films: a potential local drug delivery system for antibiotics. *Clin Orthop Relat Res* 2008;466(6):1377-82.
47. Ma L, Gao C, Mao Z, Zhou J, Shen J, Hu X, Han C. Collagen/chitosan porous scaffolds with improved biostability for skin tissue engineering. *Biomaterials* 2003;24(26):4833-41.
48. Stinner D, Noel S, Haggard W, Watson J, Wenke J. Local antibiotic delivery using tailorable chitosan sponges: the future of infection control? *J Orthop Trauma* 2010;24(9):592-7.
49. Noel SP, Courtney HS, Bumgardner JD, Haggard WO. Chitosan sponges to locally deliver amikacin and vancomycin: a pilot in vitro evaluation. *Clin Orthop Relat Res* 2010;468(8):2074-80.
50. Jennings JA, Courtney HS, Haggard WO. Cis-2-decenoic acid inhibits *S. aureus* growth and biofilm in vitro: a pilot study. *Clin Orthop Relat Res* 2012;470(10):2663-70.
51. Zhang M, Li XH, Gong YD, Zhao NM, Zhang XF. Properties and biocompatibility of chitosan films modified by blending with PEG. *Biomaterials* 2002;23(13):2641-8.
52. Wang Q, Zhang N, Hu X, Yang J, Du Y. Chitosan/polyethylene glycol blend fibers and their properties for drug controlled release. *Journal of Biomedical Materials Research Part A* 2008;85(4):881-7.
53. Kolhe P, Kannan RM. Improvement in ductility of chitosan through blending and copolymerization with PEG: FTIR investigation of molecular interactions. *Biomacromolecules* 2003;4(1):173-180.
54. Zhao L, Zhu L, Liu F, Liu C, Shan D, Wang Q, Zhang C, Li J, Liu J, Qu X and others. pH triggered injectable amphiphilic hydrogel containing doxorubicin and paclitaxel. *Int J Pharm* 2011;410(1-2):83-91.

55. Moribe K, Maruyama K, Iwatsuru M. Molecular localization and state of amphotericin B in PEG liposomes. *Int J Pharm* 1999;193(1):97-106.
56. Darole PS, Hegde DD, Nair HA. Formulation and evaluation of microemulsion based delivery system for amphotericin B. *AAPS PharmSciTech* 2008;9(1):122-8.
57. Moribe K, Maruyama K. Pharmaceutical design of the liposomal antimicrobial agents for infectious disease. *Curr Pharm Des* 2002;8(6):441-54.
58. Tiyaboonchai W, Limpeanchob N. Formulation and characterization of amphotericin B-chitosan-dextran sulfate nanoparticles. *International Journal of Pharmaceutics* 2007;329(1-2):142-9.
59. Zhang H, Neau SH. In vitro degradation of chitosan by bacterial enzymes from rat cecal and colonic contents. *Biomaterials* 2002;23(13):2761-6.
60. Harmsen S, McLaren AC, Pauken C, McLemore R. Amphotericin B is cytotoxic at locally delivered concentrations. *Clin Orthop Relat Res* 2011;469(11):3016-21.

APPENDIX A

PRELIMINARY FORMULATION RESEARCH

Prior to the resulting chitosan and polyethylene glycol sponge formulations described in Chapters 3 and 4 of this dissertation, extensive formulation research was performed in order to reach the final sponge formulations. The variables tested and selected for the final sponge formulations, along with the reasons for selection are reported in Table 1.

Table 1. Chitosan and polyethylene glycol sponge formulation variables tested

Variable	Variable Tested	Reason for Selection
Weight percentage	1% or 2%	Degradation
Chitosan: PEG Ratio	1:1 , 2:1, or 4:1	Elution & degradation
Chitosan Supplier	Primex or Chinitor AS	Supplier change
DDA	61%, 71%, or 82%	Supplier change
PEG MW (g/mol)	6,000 , 8,000 , or 10,000	Degradation
NaOH concentration (M)	0.25 , 0.6, or 1	Degradation & swelling
Acid type	1% Lactic/acetic acid (75:25) or 1% acetic acid	Degradation & sponge flexibility
Freezing temperature	-20°C or -80°C	Freezer space, no difference otherwise
Order of addition	Chitosan first or PEG first	Easier to dissolve chitosan
Number of lyophilizations	1 or 2	Degradation

Bold indicates the variable was selected for the final chitosan/PEG sponge formulations.

In the first round of sponge formulations, 1:1, 2:1, and 4:1 Chitosan: PEG sponges were prepared in 1% acetic acid. Chitosan with a DDA of 71% from Primex and PEG with a molecular weight of 8,000 g/mol were used for each sponge type. All of the sponges were lyophilized twice and neutralized in 1 M NaOH. The *in vitro* lysozyme based degradation of the sponges was analyzed, as well as the *in vitro* water insoluble

amphotericin B elution; both experiments were previously described in Chapter 3. The percentage of sponge remaining after two or four days of *in vitro* degradation is shown in Figure 1. None of the chitosan/PEG blended sponges exhibited any significant differences in sponge degradation over time.

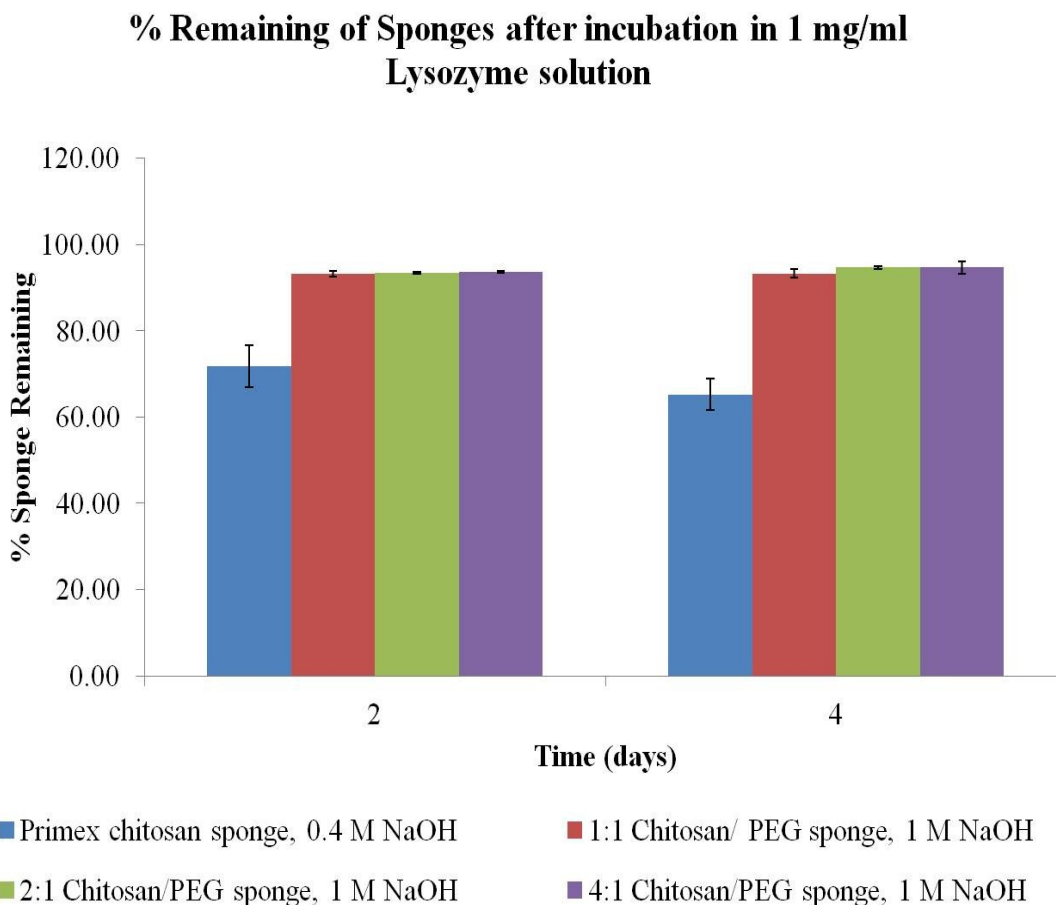


Figure 1. Mean *in vitro* lysozyme mediated degradation of first chitosan/PEG sponge formulations over time.

The elution profile of water insoluble amphotericin B from the 1:1, 2:1, and 4:1 chitosan/PEG sponges is provided in Figure 2. Once again, not many significant differences can be seen between the sponge groups, except that the 2:1 chitosan/PEG

sponge released slightly more amphotericin B after one and three hours than the other formulations. Because not many differences in degradation or antifungal elution were revealed between the three original sponge formulations, the 1:1 chitosan/PEG sponge was selected due to the belief that this sponge formulation would exhibit increased degradation after changing the sodium hydroxide concentration.

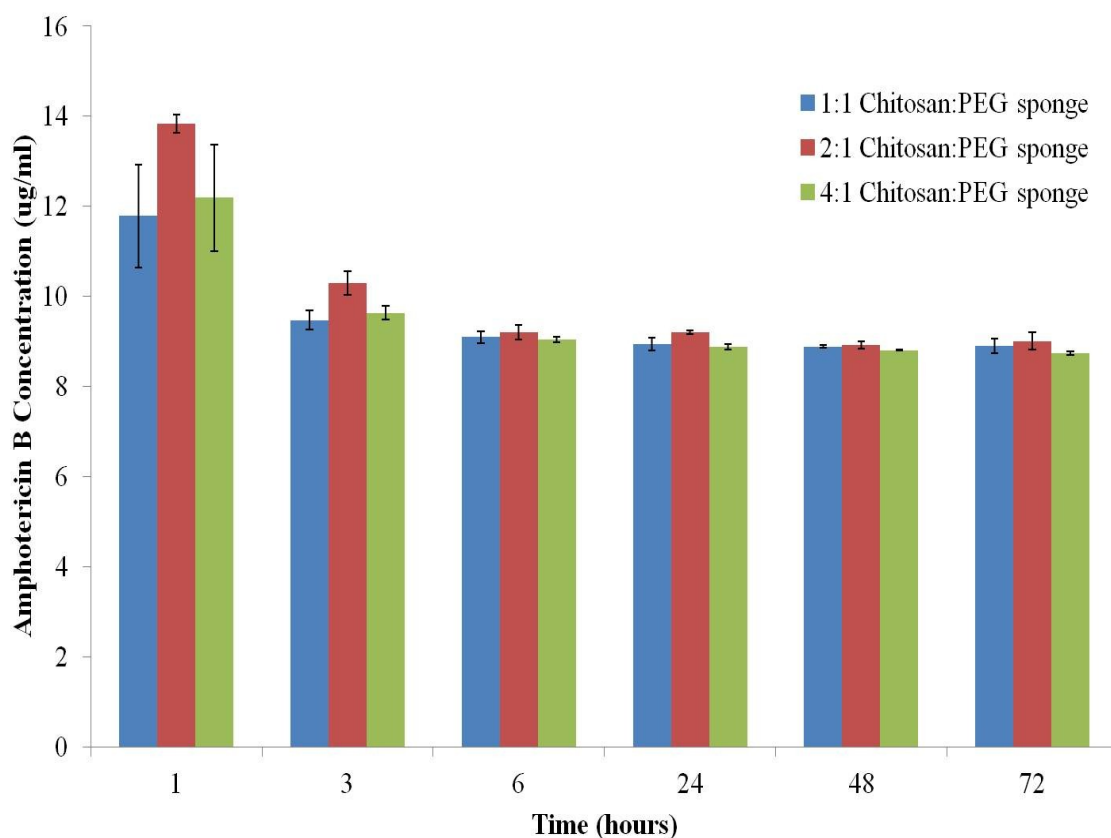


Figure 2. Mean amphotericin B (water insoluble) elution (\pm standard deviation) from first round of chitosan/PEG sponge formulations over 72 hours.

In the second round of formulation research, 1:1 chitosan/PEG sponges were developed in 1% acetic or blended (75:25 lactic: acetic) acid. Chitosan with 61% or 71% DDA and PEG with a molecular weight of 6,000 or 8,000 g/mol were utilized to make

the sponges. One sponge was made by dissolving chitosan in the acid first, followed by PEG. The remaining sponges were fabricated by dissolving PEG first. Sponges were neutralized in 0.25, 0.6, or 1 M NaOH, frozen at -80°C , and lyophilized twice. The swelling ability of the sponges in water was characterized, following the procedure described in Chapter 4 (Figure 3). The chitosan/PEG sponge neutralized in 0.25 M NaOH exhibited the highest swelling ratio compared to the other sponges. These results led to the decision to select 0.25 M NaOH for neutralizing the modified chitosan sponges.

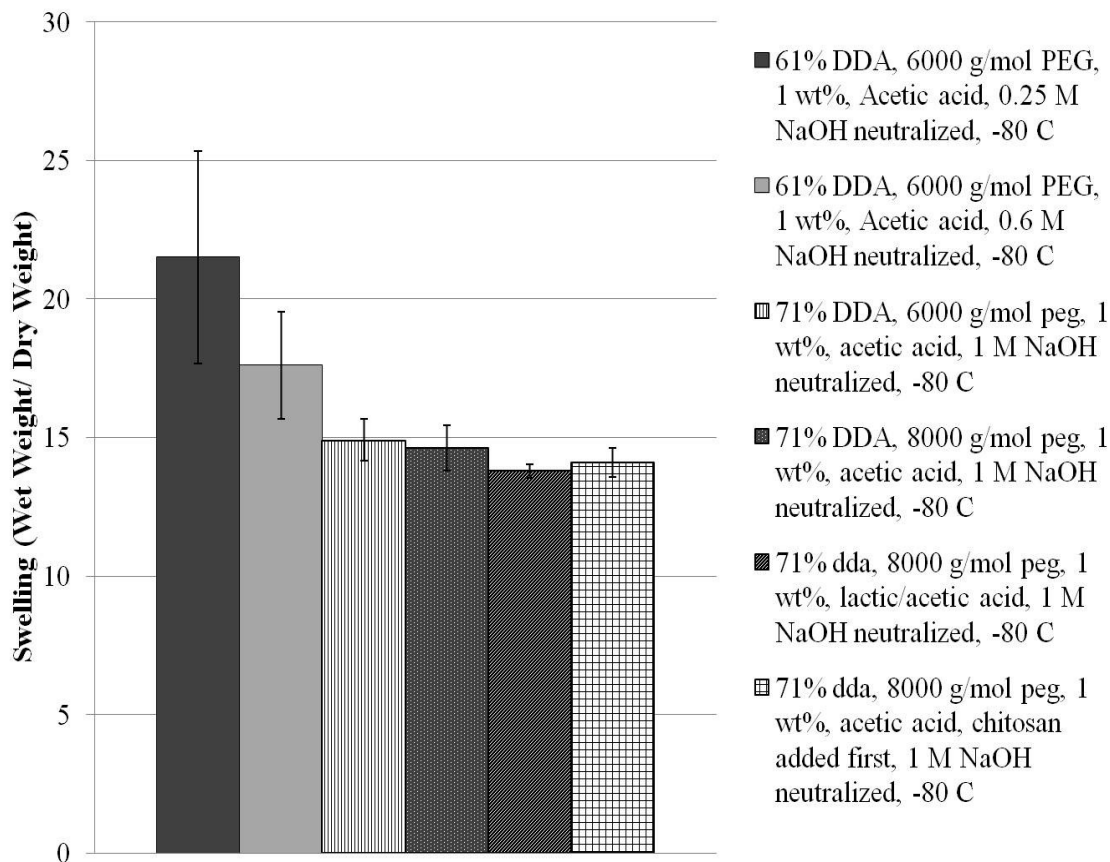


Figure 3. Swelling of second round of chitosan/PEG sponge formulations in water

In the third round of formulation research, 1:1 chitosan/PEG sponges were fabricated in 1% acetic or blended (75:25 lactic: acetic) acid. Sponges were prepared with either 61% or 71% DDA chitosan and 6,000, 8,000, or 10,000 g/mol PEG. All sponges were neutralized in 0.25 M NaOH and lyophilized twice. Another *in vitro* degradation study was conducted with these chitosan/PEG sponge formulations, and these results are provided in Figure 4.

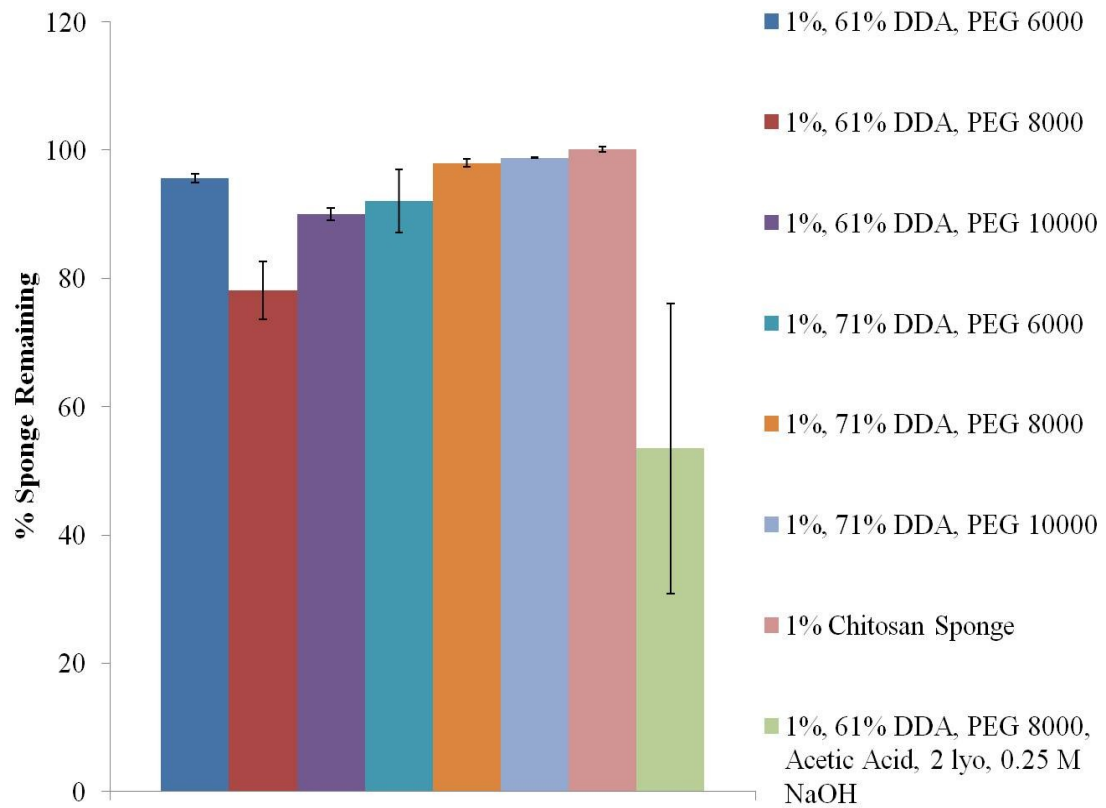


Figure 4. *In vitro* degradation of second round of chitosan/PEG sponge formulations after 4 days in 1 mg/ml lysozyme solution, all sponges were made with 1% blended acid unless otherwise noted.

As shown in the degradation results, the sponge formulated with 1% acetic acid exhibited significant increased degradation than the sponges formulated with 1% blended acid. Thus, acetic acid was selected as the sponge solvent for future chitosan/PEG sponge formulation.

After the third round of sponge formulations, our laboratory changed chitosan suppliers from Primex to Chitinor AS. Whereas Primex produced 61% and 71% DDA chitosan, Chitinor AS produced chitosan with an average 82% DDA. This specific chitosan was selected because our industrial research partner, Bionova Medical, used this chitosan to manufacture chitosan sponges.

APPENDIX B

ADDITIONAL CYTOCOMPATIBILITY EVALUATIONS

Objective

In vitro cytocompatibility of materials is a useful tool to screen potential candidates for eventual *in vivo* implantation. Cell viability results from a direct contact study with the chitosan/PEG sponges and the antimicrobial sponge eluates are reported in Chapters 3 and 4, respectively. However, additional microscopic evaluation and live/dead staining of the normal human dermal fibroblasts (NHDFs) in direct contact with the chitosan/PEG sponges was conducted in order to identify cellular morphology. Additionally, cytocompatibility of cells in contact with standard solutions of amphotericin B and vancomycin, both alone and in combination, was assessed to identify cytotoxic concentrations of the antimicrobials, independent of the antimicrobial elution from the sponges. The stock antibiotic and antifungal solutions used to load the chitosan/PEG sponges in Chapter 3 were also tested for cytocompatibility.

Live/Dead Staining

Normal human dermal fibroblasts were seeded in 12 well tissue culture plastic plates at 2.89×10^4 cells/ml in Dulbecco's Modified Eagle's Medium (DMEM) supplemented with 10% fetal bovine serum (FBS) and penicillin (100 units/mL), streptomycin (100 mg/mL), and amphotericin B (0.25 μ g/mL) under standard cell culture conditions (37°C and 5% CO₂ atmosphere). Cells were allowed to proliferate to near confluence, after which cell culture medium was aspirated and refreshed with 1 mL of fresh medium. Chitosan, chitosan/PEG, and control polyurethane sponges were soaked in pre-warmed, sterile 1 x PBS for approximately 20 minutes. A single 8 mm diameter test

specimen ($n = 5$) was then gently placed in a well in direct contact with the cell monolayer. Cultures were incubated for one day before biocompatibility and cellular morphology was assessed with the LIVE/DEAD® Viability/Cytotoxicity kit, obtained from Molecular Probes. Cell culture media was removed and replaced with Live/Dead solution, which consisted of 35 μ l of 2 mM ethidium homodimer-1 and 25 μ L of 4 mM calcein in 1 x PBS. Plates were incubated at room temperature before images of the stained cells were taken with an EVOS microscope at 4 x magnification. Representative images of stained cells after one day of direct contact with the sponges are shown in Figure 1.

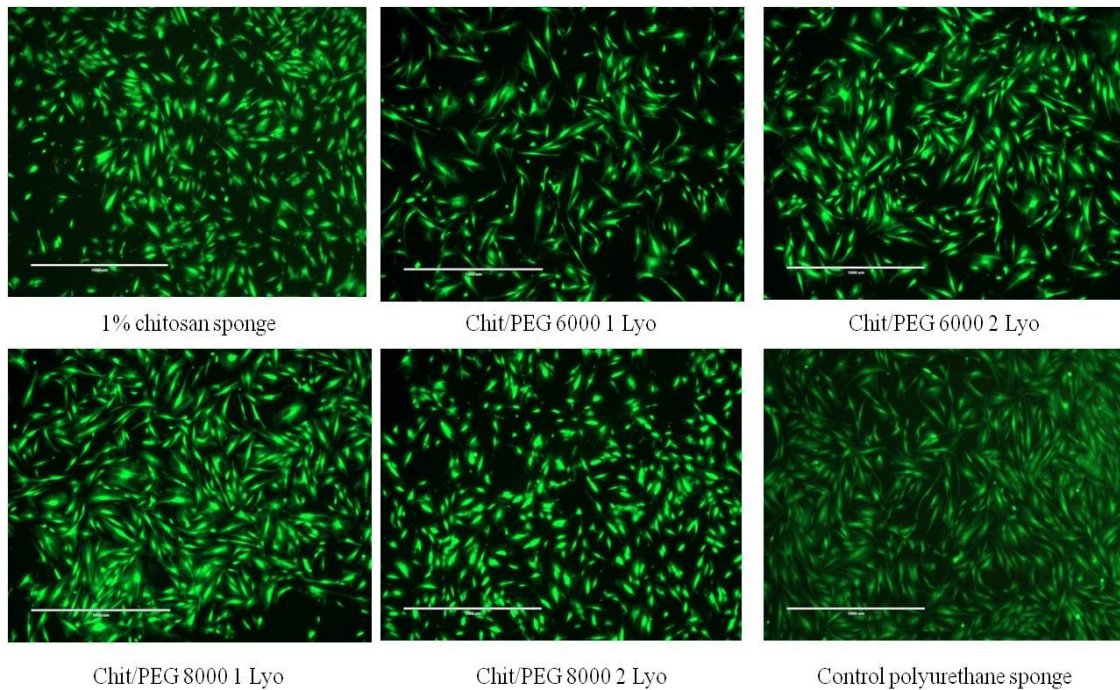


Figure 1. Images of normal human dermal fibroblasts stained with calcein (live cells) and ethidium homodimer-1 (dead cells) after one day of direct contact with the 1% chitosan sponge, chit/PEG 6000 1 lyo, chit/PEG 6000 2 lyo, chit/PEG 8000 1 lyo, chit/PEG 8000 2 lyo, and a control polyurethane sponge (at 4 x magnification)

All of the sponges exhibited good cell viability, with hardly any visible dead cells present. However, there are a few differences in cellular morphology. While the chitosan/PEG 6000 1 lyo, chitosan/PEG 6000 2 lyo, and chitosan/PEG 8000 1 lyo sponges all exhibited similar effects on cell morphology as the polyurethane sponges, the 1% chitosan and chitosan/PEG 8000 2 lyo sponges caused slight cellular malformation. The cells exposed to these two sponge groups exhibited reduced elongation. This effect on *in vitro* cellular morphology led to the decision to exclude the chitosan/PEG 8000 2 lyo sponge from future experimental analysis.

Antimicrobial Solution Cytocompatibility

To evaluate the effects of both stock and standard solutions of amphotericin B and vancomycin, both alone and in combination, normal human dermal fibroblasts were seeded at 2.5×10^4 cells/ml in 48 well plates in the same cell culture conditions described in Chapter 4. Standard concentrations of amphotericin B and vancomycin at 1000, 100, 10, and 1 $\mu\text{g/ml}$ and 4000, 400, 40, and 4 $\mu\text{g/ml}$, respectively, were prepared in 1:1 dilutions in sterile pre-warmed media. Standard concentrations of vancomycin and amphotericin B in combination were also prepared at a total antimicrobial concentration of 5000, 500, 50, and 5 $\mu\text{g/ml}$ (4000, 400, 40, and 4 $\mu\text{g/ml}$ and 1000, 100, 10, and 1 $\mu\text{g/ml}$ of vancomycin and amphotericin B combined). The original stock loading solutions of amphotericin B and vancomycin, both alone and in combination, from Chapter 4 were also diluted in media, along with a PBS control.

After cells reached near confluence, culture media was removed and replaced with the antimicrobial solution dilutions. Cells were incubated for one or three days, after which cell viability was assessed with the Cell Titer-Glo® Luminescent Cell

Viability assay, purchased from Promega. The luminescent signal, which corresponded to the amount of adenosine triphosphate and the number of viable cells through a standard dilution of known concentrations of cells, was recorded at 590 nm using a BioTek Synergy H1 plate reader. Cell concentrations were converted to percentage of cell viability by comparison to tissue culture plastic controls, which were represented as 100% cell viability.

Results from the cytocompatibility study with standard antimicrobial solutions are provided in Figure 2, while the cytocompatibility data from stock antimicrobial solutions used to load chitosan and chitosan/PEG sponges is shown in Figure 3. As expected, a large difference in cell viability exists between the vancomycin and amphotericin B solutions, both in the standards and stock solutions. Amphotericin B is known to be toxic at high levels; one previous study has found that concentrations of 100 $\mu\text{g/ml}$ caused cell death after five hours.⁶⁰ However, the modified sponges studied in this work did not release amphotericin B at levels high enough to cause severe cell death, as seen in the 1000 and 100 $\mu\text{g/ml}$ samples in Figure 2. Not surprisingly, the dual vancomycin and amphotericin B solutions also exhibited similar cytotoxicity to amphotericin B alone; the dual solutions contained the same amount of amphotericin B as the single solutions. Interestingly, the vancomycin solutions exhibited larger decreases in cell viability from one to three days of treatment than the amphotericin B and dual antimicrobial solutions. However, the PBS group also exhibited this decreased cell viability, which indicates this effect might be simply due to the dilution of media over three days.

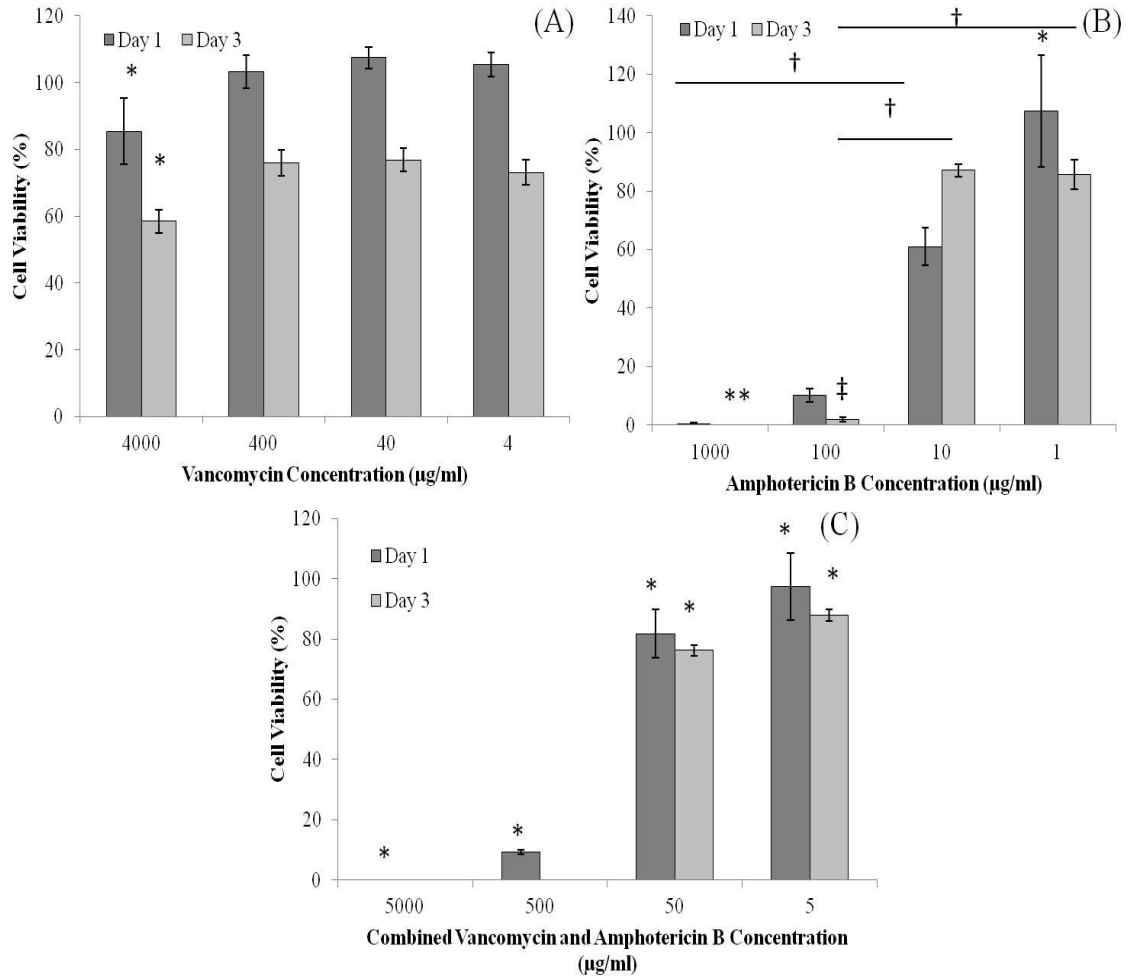


Figure 2. Cytocompatibility (mean \pm standard deviation) of (A) standard vancomycin solutions ($n = 3$), (B) standard amphotericin B solutions ($n = 3$), and (C) standard vancomycin and amphotericin B combination solutions to normal human dermal fibroblasts after one and three days. Cells were analyzed using Cell Titer-Glo[®] luminescent assay and resulting cell numbers were converted to percent cell viability by normalization to tissue culture plastic (TCP) controls. (* indicates $p < 0.05$ versus all, ** indicates $p < 0.05$ versus all except ‡, and † denotes $p < 0.05$ pairwise)

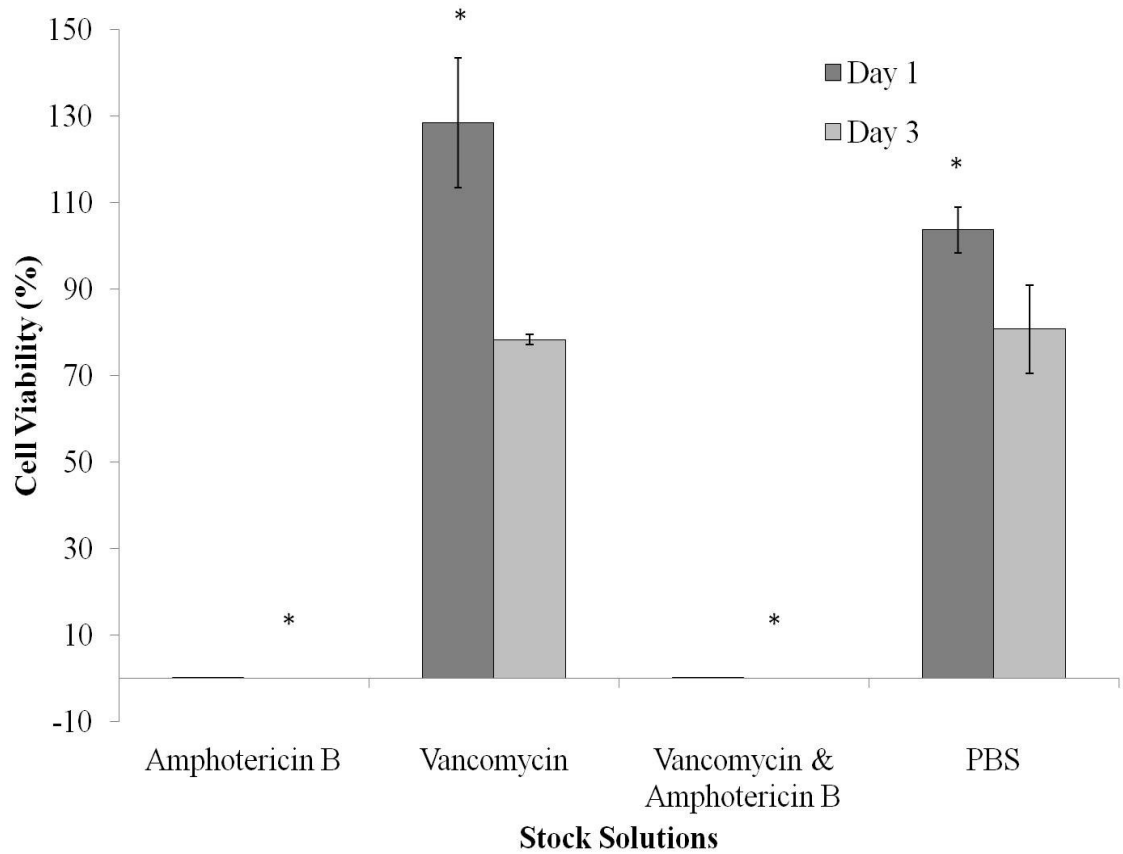


Figure 3. Cytocompatibility (mean \pm standard deviation) of normal human dermal fibroblasts after one and three days of treatment of stock amphotericin B, vancomycin, and combination vancomycin and amphotericin B solutions (n = 3) used to load chitosan/PEG and chitosan sponges in *in vitro* antimicrobial elutions. (* indicates $p < 0.05$ versus all within respective timepoint)

APPENDIX C

EVALUATION OF TWO SOURCES OF CALCIUM SULFATE FOR A LOCAL DRUG DELIVERY SYSTEM: A PILOT STUDY

Introduction

Wound infection and osteomyelitis can be challenging to treat especially with complex musculoskeletal trauma in civilian and military populations, and can result in multiple surgeries and increased costs [1,2]. Local drug delivery is emerging as a useful route for treating acute and chronic wound infections. Because drugs are delivered to the entire body in systemic drug delivery, toxicity issues can often arise as well as antibiotic resistance [3]. Organisms that are typically antibiotic-resistant in systemic delivery can be more susceptible to the higher levels of antibiotics provided through local delivery [3]. Additionally, the drug can take a longer time to reach the wound when delivered systemically and some avascular areas of the body are unreachable [3]. In local drug delivery, the wound area is targeted and the drug does not substantially affect other parts of the body; however, local drug delivery systems do not completely eliminate toxicity issues and antibiotic resistance. The ideal local drug delivery system would be implanted, deliver antibiotics at appropriate levels and lengths of time based on application, and then degrade so there would be no need for a second surgical procedure for removal [3].

Another difficult challenge with complex musculoskeletal trauma is resistant bacteria. Wound infection can be complicated by wound contamination with antibiotic-resistant bacteria, which can increase treatment difficulty. Methicillin-resistant *Staphylococcus aureus* (MRSA) is a serious concern in modern medicine and serves as a problem in wound treatment. Antibiotic-resistant bacteria have created a need for newer

antibiotics as an adjunct for past antibiotic selections such as vancomycin. Daptomycin is a semisynthetic antibiotic with activity against Gram-positive bacteria and has demonstrated activity against MRSA [4,5]. Daptomycin has been previously researched combined with a calcium sulfate (CaSO_4) carrier, and daptomycin reportedly elutes similarly to tobramycin in vitro [6,7]. However, like with many antibiotics used for infected wound treatment, bacterial resistance to daptomycin has been recently reported [8].

CaSO_4 has been previously used as a bone void filler and in bone defects is absorbed by the surrounding tissue, possibly accelerating bone healing [9]. CaSO_4 is a biocompatible, biodegradable material with osteoconductive properties that exhibits a bolus, or burst, release followed by an extended drug release from several hours to weeks depending on the formulation [10,11]. CaSO_4 has been used to deliver vancomycin, gentamycin, tobramycin, lincomycin, cefazolin, teicoplanin, and fucidin [12-14]. Another, and the most common, material used for local drug delivery is polymethylmethacrylate (PMMA) [15]. Although PMMA implants are not biodegradable, their removal may be necessary at times for planned staged reconstruction or late bead failure [16]. Because CaSO_4 degrades over time, the need for surgical removal is eliminated. Clinical studies and animal models suggest using antibiotic-loaded calcium sulfate pellets minimizes infection [17-19]. Although there are numerous potential applications in which calcium sulfate is beneficial as a drug delivery material, the mechanical properties of calcium sulfate do make it insufficient for load-bearing applications [20]. Recently, two sources of CaSO_4 that are commercially available have been studied for their use in local antibiotic delivery. To make pellets with daptomycin

from one type of CaSO₄ (hemihydrate synthesized from naturally occurring USP grade gypsum), a catalyst, K₂SO₄, is required [7]. It has been proposed the K₂SO₄ catalyst would not be necessary to form pellets from a synthetic CaSO₄. A comparison of antibiotic elution, pellet degradation, and the need for a catalyst of these two CaSO₄ sources has not been investigated.

We asked the following questions: (1a), is the pellet degradation and (1b), daptomycin elution profile different for two different forms of CaSO₄, naturally sourced from gypsum and synthetic; (2) does the presence of a catalyst, potassium sulfate (K₂SO₄), affect the degradation and the daptomycin elution profile of the CaSO₄ pellets manufactured from two different sources; and (3) is the daptomycin released from both sources of CaSO₄ pellets active against bacteria associated with osteomyelitis, specifically *S. aureus*?

Materials and Methods

To determine whether the pellet degradation, daptomycin elution profile, and activity against *S. aureus* were affected by the type of CaSO₄ or the presence of a catalyst, we prepared the CaSO₄ pellets in three groups, synthetic CaSO₄ and 3% K₂SO₄, synthetic CaSO₄ and 0% K₂SO₄, and naturally sourced CaSO₄ with 3% K₂SO₄ as seen in Figure 1. Four of each type of pellet was placed in each vial and there were four total replications, or vials, for each group in each test. Each pellet group was tested in an elution study, degradation study, and activity testing with the dependent variables being daptomycin concentration, degradation rate, and turbidity, respectively.

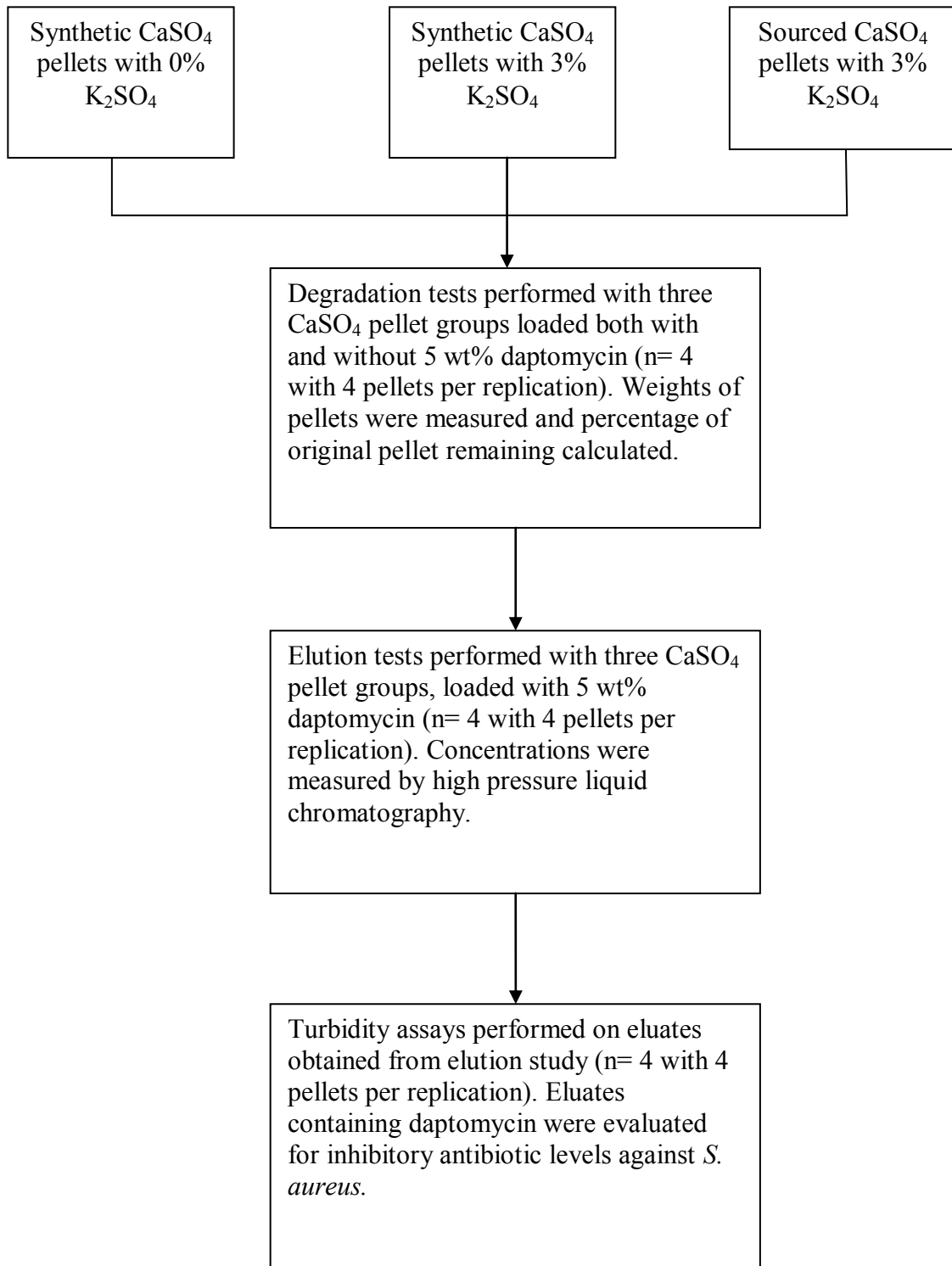


Figure 1. A flowchart demonstrates the study design with the three test groups and the key variables from three property characterization tests.

The two types of CaSO₄ used in our study were Osteoset (Wright Medical Technology, Arlington, TN), a sterile surgical grade, CaSO₄ α-hemihydrate from naturally sourced United States Pharmacopeia (USP) grade gypsum, and Stimulan (Biocomposites, Wilmington, NC), a high-purity, completely synthetic sterile CaSO₄α-hemihydrate. The naturally sourced and synthetic CaSO₄ pellets were both cast with 4.75 g of CaSO₄, with and without 5 wt%, 0.25 g, of daptomycin (Cubist Pharmaceuticals Inc, Lexington, MA; Lot MCB2007). The 5 wt% was previously determined using prior research on naturally sourced CaSO₄ pellets [6,7]. Throughout our study, we used aseptic techniques in the fabrication of the pellets. The synthetic CaSO₄ pellets were made with and without 2.5 mL of sterilized 3% K₂SO₄ solution, whereas the naturally sourced CaSO₄ pellets were only made with 2.5 mL of 3% K₂SO₄ solution. Previous research has determined that a concentration of 3% K₂SO₄ is necessary for the naturally sourced CaSO₄ pellets because the pellets will not retain their shape without the catalyst [6]. The 3% K₂SO₄ solution was substituted with 1.7 mL of sterile phosphate-buffered saline for the synthetic CaSO₄ pellets with 0% K₂SO₄. We carried out all experiments in four replications (n = 4). Pellets were cast using 3-mm OSTEOSET® Resorbable Mini-Bead Kits (Wright Medical Technology; Catalog 8400-0511; Lot LB04-0028-27) and following the mixing method used by Wright Medical Technology described in previous research [6,7].

We performed the elution statically with four sets of each pellet variation distributed into four steam autoclaved 20-mL glass scintillation vials. The elution was conducted without stirring to maintain the structure of the pellets. We loaded 4 mL of phosphate-buffered saline (PBS) into each vial and placed them in an oven at 37° C. The

eluates were mixed and 1-mL samples were taken at Days 1, 2, 4, 6, 8, and 10. The elution studies were stopped at 10 days because the antibiotic levels were below the HPLC detection limit. After each day's eluate sample was collected, we replaced the remaining liquid with a fresh 4 mL PBS and the vials were returned to the 37° C oven. Eluate samples were immediately frozen in a Fisher Scientific Isotemp freezer at -20° C.

To measure the initial daptomycin concentration loaded in the pellets, samples were made of each pellet variation were constructed and crushed before placing them into a PBS solution. The drug content of the pellets was measured before the elution because previous CaSO₄ and daptomycin pellets had some daptomycin loss from initial loading. The percent daptomycin content loaded into the pellets was compared with the percent daptomycin released from the elution.

To determine the eluate's antibiotic concentration, we performed high-pressure liquid chromatography (HPLC) testing according to previously used methods [7]. The Varian (Palo Alto, CA) HPLC system was comprised of a ProStar 240 Solvent Delivery, ProStar 410 Autosampler, and ProStar 325 UV-Vis Detector modules. We performed module control and data processing using Varian's Galaxie Chromatography Data System (Version 1.8.508.1). The mobile phase consisted of a HPLC-grade acetonitrile and water (62:38, v/v) solution including 4 mM ammonium dihydrogen phosphate brought to a pH of 3.25 using glacial acetic acid. Separation was accomplished using a Varian Microsorb-MV C8 column, 150-mm length and 4.6-mm inner diameter, with a flow rate of 1 mL/min. Daptomycin was detected at 232 nm with a retention time of 13.8 minutes. We performed the method in a temperature range of 23.3 ± 1.1° C.

We determined the CaSO₄ pellets' degradation by a common weight-based experiment¹⁻³. Initially, the weights of clean 20-mL glass scintillation vials were established and then the weight of each vial with four pellets of an individual variation was measured. We loaded 4 mL of PBS into each vial and stored them at 37° C. At 1-, 2-, 4-, 6-, 8-, and 10-day time points, the PBS was removed and the pellets were allowed to dry at 70° C until a constant vial and pellet weight was obtained. After each time point's sample was collected, we placed 4 mL PBS into the vials and they were returned to 37° C storage. The degradation was determined by the percent of pellets remaining at each time point calculated using the following relationship:

$$\text{Percent remaining (\%)} = \frac{(\text{vial and pellets at } \times \text{ hours weight} - \text{vial weight})(\text{mg})}{(\text{vial and initial pellets weight} - \text{vial weight})(\text{mg})} \times 100$$

We determined antibiotic activity against *S. aureus* (Cowan I strain obtained from Dr David Hasty, University of Tennessee Health Science Center) by using antibiotic elution samples in a turbidity assay. In this experiment, solution clarity after sufficient bacterial incubation with antibiotic eluates indicated bacterial inhibition resulting from antibiotic activity. As instructed by the protocol provided by the manufacturer, we supplemented BBL™ Mueller Hinton II Broth (Becton, Dickinson and Co, Sparks, MD; Lot 0071612) with 25 µg/mL Ca²⁺ in order to achieve a total Ca²⁺ concentration of 50 µg/mL. Two hundred microliters of daptomycin eluates were added to the inoculum containing 1.75 mL Mueller Hinton II Broth + Ca²⁺ and 50 µL *S. aureus* in 5-mL polystyrene test tubes. The experimental setup created a 1:10 dilution of all eluates. Experimental groups, blanks containing neither *S. aureus* nor eluate samples, and positive controls containing *S. aureus* without antibiotic eluates were mixed and incubated at 37°

C. After approximately 20 hours of incubation at 37° C, we vortexed the tubes and the absorbance at 530 nm was recorded.

All data are presented as mean \pm SD and met the assumptions of a parametric test. We determined differences in percent degradation and daptomycin concentration between the pellets made from two different types of CaSO₄ and the pellets made with and without K₂SO₄ using repeated measures analysis of variance and Tukey's post hoc analysis using 2007 Microsoft Office Excel (Microsoft Inc, Redmond, WA) and 2004 SigmaStat (San Jose, CA). Differences in degradation were also analyzed with Kaplan-Meier survival analysis with log rank, where 10% of the original pellet remaining was classified as failure of the pellets. When only 10% of the original pellet remains, the antibiotic concentration in the pellets is typically too low and the pellets are too small to accurately measure.

Results

The degradation studies indicated differences between the sourced and synthetic CaSO₄ pellets with 3% K₂SO₄ without daptomycin at Days 2 ($p = 0.002$), 4, 6, and 8 ($p < 0.001$), as seen in Figure 2. However, Kaplan Meier analysis with log rank revealed no overall differences between all three CaSO₄ groups without daptomycin ($p = 0.368$). When 5 wt% daptomycin was incorporated into the pellets (Figure 3), differences were seen between the sourced CaSO₄ pellets and the synthetic CaSO₄ with 0% K₂SO₄ at Days 1 through 10 ($p < 0.001$).

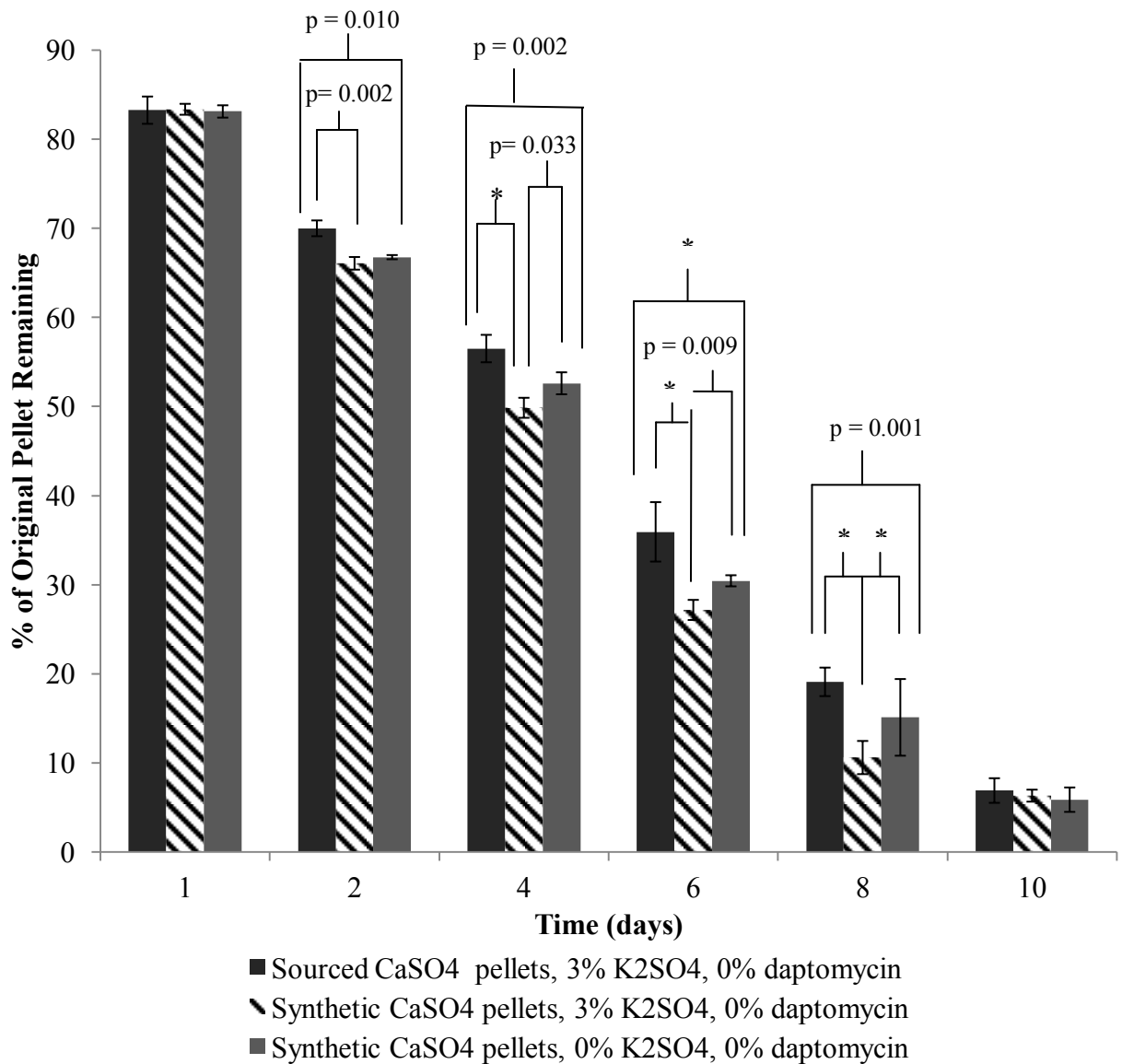


Figure 2. The graph shows the degradation results of the naturally sourced and synthetic CaSO₄ pellets with 0% daptomycin present. There were differences in average degradation of naturally sourced and synthetic CaSO₄ pellets with 3% K₂SO₄ and naturally sourced and synthetic CaSO₄ pellets with 0% K₂SO₄ at Days 2, 4, 6, and 8. Differences were observed between the synthetic CaSO₄ pellets with 3% and 0% K₂SO₄ at Days 4, 6, and 8. Degradation is reported in wt% of original pellet remaining ± SD with n = 4 (* corresponds to p < 0.001).

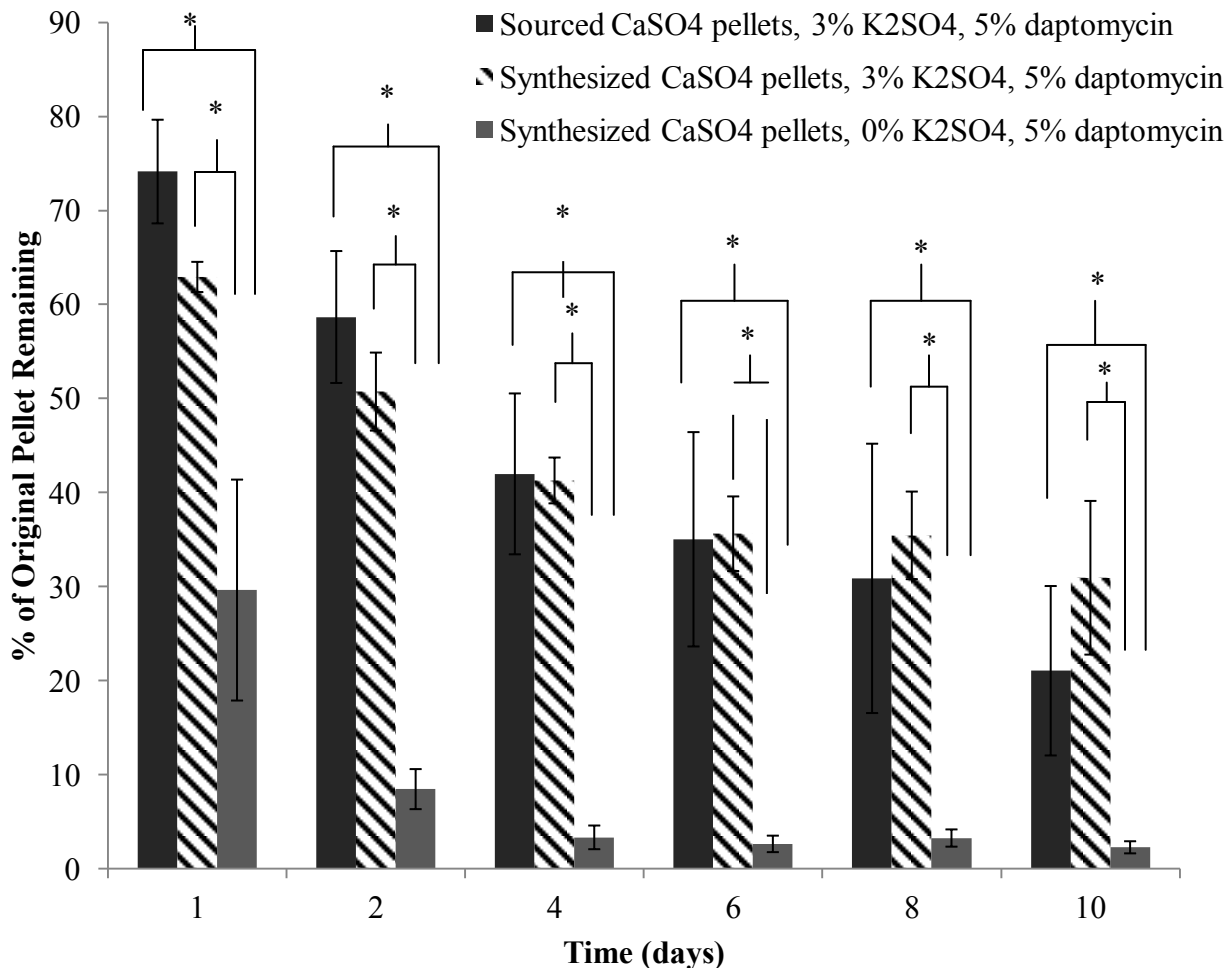


Figure 3. The graph shows the degradation results of the naturally sourced and synthetic CaSO₄ pellets with 5% daptomycin present. We observed differences in average degradation of naturally sourced and synthetic CaSO₄ pellets with 0% K₂SO₄ and synthetic CaSO₄ pellets with 3% and 0% K₂SO₄ at Days 1-10. Degradation is given in wt% of original pellet remaining ± SD with n = 4 (* corresponds to p < 0.001).

Using Kaplan Meier analysis with log rank, overall differences were seen between the sourced and synthetic CaSO₄ pellets with 0% K₂SO₄ (p < 0.001) and between the synthetic CaSO₄ pellets with 3% and 0% K₂SO₄ (p < 0.001). However, no differences were seen between the degradation of the sourced and the synthetic CaSO₄ pellets with 3% K₂SO₄ (p > 0.05) from the ANOVA or Kaplan Meier survival analysis.

We observed differences in the elution profile of the sourced CaSO_4 pellets and the synthetic CaSO_4 pellets with 3% K_2SO_4 at Day 1 ($p < 0.001$) and Day 2 ($p = 0.002$) (Figure 4). The sourced CaSO_4 pellets released the highest amount of daptomycin on Day 1 and correspondingly had the highest amount of cumulative daptomycin eluted (Figure 5), but the synthetic CaSO_4 pellets with 3% K_2SO_4 released the largest amount of antibiotic on Day 2.

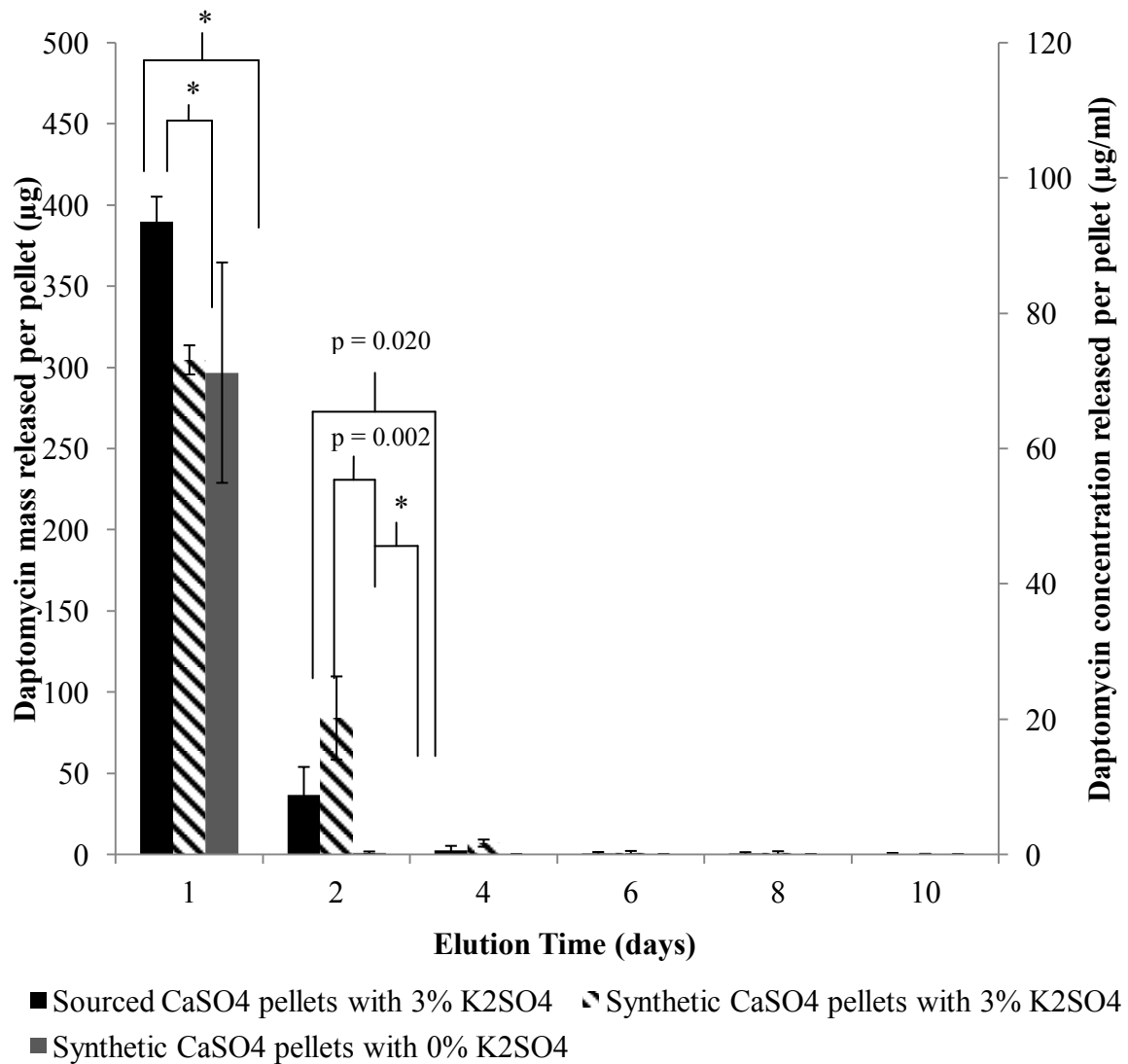


Figure 4. The graph shows the elution results from the naturally sourced and synthetic CaSO₄ pellets with 5% daptomycin loaded, with mass and concentration of daptomycin released on the primary and secondary y axes, respectively. We found differences in the average mass and concentration of daptomycin released in the eluates between the naturally sourced and synthetic CaSO₄ pellets with 3% and 0% K₂SO₄ at Days 1 and 2. Differences are shown in average mass and concentration of daptomycin released in the eluates between the synthetic CaSO₄ pellets with 3% and 0% K₂SO₄ at Day 2. Mass and concentration are given in micrograms and micrograms per milliliter, respectively, of daptomycin released per pellet ± SD with n = 4 (* corresponds to p < 0.001).

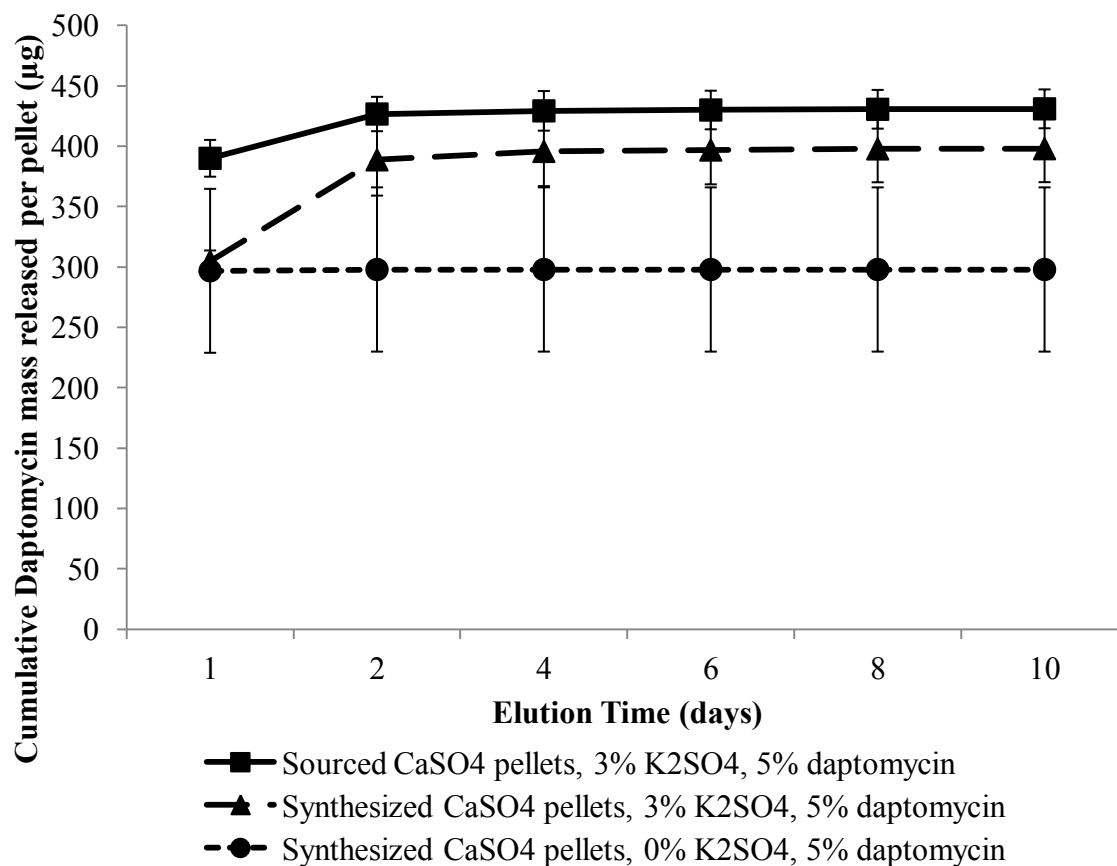


Figure 5. The graph shows the elution results in the cumulative release form from the naturally sourced and synthetic CaSO₄ pellets, with and without 3% K₂SO₄, with 5% daptomycin loaded. Mass is given in micrograms of daptomycin released per pellet ± SD with n = 4.

For evaluation of mass balance in these studies, the average percent daptomycin loaded and released from the three types of pellets was measured. The average percent of daptomycin for the sourced CaSO₄ pellets was highest at loading, at 85.1%, but the percent daptomycin released was highest in the synthetic CaSO₄ pellets with 3% K₂SO₄ at 48.8% (Table 1). The average percent daptomycin was lowest, both loaded and released, in the synthetic CaSO₄ pellets with 0% K₂SO₄.

Table 1. Average percent daptomycin loaded in pellets and released in elution testing

Pellet Type	% Daptomycin Loaded	% Daptomycin Released
Sourced CaSO ₄ Pellets with 3% K ₂ SO ₄	85.1	42.8
Synthesized CaSO ₄ Pellets with 3% K ₂ SO ₄	81.8	48.8
Synthesized CaSO ₄ Pellets with 0% K ₂ SO ₄	45.8	39.3

Values are mean (n = 4)

The presence or absence of K₂SO₄ created differences in the degradation and the elution in the synthetic CaSO₄ pellets. The synthetic CaSO₄ pellets with 0% K₂SO₄ and 5 wt% daptomycin degraded much more quickly than both types of pellets with 3% K₂SO₄, and as previously mentioned, differences were seen in degradation between the synthetic CaSO₄ pellets with 0% K₂SO₄ and the other pellets using ANOVA and Kaplan Meier analysis. Differences were seen in the elution (Fig 4) between the synthetic CaSO₄ pellets with 0% K₂SO₄ and 3% K₂SO₄ at Day 2 (p < 0.001) and the naturally sourced CaSO₄ pellets with 3% K₂SO₄ at Day 1 (p < 0.001) and Day 2 (p = 0.002).

The eluates of the sourced CaSO₄ pellets with 3% K₂SO₄ and 5 wt% daptomycin demonstrated sufficient activity against *S. aureus* with no bacterial growth at Days 1, 4, and 6 (Table 2). Eluates from synthesized CaSO₄ pellets with 0% K₂SO₄ were only active against *S. aureus* at Days 1 and 2; however, the eluates from the synthesized CaSO₄ pellets with 3% K₂SO₄ were active against *S. aureus* at all time points except at 10 days.

Table 2. The average activity for 5% loaded daptomycin (1:10 dilution) against of *Staphylococcus aureus*

Pellet Type	Time points (days)					
	1	2	4	6	8	10
Sourced CaSO ₄ Pellets with 3% K ₂ SO ₄	-	+	-	-	+	+
Synthesized CaSO ₄ Pellets with 3% K ₂ SO ₄	-	-	-	-	-	+
Synthesized CaSO ₄ Pellets with 0% K ₂ SO ₄	-	-	+	+	+	+

(-) indicates inhibition of *S. aureus*, (+) indicates growth of *S. aureus*, (n = 4)

Discussion

The treatment of osteomyelitis is becoming complicated by the increased emergence of antibiotic-resistant bacteria and increases the need for local drug delivery over systemic delivery. The purpose of our study was to evaluate parameters of a local CaSO₄ drug delivery system, including (1a) to determine if the pellet degradation and (1b) daptomycin elution profile is different for two different commercially available forms of CaSO₄; (2) to examine if the presence of a catalyst, K₂SO₄, affects the degradation and antibiotic elution profile of the CaSO₄ pellets; and (3) to verify the daptomycin released from both types of CaSO₄ pellets is active against *S. aureus*, a bacterium commonly associated with osteomyelitis.

Our study is limited by several factors. First, a common limitation of most in vitro research is the difficulty of translating in vitro studies to in vivo studies [16]. Release characteristics in an in vivo environment, especially associated with a wound, are different than antibiotic release characteristics in vitro, in which a set volume of eluate and PBS is exchanged at certain intervals [16]. This study is not meant to serve as a surgical wound model itself, but as a supplement to in vivo studies. Additionally, although we are testing four pellets at one time, elution, degradation, and activity properties of these pellets may be completely different in vivo in larger pellet quantities.

Second, we tested activity of the antibiotic to planktonic *S. aureus* and did not test inhibitory activity to bacteria within biofilms, which can be more resistant to antibiotic therapy and typically require additional antibiotic levels required for inhibition of planktonic bacteria [23]. Third, we used only one antibiotic. Increasing the number of evaluated antibiotics could predict if the CaSO₄ type or presence of K₂SO₄ impacts drug elution and pellet degradation in different ways. Fourth, both elution and degradation are dependent on numerous factors, including physical and chemical properties of materials, elution volumes with and without fluid exchange, and antibiotic interactions and thus we cannot predict elution and degradation performance across all potential applications. Both elution and degradation studies only provide details about the release and degradation characteristics of the local delivery vehicle itself, and do not account for affects from a local wound and the interactions between the delivery system, fluid, and drug.

Our preliminary data indicate differences in degradation and elution between both forms of CaSO₄ pellets, naturally sourced and synthetic, that could affect the clinical selection of a local delivery system. As with previously researched sourced CaSO₄ pellets, all pellets exhibited a bolus release of antibiotics on Day 1 [21,26]. However, the total percent release of daptomycin from the naturally sourced CaSO₄ pellets was higher and the concentration of daptomycin released on Day 1 was lower than previously reported (Table 3) [6,7]. The initial daptomycin released from the naturally sourced and synthetic calcium sulfate pellets is closer to initial antibiotics eluted from PMMA beads (Table 3) [24-26]. An explanation for the higher total release of the antibiotic could be the result of faster elution to measurement activities in comparison to previous studies.

Extended elution and storage could impact stability of daptomycin in solution. The lower initial daptomycin concentration could be explained by the larger size of the previously researched CaSO₄ pellets [21,26]. Although the synthetic CaSO₄ pellets also exhibited a bolus release, more daptomycin was eluted on Day 2 compared with the naturally sourced CaSO₄ pellets, which could demonstrate a slower antibiotic release.

The difference in daptomycin release could be partially explained by the degradation differences between the types of pellets. The synthetic CaSO₄ pellets with 3% K₂SO₄ and 5% daptomycin demonstrated the slowest degradation, as compared to the other two types of pellets. Although the naturally sourced CaSO₄ pellets had a faster degradation than the synthetic CaSO₄ pellets with 3% K₂SO₄, the degradation of the naturally sourced CaSO₄ pellets in our study was slower than previously reported [7]. However, the results could have been different because distilled water was used for the degradation solution instead of PBS in the previous research [7]. The presence of daptomycin increased the degradation rate in all three pellet types studied, but had the greatest effect on the degradation of the synthetic CaSO₄ pellets with 0% K₂SO₄. An explanation for this difference in degradation that has been previously reported could be that when the K₂SO₄ is absent, the daptomycin prevents the setting reaction of the CaSO₄, which impacts the stability of pellets [21].

Table 3. Comparisons of present study with previous research on CaSO₄ and PMMA

Study	Type of material	Antibiotic	Catalyst/additive	Drug release on Day 1	Degradation	Activity testing
Richelsoph et al. [21]	Sourced CaSO ₄	Daptomycin or tobramycin	K ₂ SO ₄	537.3 µg/mL/g daptomycin and 827.6 µg/mL/g tobramycin	Yes 100% degraded at 6 days	No
Webb et al. [26]	Sourced CaSO ₄	Daptomycin	K ₂ SO ₄	697.4 µg/mL/g for clinical pellets	N/A	Yes: inhibition through 28 days, except Days 10 & 14
Kanellakopoulou et al. [11]	Synthetic CaSO ₄	Daptomycin	None	1320.1 µg/mL	N/A	No
McLaren et al. [18]	PMMA	Daptomycin	None, xylitol or glycine	84.375 µg/mL with xylitol	N/A	No
Lewis and Janna [13]	PMMA	Gentamicin sulfate	None	≈ 10 x 10 ⁻³ g/mL/h for 4.25 wt% loading	N/A	N/A
Lewis et al. [12]	PMMA	Daptomycin	None	< 50 µg/mL/g for 4.5 wt% loading	N/A	Yes: inhibition through 7 days
Parker et al. (current study)	Sourced CaSO ₄	Daptomycin	K ₂ SO ₄	97.48 µg/mL	Yes 21% of original pellets remaining at 10 days	Yes: inhibition at Days 1, 4, and 6

Table 3 continued. Comparisons of present study with previous research on CaSO₄ and PMMA

Study	Type of material	Antibiotic	Catalyst/additive	Drug release on Day 1	Degradation	Activity testing
Parker et al (current study)	Synthetic CaSO ₄	Daptomycin	K ₂ SO ₄	76.16 µg/mL with 3% K ₂ SO ₄ and 74.19 µg/mL with 0% K ₂ SO ₄	Yes 30.9% & 2.25% of original pellets with 3% & 0% K ₂ SO ₄ remaining at 10 days	Yes: inhibition at Days 1 and 2 with 0% K ₂ SO ₄ and Days 1-8 with 3% K ₂ SO ₄

PMMA = polymethylmethacrylate; N/A = not applicable

Although it has been previously determined that K₂SO₄ is necessary to form pellets of naturally sourced CaSO₄ [7], we were able to form pellets out of synthetic CaSO₄ without the K₂SO₄ catalyst. By not incorporating K₂SO₄ into the pellets, the synthetic CaSO₄ pellets degraded much more rapidly and released less daptomycin than the other pellets with the catalyst present. The daptomycin released from the synthetic CaSO₄ pellets with 0% K₂SO₄ is substantially less than the amount released from the same type of CaSO₄ with 0% K₂SO₄ that was previously reported (Table 3) [27]. However, the local delivery pellets used in these previous research studies were much larger than the pellets in this current research, 160 by 100-mm compared with 3-mm pellets, and Mueller Hinton broth was used as the elution vehicle instead of PBS [27].

Our preliminary data suggest the eluted daptomycin from both naturally sourced and synthetic CaSO₄ pellets, with and without K₂SO₄, is active against *S. aureus*, inhibiting bacterial growth for varying lengths of time. While the synthetic CaSO₄ pellets

with 3% K₂SO₄ demonstrated the highest activity against *S. aureus*, the synthetic pellets with 0% K₂SO₄ provided inhibition of *S. aureus* on Days 1 and 2 only, which can be explained by the low amount of daptomycin eluted from the pellets compared to the pellets with K₂SO₄. The inhibitory activity of the synthetic pellets with 0% K₂SO₄ is much lower than previously reported daptomycin inhibition of *S. aureus* from CaSO₄ and PMMA; however, the bacterial inhibition of the synthetic CaSO₄ pellets with 3% K₂SO₄ is much higher than the same reported data [12,26]. The positive growth measured on Day 2 for the naturally sourced CaSO₄ pellets may have been caused by an unknown contaminant because there were similar amounts of daptomycin present in the pellets on Days 4 and 6. Additionally, similar naturally sourced CaSO₄ pellets were previously reported to inhibit *S. aureus* for 10 days without any contamination and inhibited *S. aureus* for 28 days with two cases of contamination [6].

This preliminary research provides researchers and clinicians with additional information on the two commercially available forms of CaSO₄ for a local delivery system for infection prevention or treatment. Our study has also shown although K₂SO₄ is not necessary for forming pellets from synthetic CaSO₄, it may be helpful for decreased degradation, an increased daptomycin elution profile, and potentially extended activity against susceptible organisms. Further investigations, including preclinical in vivo studies and biofilm associated investigations, are needed to determine functional differences and applications of these local drug delivery systems.

References

1. Nandi SK, Mukherjee P, Roy S, Kundu B, De DK, Basu D. Local antibiotic delivery systems for the treatment of osteomyelitis- A review. *Materials Science and Engineering C* 2009;29:2478-2485.
2. Finney MS, Crank CW, Segreti J. Use of daptomycin to treat drug-resistant Gram-positive bone and joint infections. *Curr Med Res Opin* 2005;21(12):1923-6.
3. Hanssen AD. Local antibiotic delivery vehicles in the treatment of musculoskeletal infection. *Clin Orthop Relat Res* 2005(437):91-6.
4. Enoch D, Bygott JM, Daly M, Kara JA. Daptomycin. *J Infect* 2007;55:205-213.
5. Louie A, Kaw P, Liu W, Jumbe N, Miller MH, Drusano GL. Pharmacodynamics of daptomycin in a murine thigh model of *Staphylococcus aureus* infection. *Antimicrobi Agents Chemother* 2001;45:845-851.
6. Webb ND, McCanless JD, Courtney HS, Bumgardner JD, Haggard WO. Daptomycin Eluted From Calcium Sulfate Appears Effective Against *Staphylococcus*. *Clin Orthop Relat Res* 2008;466:1383-1387.
7. Richelsoph KC, Webb ND, Haggard WO. Elution Behavior of Daptomycin-loaded Calcium Sulfate Pellets. *Clinical Orthopaedics and Related Research* 2007;461:68-73.
8. van Hal SJ, Paterson DL, Gosbell IB. Emergence of daptomycin resistance following vancomycin-unresponsive *Staphylococcus aureus* bacteraemia in a daptomycin-naive patient-a review of the literature. *Eur J Clin Microbiol Infect Dis* 2010.
9. Peltier L. The use of plaster of Paris to fill large defects in bone. *Am J Surg* 1959;97:11-15.
10. Thomas DB, Brooks DE, Bice TG, DeJong ES, Lonergan KT, Wenke JC. Tobramycin-impregnated calcium sulfate prevents infection in contaminated wounds. *Clin Orthop Relat Res* 2005;441:366-71.
11. Jackson SR, Richelsoph KC, Courtney HS, Wenke JC, Branstetter JG, Bumgardner JD, Haggard WO. Preliminary In Vitro Evaluation of an Adjunctive Therapy for Extremity Wound Infection Reduction: Rapidly Resorbing Local Antibiotic Delivery. *Journal of Orthopaedic Research* 2008;7:903-908.
12. Dacquet V, Varlet A, Tandogain R, Tahon M, Fournier L, Jehl F, Monteil H, Bascoulergue G. Antibiotic-impregnated plaster of Paris beads-trials with teicoplanin. *Clin Orthop Relat Res* 1992;282:241-249.

13. Heijink A, Yaszemski M, Patel R, Rouse M, Lewallen D, Hanssen A. Local antibiotic delivery with osteoset, DBx, and collagraft. *Clin Orthop Relat Res* 2006;451:29-33.
14. Mackey D, Varlet A, Debeaumont D. Antibiotic loaded plaster of Paris pellets: an in vitro study of a possible method of local antibiotic therapy in bone infection. *Clin Orthop Relat Res* 1982;167:263-268.
15. Diefenbeck M, Muckley T, Hofmann GO. Prophylaxis and treatment of implant-related infections by local application of antibiotics. *Injury* 2006;37:S95-S104.
16. McLaren AC. Alternative materials to acrylic bone cement for delivery of depot antibiotics in orthopaedic infections. *Clin Orthop Relat Res* 2004(427):101-6.
17. Turner T, Urban R, Hall D, Chye P, Segreti J, Gitelis S. Local and systemic levels of tobramycin delivered from calcium sulfate bone graft substitute pellets. *Clin Orthop Relat Res* 2005;437:97-104.
18. McKee M, Wild L, Schemitsch E, Waddell J. The use of an antibiotic-impregnated, osteoconductive, bioabsorbable bone substitute in the treatment of infected long bone defects: early results of a prospective trial. *J Orthop Trauma* 2002;16(9):622-627.
19. Branstetter J, Jackson S, Haggard W, Richelsoph K, Wenke J. Locally-administered antibiotics in wounds in a limb. *J Bone Joint Surg Br* 2009;91(8):1106-1109.
20. Gitelis S, Virkus W, Anderson D, Piasecki P, Yao TK. Functional outcomes of bone graft substitutes for benign bone tumors. *Orthopedics* 2004;27(1 Suppl):s141-4.
21. Cai Z-Y, Yang D-A, Zhang N, Ji C-G, Zhu L, Zhang T. Poly(propylene fumarate)/(calcium sulphate/B-tricalcium phosphate) composites: Preparation, characterization and in vitro degradation. *Acta Biomaterialia* 2009;5:628-635.
22. Tomihata K, Ikada Y. In vitro and in vivo degradation of films of chitin and its deacetylated derivatives. *Biomaterials* 1997;18(7):567-75.
23. Costerton JW, Lewandowski Z, Caldwell DE, Korber DR, Lappin-Scott HM. Microbial biofilms. *Annu Rev Microbiol* 1995;49:711-45.
24. McLaren AC, McLaren SG, Smeltzer M. Xylitol and glycine fillers increase permeability of PMMA to enhance elution of daptomycin. *Clin Orthop Relat Res* 2006;451:25-8.
25. Lewis G, Brooks JL, Courtney HS, Li Y, Haggard WO. An Approach for determining antibiotic loading for a physician-directed antibiotic-loaded PMMA bone cement formulation. *Clin Orthop Relat Res* 2010;468(8):2092-100.

26. Lewis G, Janna S. Estimation of the optimum loading of an antibiotic powder in an acrylic bone cement: gentamicin sulfate in SmartSet HV. *Acta Orthop* 2006;77(4):622-7.
27. Kanellakopoulou K, Panagopoulos P, Giannitsioti E, Tsaganos T, Carrer D-P, Efstathopoulos N, Giamerellos-Bourboulis E. In Vitro Evaluation of Daptomycin by a Synthetic Crystalline Semihydrate Form of Calcium Sulfate, Stimulan. *Antimicrobial Agents and Chemotherapy* 2009;July 2009:3106-3107.

APPENDIX D

A DAPTOMYCIN-XYLITOL-LOADED POLYMETHYLMETHACRYLATE BONE CEMENT HOW MUCH XYLITOL SHOULD BE USED?

Introduction

A recurring challenge with total joint arthroplasty (TJA) is periprosthetic joint infection (PJI) [13, 39, 49]. The prevalence of this phenomenon is variable, ranging from 0.3% to 9% for primary cases [11, 48] and from 2% to 40% for revision cases [24, 49]. The ramifications are serious for the patient (in most cases, revision is necessary using, for example, the two-stage method [38]) and treatment costs are high (for example, in 2009, in the United States, the mean total charge for revision of an infected THA was approximately USD 94,000 [21]). Thus, there have been many efforts to reduce the likelihood of PJI [13, 24] and improve treatment options [38, 45].

One approach to improving treatment is to use an antibiotic-loaded polymethylmethacrylate (PMMA) bone cement (ALABC) in which the cement powder is blended with a novel antibiotic [15, 31]. Novel antibiotics are considered those with potential to have rapid and effective bactericidal activity against pathogens, such as methicillin-resistant *Staphylococcus aureus* and *Staphylococcus epidermidis*, that have become resistant to many of the common antibiotics used in current approved commercially available ALABC brands or orthopaedic surgeon-prepared/directed formulations (such as gentamicin, tobramycin, and vancomycin [13, 39, 45]). Although there is a growing number of these novel antibiotics (eg, dalbavancin, daptomycin, telavancin, and tigecycline) [4, 8, 10, 12, 15, 19, 31, 42, 45], only a few, such as daptomycin and telavancin, have been used in PJI treatment [15, 31].

Several studies have reported the in vitro properties of either low-dose daptomycin-loaded PMMA bone cement (low-dose is defined as ≤ 1 g daptomycin per 40 g cement powder [13]) [5, 14, 26] or a higher-dose variant (≥ 2 g) [5, 14, 26, 41]. These reports show the daptomycin release profile in phosphate-buffered saline (PBS) solution, at 37° C, is characterized by a burst followed by a period of slow decrease [5, 14, 26]. At relatively low amounts (up to 7.5% of the mass of the dry cement powder-daptomycin mixture), the daptomycin exerts a marginal influence on the cement's fatigue limit, tensile strength, yield strength, compressive strength, and compressive modulus (compared to the value for a cement that did not contain the antibiotic) [14, 26, 41], but with a higher amount of daptomycin (11 wt/wt%), there is an appreciable drop in the cement's fatigue limit [26]. There is a sizeable literature on methods to improve the release profile of antibiotics from ALABC cylinders, including incorporation of a particulate filler (such as lactose, mesoporous silica nanoparticles, or xylitol) in the cement powder [9, 37, 43] and subjection of cured cement specimens to continuous or intermittent watt-level low-frequency ultrasound [3]. However, none of these reported methods have been evaluated for daptomycin-loaded PMMA bone cement. Also, in the case of an ALABC loaded with a poragen, the question as to the appropriate poragen amount has not been fully investigated.

We therefore asked: What is an appropriate amount of xylitol to be used in a daptomycin-xylitol-loaded PMMA bone cement?

Materials and Methods

The study design comprised three parts as seen in Figure 1. (1) We prepared four groups of cement, one not loaded with the xylitol and three having different xylitol

masses, namely, 0.7, 1.4, and 2.7 g; (2) For each of these four groups, we determined the following cement properties: fracture toughness, fatigue limit, daptomycin release rate, coefficient of diffusion for outflow of daptomycin (D_{dapt}), an index of activity of the daptomycin eluate against *S aureus*, polymerization rate at 37° C, coefficient of diffusion for intake of 1X PBS solution, and radiopacity (see Figure 1 for numbers of specimens or replicates used for each type of testing). These determined properties are of clinical relevance [17, 25, 29, 35, 41, 43, 44]. (3) We used an optimization method to assess an appropriate xylitol amount.

The materials used were a commercially available brand of PMMA bone cement (Orthoset[®] 1; Wright Medical Technology, Inc, Arlington, TN, USA), daptomycin (Cubicin[®]; Cubist Pharmaceuticals, Lexington, MA, USA), and xylitol (XyloSweet[®]; XLEAR, Orem, UT, USA). The daptomycin amount used (1.36 g/40 g dry cement powder) was determined, from our previous work [26], based on the fatigue life, rate of release of daptomycin, and activity of the released daptomycin against *S aureus* of daptomycin-loaded Orthoset[®] 1 cement. The xylitol amounts (X) of the cements in the four study groups were 0, 1.66, 3.27, and 6.13 wt/wt% of the total dry cement powder mixture mass. In a separate study, we used a volumetric displacement method in a liquid in which the powder was not soluble to determine the densities of the dry cement powder, daptomycin, and xylitol to be 1.25, 1.20, and 1.50 g cm⁻³, respectively. Thus, the corresponding xylitol amounts were 0, 1.39, 2.74, and 5.16 vol/vol% of the total dry cement powder mixture volume.

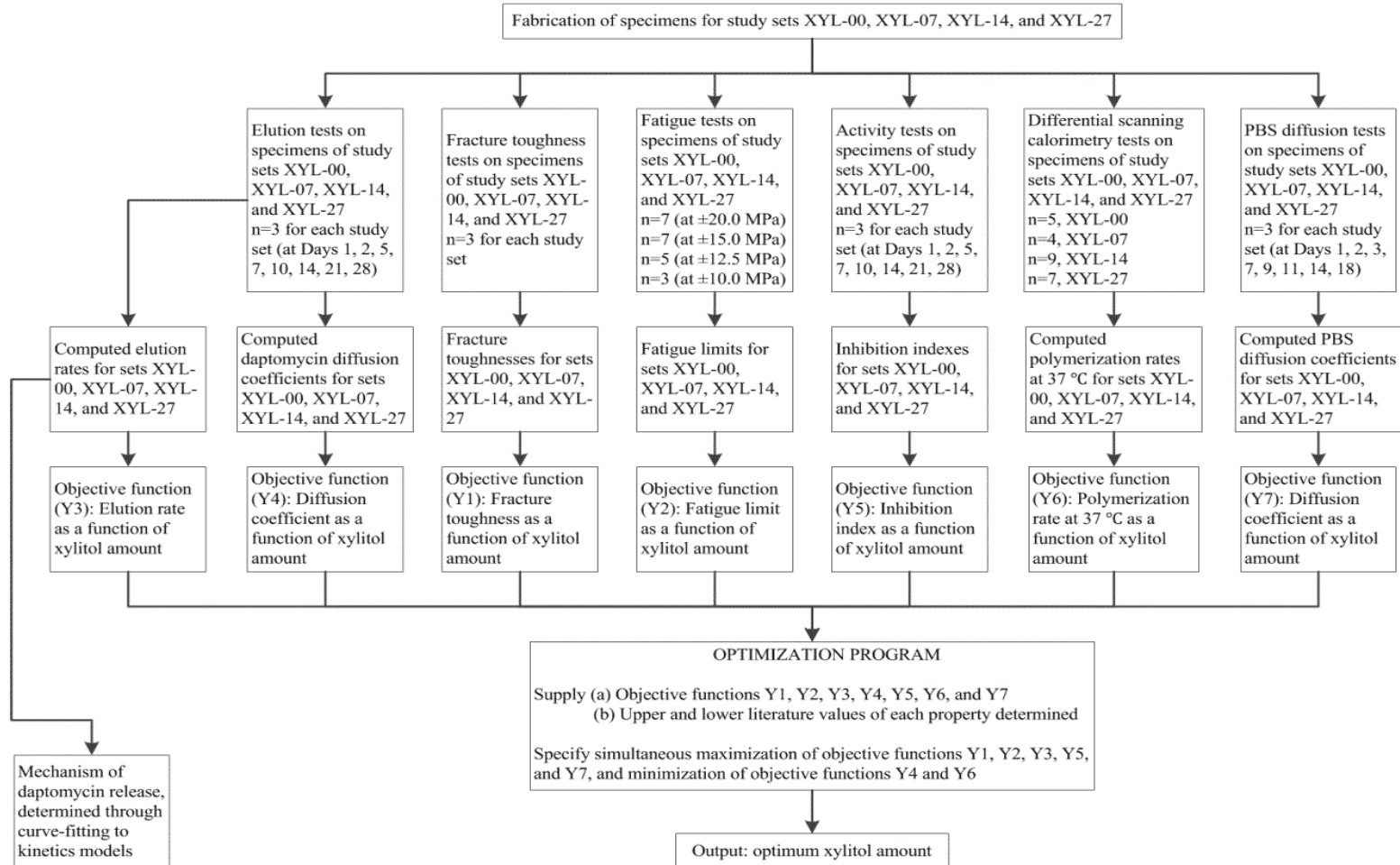


Figure 1. A flowchart shows the study design. The key features of the eight cement property characterization tests conducted are shown: fracture toughness (Y1), fatigue limit (Y2), daptomycin elution rate (Y3), diffusion coefficient for daptomycin egress (Y4), inhibition index (Y5), polymerization rate, at 37° C (Y6), diffusion coefficient for PBS intake (Y7), and normalized radiopacity (Y8). Study sets were no xylitol (XYL-00), 0.7 wt/wt% xylitol (XYL-07), 1.4 wt/wt% xylitol (XYL-14), and 2.7 wt/wt% xylitol (XYL-27).

Before the preparation of the cement groups, the daptomycin was stored at $4^{\circ} \pm 1^{\circ}$ C, while the xylitol and the cement powder and liquid monomer were stored in ambient laboratory conditions (temperature and relative humidity of $21^{\circ} \pm 1^{\circ}$ C and $57\% \pm 2\%$, respectively). A commercially available cement powder mixer (OmoMix[®]; Tecres SpA, Verona, Italy) was used to mix the dry cement powder, daptomycin, and xylitol. For the fracture toughness tests, the final powder mixture and the liquid monomer of the cement (18.37 mL) were vacuum-mixed using a commercially available unit (MixeVac[®] II High-Vacuum System; Stryker Instruments, Kalamazoo, MI, USA), with an evacuation pressure of 74 ± 1 kPa. The prepared cement dough was injected into a stainless steel mold whose internal configuration and dimensions were of a compact tension test specimen, whose dimensions conformed to those stipulated in ASTM D5045 [2]: overall nominal height, width, and thickness = 35.7 mm, 37.2 mm, 14.9 mm, respectively. The protocols used for finishing the specimens, accepting specimens for testing, conditioning the accepted specimens, performing the tests, and treating the results to obtain the fracture toughness (K_{IC}) of the cement were the same as those given in our previous work [30].

For the fatigue tests, the prepared cement dough was injected into a four-celled silicone mold, with each cell having internal configuration and dimensions of a solid cylindrical dog bone, whose dimensions conformed to those stipulated in ASTM F2118-03 [1]: overall nominal diameter and length = 8.5 mm and 62 mm, respectively. Protocols for inspecting the fabricated specimens, selecting acceptable specimens, choosing the specimens to be tested from the acceptable ones, conditioning the test

specimens, and performing the tests were the same as those given in our previous work [26]. Per ASTM F2118-03, acceptable specimens are those with no surface defects in the gage or transition sections and no internal defects with major diameter of larger than 1 mm in the gage section. The acceptable specimens were conditioned in 1X PBS, at $37^{\circ} \pm 1^{\circ}$ C, for 7 days before the tests. During the tests, the specimen was immersed in 1X PBS, at $37^{\circ} \pm 1^{\circ}$ C. For each cement group, the combination of applied stress (S) and number of specimens used were ± 20 MPa (seven specimens), ± 15 MPa (seven specimens), ± 12.5 MPa (five specimens), and ± 10 MPa (three specimens). These stresses have been used in many literature studies [7, 22, 26, 47], with ± 10 MPa being of the order postulated to be experienced in the cement mantle in a cemented TJA [18]. The test results were presented in the form of S versus number of cycles to fracture, N_f (as before [26], run-out was defined as no fracture after 1.557 million loading cycles). The method used for estimating the fatigue limit of the cement was the same as that used in our previous work [26].

For each cement group, 75% to 89% of the fabricated specimens were found acceptable for fatigue testing but not all were used. From among those not used, three were selected at random for the daptomycin release tests. These elution tests were performed using the protocols in our previous study [26]. The amount of daptomycin released was measured in 10 mL 1X PBS solution, at $37^{\circ} \pm 1^{\circ}$ C, at eight time points (t) of 1, 2, 5, 7, 10, 14, 21, and 28 days, with complete PBS refreshment at each time point. The release results were compiled as current amount of daptomycin released (W) versus t and cumulative amount (M) versus t. A commercially available software package (MATLAB[®] R2011b; The MathWorks, Natick, MA, USA) was used to obtain the best-fit

relationship between W and t . The daptomycin release rate was then computed as the derivative of this W -versus- t relationship calculated at the value of t midway between the burst release point and the point at which the W -versus- t curve began to flatten.

The release of daptomycin from a test specimen was approximated using the expression for release of a drug from a specimen possessing aspects of both a long cylinder and a thin disc [40]. With the aid of a scientific calculator (TI-89 Titanium; Texas Instruments, Inc, Dallas, TX, USA), the M -versus- t results and the aforementioned expression were used to compute D_{dapt} .

After the daptomycin release tests were completed, eluates at each of the eight time points were tested for an index of antimicrobial activity against *S aureus*, as described previously [26]. Thus, 200 μL of eluates were added to 1.75 mL Mueller Hinton II broth supplemented with 25 μg CaCl_2 per mL followed by the addition of an inoculum of *S aureus* ($\sim 10^4$ colony-forming units [CFUs]) and an overnight incubation at 37° C. Growth was determined by measuring the optical density (OD) of the solutions, at 530 nm, using an ultraviolet spectrophotometer (GENESYS™ 20; Thermo Scientific, West Palm Beach, FL, USA). The inhibition index (I) was computed as before [26]. The differential scanning calorimetry work was performed at a heating rate of 15 K minute^{-1} (DuPont 910; Instrument Specialists, Inc, Spring Grove, IL, USA). The protocols used and the steps employed in treating the results to obtain the cement polymerization rate at 37° C (k') were as described in our previous work [30].

The PBS intake test involved measuring the mass gain of a circular cross-sectioned cement disc specimen cut from the end of an acceptable fatigue test specimen (nominal diameter and thickness of 8.50 mm and 3.00 mm, respectively) immersed in 15

mL 1X PBS solution at $37^{\circ} \pm 1^{\circ}$ C. Measurement continued until there was no observable increase in mass gain. Details of all the steps involved in using the mass gain versus time in PBS results to compute the PBS diffusion coefficient (D_{PBS}) were given in our previous work [30].

The experimental protocols followed for the determination of the radiopacity (R) of the cement were the same as presented in our previous work [28]. However, in the present work, R was calculated as the ratio of the linear attenuation coefficient (μ) for the cement (slope of the linear regression plot of the logarithm of OD of cement disc versus cement disc thickness) to μ for Al (slope of the linear regression plot of OD of Al step-wedge versus Al step-wedge thickness) and expressed as equivalent Al% [36]. The normalized radiopacity (R') was computed as the ratio of R to the mass fraction of the radiopacifier in the cement powder (9.1 wt/wt% BaSO₄ for each cement group).

The optimization method used to assess the appropriate xylitol loading comprised seven steps: (1) for each of the eight cement properties, obtain the best-fit relationship between the determined values and X; this relationship is called an “objective function”; (2) for each of the cement properties, find the highest and lowest value, as given in previous literature; (3) for each cement property, calculate the its fractional objective function at a given value of X (within the range 0 - 6.13 wt/wt%) as follows: (value of the objective function at X – lowest literature value of property) divided by (highest literature value of property – lowest literature value of property); (4) for a property that should be as high as possible (for example, fatigue limit), calculate the quantity, (fractional objective function)² at the X value . Call this quantity Y1. Alternatively, for each property that should be as low as possible (for example, k'), calculate the quantity [1-

(fractional objective function)]² at the X level Call this quantity Y2; (5) repeat steps (3) and (4) for all the properties and hence calculate the master modified fractional objective function (MMFOF) as equal to (sum of all the values of Y2)-(sum of all the values of Y1); (6) repeat steps (3) – (5) at other values of X (within the range 0 – 6.13 wt/wt%); (7) determine the appropriate value of X as that at which the maximum value of MMFOF, when plotted against X, occurs. Thus, this appropriate value is the one that gives the best tradeoff among the cement properties. The calculations in step (1) and those in steps (3) – (7) were carried with the aid of commercially available software packages (TableCurve 2D v5.01; SYSTAT Software Inc, Chicago, IL (USA) and Microsoft[®] Excel[®] Solver; Microsoft Corp, Redmond, WA, USA), respectively.

Results

The results of the daptomycin release profile, the activity of the released daptomycin against *S aureus*, fatigue lives, and the other cement properties are presented in Figure 2, Table 1, Figure 3, and Table 2, respectively.

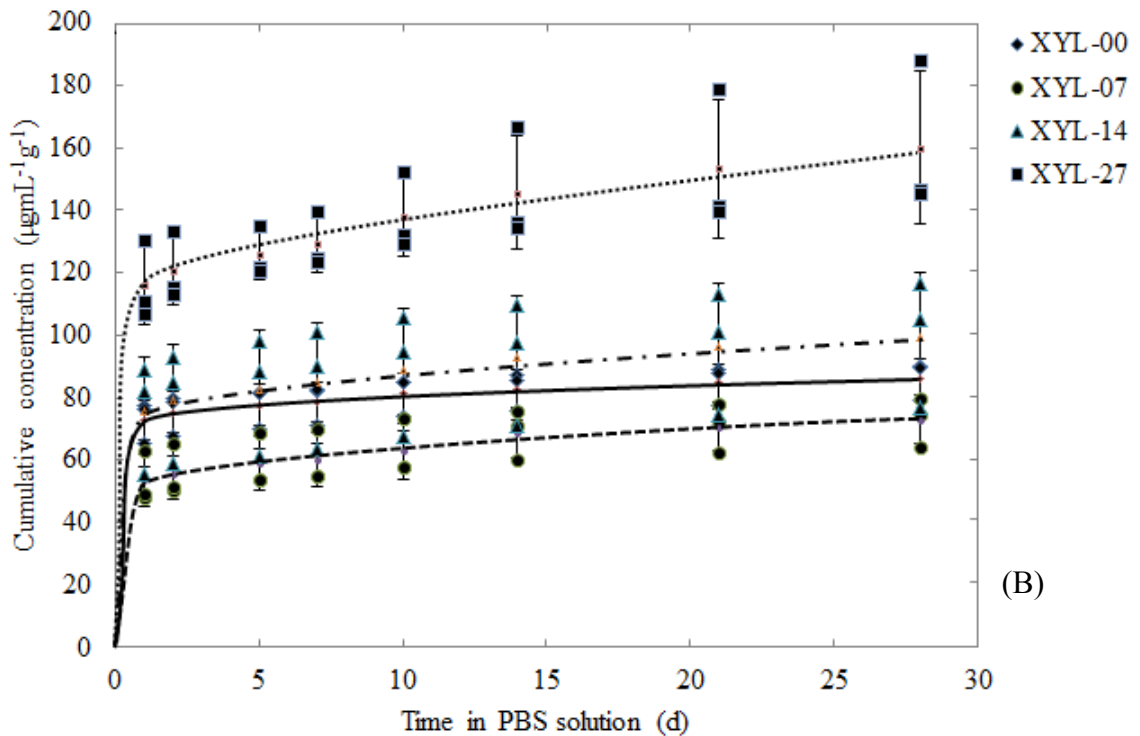
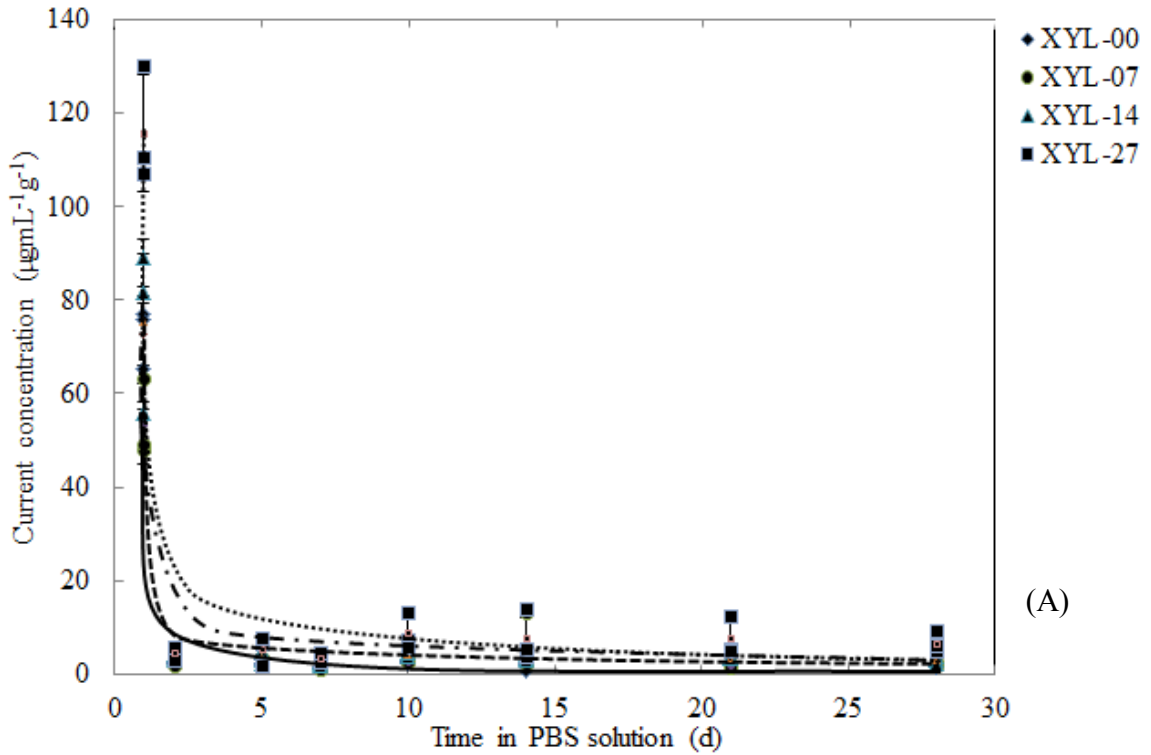


Figure 2A–B. Graphs show the daptomycin release profiles in (A) current amount and (B) cumulative amount. Study sets were no xylitol (XYL-00), 0.7 wt/wt% xylitol (XYL-07), 1.4 wt/wt% xylitol (XYL-14), and 2.7 wt/wt% xylitol (XYL-27). The daptomycin release profile depended on the xylitol amount.

Table 1. Summary of values of cement properties

Cement	K_{IC} (MPa \sqrt{m})*	Fatigue limit (MPa) [†]	Daptomycin release rate ($\mu\text{g mL}^{-1} \text{d}^{-1}$ g^{-1})*	D_{dapt} (10^{-11} $\text{m}^2 \text{s}^{-1}$)*	k' (10^{-3}s^{-1})	D_{PBS} (10^{-12} $\text{m}^2 \text{s}^{-1}$)*	R' (equivalent AI% MR ⁻¹) ^{‡§}
XYL-00	1.92 \pm 0.04	9.9 (8.3, 11.6)	45.2	3.75 \pm 0.21	2.59 \pm 2.10	4.49 \pm 1.05	4.51
XYL-07	1.89 \pm 0.06	9.8 (8.3, 11.3)	34.6	2.53 \pm 0.63	2.21 \pm 1.20	4.34 \pm 1.60	3.30
XYL-14	1.96 \pm 0.02	8.8 (6.2, 11.4)	50.0	2.72 \pm 0.26	0.67 \pm 0.32	3.37 \pm 1.33	3.41
XYL-27	1.88 \pm 0.04	9.7 (8.6, 10.8)	74.3	2.44 \pm 0.29	0.61 \pm 0.22	5.92 \pm 1.15	3.63

*Values are expressed as mean \pm SD; [†] values are expressed as mean, with 95% CIs in parentheses; [‡] values are expressed as mean only; [§] MR = mass ratio of the radiopacifier in the cement powder (9.1 wt/wt% BaSO₄); K_{IC} = fracture toughness; D_{dapt} = coefficient of diffusion for outflow of Daptomycin; k' = cement polymerization rate at 37°C; D_{PBS} = coefficient of diffusion for intake of 1X phosphate-buffered saline solution; R' = normalized radiopacity; XYL-00 = no xylitol; XYL-07 = 0.7 wt/wt% xylitol; XYL-14 = 1.4 wt/wt% xylitol; XYL-27 = 2.7 wt/wt% xylitol.

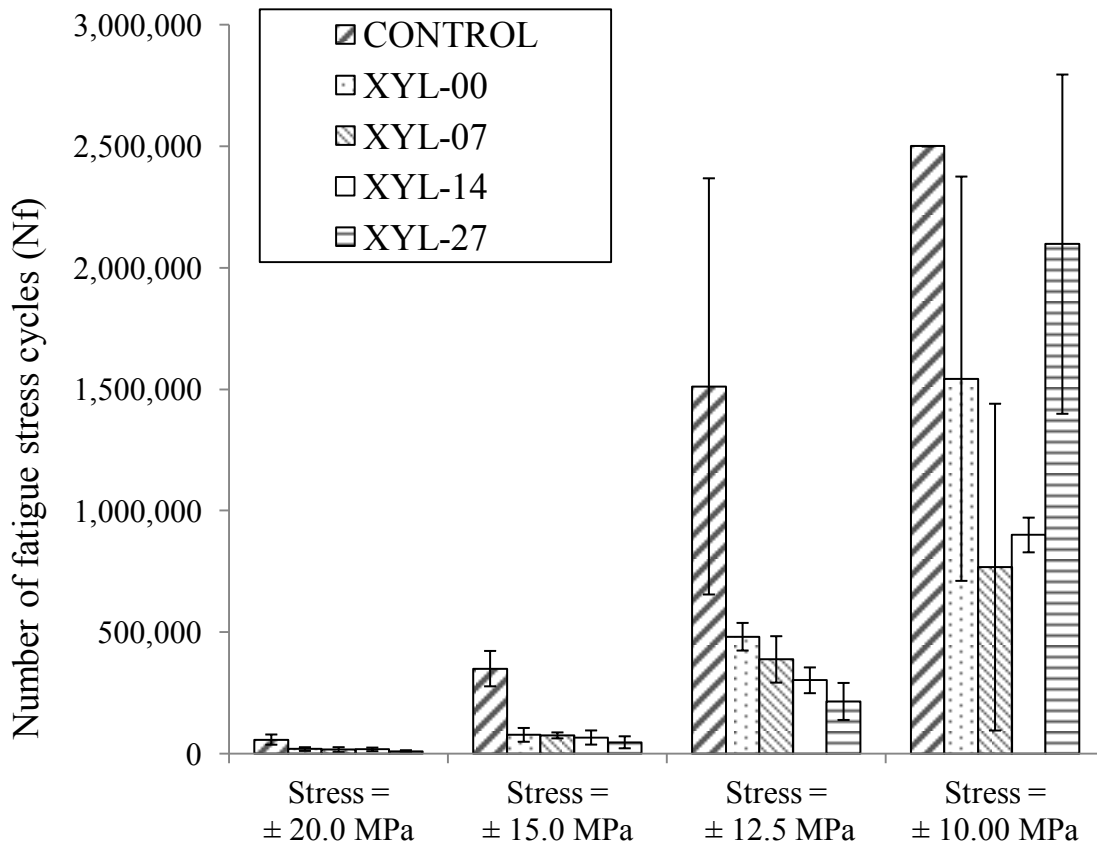


Figure 3. A graph summarizes the fatigue test results. At stresses of the order experienced in the cement mantle in a cemented TJA (10 MPa), xylitol did not adversely affect fatigue life. Study sets were no xylitol (XYL-00), 0.7 wt/wt% xylitol (XYL-07), 1.4 wt/wt% xylitol (XYL-14), and 2.7 wt/wt% xylitol (XYL-27). Values are shown as mean with standard deviation.

Table 2. Summary of activity test results

Cement	Growth/inhibition of <i>Staphylococcus aureus</i> *								Mean inhibition index [†] (%)
	Elution time (days)								
	1	2	5	7	10	14	21	28	
XYL-00	-	-	-	-	-	+	+	+	62.5
XYL-07	-	-	-	-	-	-	-	-	100
XYL-14	-	-	-	-	-	-	-/+ [‡]	-	95.8
XYL-27	-	-	-	-	-	-	-	-	100

* + = growth of *S. aureus* (inhibition index = 0); - = inhibition of *S. aureus* (inhibition index = 100%); [†] for a cement, index = (sum of inhibition indexes/total number of test specimens (= 24)); [‡] of the three samples tested, two inhibited and one allowed growth of *S. aureus*; XYL-00 = no xylitol; XYL-07 = 0.7 wt/wt% xylitol; XYL-14 = 1.4 wt/wt% xylitol; XYL-27 = 2.7 wt/wt% xylitol.

Using these results, the objective functions (which are given in Table 3), and the optimization method presented, we determined the appropriate xylitol amount to be 4.45 wt/wt% (equivalent to final dry powder mixture composition of 1.93 g xylitol, 1.36 g daptomycin, and 40 g cement powder).

Table 3. Summary of the objective functions (that is, best-fit relationships between each of the properties determined and the xylitol loading (X))

Cement property	Best-fit relationship	Adjusted R ^{2a}
Fracture toughness (Y1)	$Y1 = 1.924 - 9.205x \cdot 10^{-5} * e^X$	0.089
Fatigue limit (Y2)	$Y2 = 9.378 + 0.5603 * e^{-X}$	0.0799
Daptomycin elution rate (Y3)	$Y3 = 0.03583 + 0.000327 * X^{2.5}$	0.7163
Diffusion coefficient for daptomycin egress (Y4)	$Y4 = 2.587 \times 10^{-11} - 2.022 \times 10^{-13} * \ln(X)$	0.8933
Inhibition index (Y5)	$Y5 = 96.77 * X^{0.01578}$	0.9575
Polymerization rate, at 37 °C (Y6)	$Y6 = 0.002656 / (1.0 + (x / 2.598)^{2.728})$	0.7776
Diffusion coefficient for PBS intake (Y7)	$Y7 = 4.036 \times 10^{-12} + 4.053 \times 10^{-15} * e^X$	0.2028
Normalized radiopacity (Y8)	$Y8 = 1 / (0.292 - 0.069 * e^X)$	0.5824

^aCoefficient of multiple determination, adjusted for the degrees-of-freedom of the equation.

Discussion

In TJAs, it is common practice to use either a commercially available brand or an orthopaedic surgeon-prepared/directed formulation of an ALABC as a prophylaxis agent against PJI [13, 39, 49]. There are many reports of substantial decrease in susceptibility

of the pathogens involved in PJI (such as methicillin-resistant *S aureus*) to the antibiotic incorporated in the cement powder (usually, gentamicin, tobramycin, or vancomycin) [45]. This decrease in susceptibility provides opportunity to develop novel antibiotics. Among novel antibiotics, there are reports of the effectiveness of daptomycin and telavancin against these pathogens [15, 31]. Literature reports on daptomycin-loaded cement cylinders show the daptomycin release rate is low [5, 14, 26]. When a poragen was added to the cement powder of an ALABC, antibiotic release rate from cylindrical specimens increased, but there are limited data on the impact on other cement properties [37]. The question as to what should be an appropriate poragen amount in an ALABC that contains a poragen has not been posed. In this study, we determined the appropriate amount of xylitol to be used in a daptomycin-xylitol-loaded PMMA bone cement.

We recognize several limitations of our study. First, although there are reports indicating xylitol-containing dental products may be useful in preventing or reducing the progression of dental caries [32]), the question as to the safety of xylitol as a constituent of an ALABC is an open one. However, there are reports of the beneficial effects of dietary xylitol against weakening of bone in aged animal models [33]. Thus, a xylitol-loaded ALABC may be viable for use in cemented TJAs. Second, we used one cement brand, one antibiotic, and one brand of xylitol. Given the large numbers of cement brands and antibiotics available, the present approach is justified from the perspective of study time and cost. Third, the conditions under which the daptomycin release tests were conducted are different in a number of respects, notably fluid dynamics and sink details, from the in vivo medium in which a TJA is located [6, 23]. However, these experimental conditions reportedly produce vancomycin elution levels that are highly correlated with

those obtained from the hip of an animal model [50]. Fourth, we used a generalized measure of the activity of the released daptomycin against *S aureus*, rather than a specific one, such as the number of bacteria on a cement specimen (CFUs/surface area of the specimen). However, the former method was used in each of the other literature studies of daptomycin release from ALABC cylinders [5, 14, 26]; thus, we can compare present trends to those in these reports. We note two caveats regarding the appropriate xylitol loading we determined: (1) Even though a large and diverse array of cement properties was determined, there are other important ones that were not. One such property is resistance of a cement specimen to the formation of biofilm of a given pathogen implicated in PJI on its surface, a phenomenon that may result in a substantial reduction of the susceptibility of the pathogens to daptomycin [46]. Other undetermined properties are working time, which gives insight into the time window between packing the cement dough in the bone bed and placement of the prosthesis in that bed [20]; residual monomer content, which provides an indication of the potential for phenomena such as chemical necrosis of periprosthetic tissues [16]; and fatigue crack propagation rate in PBS, at 37° C, which may be related to the in situ life of a TJA [34]. (2) Weighting factors for the determined cement properties were not used; for example, considering the clinical application, in a head-to-head comparison between daptomycin release rate and fatigue limit, the former may be given a higher weighting factor. An investigation of the sensitivity of the assessed appropriate xylitol loading to the number of cement properties determined and the calculation of weighting factors for the cement properties determined are outside the confines of the present study. None of the above-mentioned limitations and caveats jeopardizes the assessed appropriate xylitol amount. However, these issues

should be taken into account if the present appropriate xylitol amount result is to be used in the clinical setting.

In a related study, Nugent et al. [37] investigated the influence of xylitol amount on the properties of ALABC cylindrical specimens and found antibiotic release increased progressively and compressive strength of the cement decreased, with increase in xylitol amount. However, Nugent et al. [37] used a medium-viscosity cement [20], the antibiotic tobramycin, and xylitol amounts from 1 g to 16 g of xylitol per 40 g of cement powder; hand-mixed the final powder mixture with the cement liquid monomer; and did not assess an appropriate xylitol amount. In contrast, we used a high-viscosity cement brand [20], daptomycin, and xylitol amounts from 0.7 g to 2.7 g of xylitol per 40 g of cement powder; vacuum-mixed the final powder mixture with the cement liquid monomer; and assessed an appropriate xylitol amount. Two other relevant studies were by Lewis et al. [26, 27] on the computation of the appropriate amount of the antibiotic in an ALABC. Two methodologies were used in one study [27], each involving changes of each of the properties determined with antibiotic dose. The methodology used in the other study [26] was the same as that used in the present work, but many more cement properties were determined in the present study (eight versus three). Thus, there are no literature studies comparable to the present investigation.

In conclusion, we found an appropriate xylitol amount for a daptomycin-xylitol-loaded PMMA bone cement was 4.46 wt/wt% (equivalent to 1.93 g xylitol mixed with 1.36 g daptomycin and 40 g cement powder). We recognize that this assessed amount is based on an analysis of a limited number of in vitro cement properties, including some

properties, such as the local minimum inhibitory concentration of the eluted daptomycin, that require confirmation from in vivo studies.

References

1. American Society for Testing and Materials. Standard F2118-03 (Reapproved 2009): standard test method for constant amplitude of force controlled fatigue testing of acrylic bone cement materials. In: *2010 Annual Book of ASTM Standards*. Volume 13.01. West Conshohocken, PA: ASTM International; 2010:994-1001.
2. American Society for Testing and Materials. Standard D5045-99 (Reapproved 2007): standard test methods for plane-strain fracture toughness and strain energy release rate of plastic materials. In: *2012 Annual Book of ASTM Standards*. Volume 08.02. West Conshohocken, PA: ASTM International; 2012:763-771.
3. Cai XZ, Chen XZ, Yan SG, Ruan ZR, Yan RJ, Ji K, Xu J. Intermittent watt-level ultrasonication facilitates vancomycin release from therapeutic acrylic bone cement. *J Biomed Mater Res B Appl Biomater*. 2009;90:11-17.
4. Cai Y, Wang R, Liang B, Bai N, Liu Y. Systematic review and meta-analysis of the effectiveness and safety of tigecycline for treatment of infectious disease. *Antimicrob Agent Chemother*. 2011;55:1162-1172.
5. Chang Y, Chen WC, Hsieh PH, Chen DW, Lee MS, Shih HN, Ueng SW. In vitro activities of daptomycin-, vancomycin-, and teicoplanin-loaded polymethylmethacrylate against methicillin-susceptible, methicillin-resistant, and vancomycin-intermediate strains of *Staphylococcus aureus*. *Antimicrob Agent Chemother*. 2011;55:5480-5484.
6. Cunningham B, McLaren AC, Pauken C, McLemore R. Liposomal formulation increases local delivery of amphotericin from bone cement: a pilot study. *Clin Orthop Relat Res*. 2012;470:2671-2676.
7. Davies JP, O'Connor DO, Burke DW, Harris WH. Influence of antibiotic impregnation on the fatigue life of Simplex P and Palacos R acrylic bone cements, with and without centrifugation. *J Biomed Mater Res*. 1989;23:379-397.
8. Doan TL, Fung HB, Mehta D, Riska PF. Tigecycline: a glycoacycline antimicrobial agent. *Clin Ther*. 2006;28:1079-1086.
9. Frutos G, Pastor JY, Martinez N, Virto MR, Torrado S. Influence of lactose addition to gentamicin-loaded acrylic bone cement on the kinetics of release of the antibiotic and the cement properties. *Acta Biomater*. 2010;6:804-811.
10. Higgins DL, Chang R, Debarov DV, Leung J, Wu T, Krause KM, Sandvik E, Hubbard JM, Kaniga K, Schmidt DE Jr, Gao Q, Cass RT, Karr DE, Benton BM,

- Humphrey PP. Telavancin, a multifunctional lipoglycopeptide, disrupts both cell wall synthesis and cell membrane integrity in methicillin-resistant *Staphylococcus aureus*. *Antimicrob Agent Chemother*. 2005;49:1127-1134.
11. Hirakawa K, Stulberg BN, Wilde AH, Bauer TW, Secic M. Results of 2-stage reimplantation for infected total knee arthroplasty. *J Arthroplasty*. 1998;13:22-28.
 12. Huang V, Cheung CM, Kaatz GW, Rybak MJ. Evaluation of dalbavancin, tigecycline, minocycline, tetracycline, teicoplanin and vancomycin against community-associated and multidrug-resistant hospital-associated methicillin-resistant *Staphylococcus aureus*. *Int J Antimicrob Agents*. 2010;35:25-29.
 13. Jiranek WA, Hanssen, Greenwald AS. Antibiotic-loaded bone cement for infection prophylaxis in total joint replacement. *J Bone Joint Surg Am*. 2006;88:2487-2500.
 14. Kaplan L, Kurdzeil M, Baker KC, Verner J. Characterization of daptomycin-loaded antibiotic cement. *Orthopedics*. 2012;35:e503-e509.
 15. Kaushal R, Hassoun A. Successful treatment of methicillin-resistant *Staphylococcus aureus*: prosthetic joint infection with telavancin. *J Antimicrob Chemother*. 2012;67:2052-2053.
 16. Kindt-Larsen T, Smith DB, Jensen JS. Innovations in acrylic bone cement and application equipment. *J Appl Biomater*. 1995;6:75-83.
 17. Kjellson F, Almen T, Tanner KE, McCarthy ID, Lidgren L. Bone cement x-ray contrast media: a clinically relevant method of measuring their efficacy. *J Biomed Mater Res B Appl Biomater*. 2004;70:354-361.
 18. Krause W, Mathis RS, Grimes LW. Fatigue properties of acrylic bone cement: S-N, P-N, and P-S-N data. *J Biomed Mater Res*. 1988;22(3 suppl):221-244.
 19. Kueche DK, Landon GC, Musher DM, Noble PC. Elution of vancomycin, daptomycin, and amikacin from acrylic bone cement. *Clin Orthop Relat Res*. 1991;264:302-308.
 20. Kuhn KD. *Bone Cements: Up-to-date Comparison of Physical and Chemical Properties of Commercial Materials*. Berlin, Germany: Springer-Verlag; 2000.
 21. Kurtz SM, Lau E, Watson H, Schmier JK, Parvizi J. Economic burden of periprosthetic joint infection in the United States. *J Arthroplasty*. 2012;27(8 suppl 1):61-65.e1.
 22. Kurtz SM, Villarraga ML, Zhao K, Edidin AA. Static and fatigue mechanical behavior of bone cement with elevated barium sulfate content for treatment of vertebral compression fractures. *Biomaterials*. 2005;26:3699-3712.

23. Kweon C, McLaren AC, Leon C, McLemore R. Amphotericin B delivery from bone cement increases with porosity but strength decreases. *Clin Orthop Relat Res.* 2011;469:3002-3007.
24. Lentino JR. Prosthetic joint infections: bane of orthopedists, challenge for infectious disease specialists. *Clin Infect Dis.* 2003;36:1157-1161.
25. Lewis G. Fatigue testing and performance of acrylic bone cement: state-of-the-art review. *J Biomed Mater Res B Appl Biomater.* 2003;66:457-486.
26. Lewis G, Brooks JL, Courtney HS, Li, Y, Haggard WO. An approach for determining antibiotic loading for a physician-directed antibiotic-loaded PMMA bone cement formulation. *Clin Orthop Relat Res.* 2010;468:2092-2100.
27. Lewis G, Janna S. Estimation of the optimum loading of an antibiotic powder in an acrylic bone cement. *Acta Orthop.* 2006;77:622-627.
28. Lewis G, Towler MR, Boyd D, German MJ, Wren A, Clarkin O, Yates A. Evaluation of two novel aluminum-free, zinc-based glass polyalkenoate cements as alternatives to PMMA bone cement for use in vertebroplasty and balloon kyphoplasty. *J Mater Sci Mater Med.* 2010;21:59-66.
29. Lewis G, Xu J, Deb S, Lasa BV, San Roman J. Influence of the activator in an acrylic bone cement on an array of cement properties. *J Biomed Mater Res A.* 2007;81:544-553.
30. Lewis G, Xu J, Madigan S, Towler MR. Influence of strontia on various properties of Surgical Simplex[®] P acrylic bone cement and experimental variants. *Acta Biomater.* 2007;3:970-979.
31. Licitra CM, Crespo A, Licitra D, Wallis-Crespo MC. Daptomycin for the treatment of osteomyelitis and prosthetic joint infection: retrospective analysis of efficacy and safety in an outpatient infusion center. *Internet J Infect Dis.* 2011;9(2).
32. Macek MD. Xylitol-based candies and lozenges may reduce caries on permanent teeth. *J Evid Base Dent Pract.* 2012;12:71-73.
33. Mattila PT, Svanberf MJ, Jamsa T, Knuutila ML. Improved bone biomechanical properties in xylitol-fed aged rats. *Metabolism.* 2002;51:92-96.
34. Molino LN, Topoleski LD. Effect of BaSO₄ on the fatigue crack propagation rate of PMMA bone cement. *J Biomed Mater Res.* 1996;31:131-137.
35. Morejon L, Delgado JA, Davidenko N, Mendizabal E, Barbosa EH. Kinetic effect of hydroxyapatite types on the polymerization of acrylic bone cements. *Int J Polym Mater.* 2003;52:637-654.

36. Nomoto R, Mishima A, Kobayashi K, McCabe JF, Darvell BW, Watts DC, Momoi Y, Hirano S. Quantitative determination of radio-opacity: equivalence of digital and film x-ray systems. *Dent Mater.* 2008;24:141-147.
37. Nugent M, McLaren A, Vernon B, McLemore R. Strength of antimicrobial bone cement decreases with increased poragen fraction. *Clin Orthop Relat Res.* 2010;468:2101-2106.
38. Parvizi J, Adeli B, Zmistowski B, Restrepo C, Greenwald AS. Management of periprosthetic joint infection: the current knowledge. *J Bone Joint Surg Am.* 2012;94:e104(1-9).
39. Parvizi J, Saleh KJ, Ragland PS, Pour AE, Mont MA. Efficacy of antibiotic-impregnated cement in total hip replacement: a meta-analysis. *Acta Orthop.* 2008;79:335-341.
40. Ritger PL, Peppas N. A simple equation for description of solute release I. Fickian and non-Fickian release from non-swellable devices in the form of slabs, spheres, cylinders or discs. *J Control Release.* 1987;5:23-36.
41. Rouse MS, Piper KE, Jacobson M, Jacofsky, Steckelberg JM, Patel R. Daptomycin treatment of *Staphylococcus aureus* experimental chronic osteomyelitis. *J Antimicrob Chemother.* 2006;57:301-305.
42. Sauermann R, Rothenburger M, Graninger W, Joukhadar C. Daptomycin: a review 4 years after first approval. *Pharmacology.* 2008;81:79-91.
43. Shen SC, Ng WK, Shi Z, Chia L, Neoh KG, Tan RB. Mesoporous silica nanoparticle-functionalized poly(methyl methacrylate)-based bone cement for effective antibiotics delivery. *J Mater Sci Mater Med.* 2011;22:2283-2292.
44. Shiramizu K, Lovric V, Leung A, Walsh WR. How do porosity-inducing techniques affect antibiotic elution from bone cement? An in vitro comparison between hydrogen peroxide and a mechanical mixer. *J Orthop Traumatol.* 2008;9:17-22.
45. Song JH. What's new on the antimicrobial horizon? *Int J Antimicrob Agents.* 2008;32:S207-S213.
46. Tan H, Peng Z, Li Q, Xu X, Guo S, Tang T. The use of quaternised chitosan-loaded PMMA to inhibit biofilm formation and downregulate the virulence-associated gene expression of antibiotic-resistant staphylococcus. *Biomaterials.* 2012;33:365-377.
47. Tanner KE, Wang J-S, Kjellson F, Lidgren L. Comparison of two methods of fatigue testing bone cement. *Acta Biomater.* 2010;6:943-952.
48. Trampuz A, Osmon DR, Hanssen AD, Steckelberg JM, Patel R. Molecular and antibiofilm approaches to prosthetic joint infection. *Clin Orthop Relat Res.* 2003;414:69-88.

49. Trampuz A, Zimmerlt W. Prosthetic joint infections: update in diagnosis and treatment. *Swiss Med Wkly*. 2005;135:243-251.
50. Yan S, Cai X, Yan W, Dai X, Wu H. Continuous wave ultrasound enhances vancomycin release and antimicrobial efficacy of antibiotic-loaded acrylic bone cement in vitro and in vivo. *J Biomed Mater Res B Appl Biomater*. 2007;82:57-64.

APPENDIX E.

Animal Use Protocol Approvals

1. The University of Memphis Institutional Animal Care and Use Committee Protocol Action Form

Protocol 0720 Approval: Antibiotic-loaded biopolymer sponge for prevention of polymicrobial wound infection (Rat Model, Chapter 2)

2. Department of the Army, US Army Medical Research and Materiel Command, Animal Care and Use Review Office Protocol Approval Form

Protocol DM090455.02 Approval: Antibiotic-loaded biopolymer sponge for prevention of polymicrobial wound infection (Rat Model, Chapter 2)

3. The University of Memphis Institutional Animal Care and Use Committee Protocol Action Form

Protocol 0728 Approval: Biopolymer sponge and paste for prevention of polymicrobial wound infection (Rat Model, Chapter 3)

4. The University of Arkansas for Medical Science Institutional Animal Care and Use Committee Protocol Approval Letter

Protocol 3641 Approval: Antibiotic-loaded chitosan devices for wound infection prevention (Mouse Model, Chapter 4)



IACUC PROTOCOL ACTION FORM

To:	Warren Haggard
From	Institutional Animal Care and Use Committee
Subject	Animal Research Protocol
Date	3-18-13

The institutional Animal Care and Use Committee (IACUC) has taken the following action concerning your Animal Research Protocol No.

0720 (Antibiotic loaded sponge ...)

Your proposal is approved for the following period:

From: March 18, 2013

To: March 17, 2016

Your protocol is not approved for the following reasons (see attached memo).

Your protocol is renewed without changes for the following period:

From:

To:

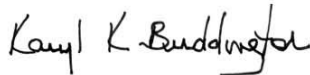
Your protocol is renewed with the changes described in your IACUC Animal Research Protocol Revision Memorandum dated

From:

To:

Your protocol is not renewed and the animals have been properly disposed of as described in your IACUC Animal Research Protocol Revision Memorandum dated


Prof. Guy Mittleman, Chair of the IACUC



Dr. Karyl Buddington, University Veterinarian
And Director of the Animal Care Facilities



REPLY TO
ATTENTION OF

DEPARTMENT OF THE ARMY
US ARMY MEDICAL RESEARCH AND MATERIEL COMMAND
504 SCOTT STREET
FORT DETRICK, MD 21702-5012

May 07, 2013

Director, Office of Research Protections
Animal Care and Use Review Office

Subject: Review of USAMRMC Proposal Number DM090455, Award Number W81XWH-12-2-0020 entitled, "Antibiotic-Loaded Biopolymer Sponge for Prevention of Polymicrobial Wound Infection"

Principal Investigator Warren Haggard
University of Memphis
Memphis, TN

Dear Dr. Haggard:

Reference: (a) DOD Instruction 3216.01, "Use of Animals in DOD Programs"
(b) US Army Regulation 40-33, "The Care and Use of Laboratory Animals in DOD Programs"
(c) Animal Welfare Regulations (CFR Title 9, Chapter 1, Subchapter A, Parts 1-3)

The above-referenced proposal is "complex," having multiple protocols associated with it under the same award. In accordance with the above references, the protocol/s listed below which is/are associated with proposal DM090455 is/are approved by the USAMRMC Animal Care and Use Review Office (ACURO) for the use of the specific species mentioned and will remain so until its modification, expiration or cancellation.

Protocol DM090455.02 entitled, "Antibiotic-Loaded Biopolymer Sponge for Prevention of Polymicrobial Wound infection," IACUC protocol number 0720, Principal Investigator Warren Haggard, is approved for the use of rats. This protocol was approved by the University of Memphis IACUC.

When updates or changes occur, documentation of the following action or events must be forwarded immediately to ACURO:

- IACUC-approved modifications, suspensions, and triennial reviews of the protocol (All amendments or modifications to previously authorized animal studies must be reviewed and approved by the ACURO prior to initiation.)
- USDA annual program/facility inspection reports
- Reports to OLAW involving this protocol regarding
 - a. any serious or continuing noncompliance with the PHS Policy;
 - b. any serious deviation from the provisions of the Guide for the Care and Use of Laboratory Animals; or

c. any suspension of this activity by the IACUC

- USDA or OLAW regulatory noncompliance evaluations of the animal facility or program
- AAALAC, International status change (gain or loss of accreditation only)

Throughout the life of the award, the awardee is required to submit animal usage data for inclusion in the DOD Annual Report on Animal Use. Please ensure that the following animal usage information is maintained for submission:

- Species used (must be approved by this office)
- Number of each species used
- USDA Pain Category for all animals used

For further assistance, please contact the Director, Animal Care and Use Review Office at (301) 619-2283, FAX (301) 619-4165, or via e-mail: usarmy.detrick.medcom-usarmmc.other.acuro@mail.mil.

NOTE: Do not construe this correspondence as approval for any contract funding. Only the Contracting Officer or Grant Officer can authorize expenditure of funds. It is recommended that you contact the appropriate Contract Specialist or Contracting Officer regarding the expenditure of funds for your project.

Sincerely,

For

GOODWIN SUSAN D DORE 1047618866

Bryan K. Ketzenberger, DVM, DACLAM
Colonel, US Army
Director, Animal Care and
Use Review Office

Copies Furnished:

Ms. Abigail Strock, US Army Medical Research Acquisition Activity (USAMRAA)
Dr. Dwayne Taliaferro, Congressionally Directed Medical Research Program (CDMRP)
Dr. Guy Mittleman, University of Memphis
Dr. Linda Heide, University of Memphis



IACUC PROTOCOL ACTION FORM

To:	Warren Haggard
From	Institutional Animal Care and Use Committee
Subject	Animal Research Protocol
Date	7-5-13

The institutional Animal Care and Use Committee (IACUC) has taken the following action concerning your Animal Research Protocol No.

Biopolymer sponge and paste for prevention of polymicrobial wound infection (0728)

Your proposal is approved for the following period:

From: July 5, 2013 To: July 4, 2016

Your protocol is not approved for the following reasons (see attached memo).

Your protocol is renewed without changes for the following period:

From: To:

Your protocol is renewed with the changes described in your IACUC Animal Research Protocol Revision Memorandum dated for the following period:

From: To:

Your protocol is not renewed and the animals have been properly disposed of as described in your IACUC Animal Research Protocol Revision Memorandum dated

Prof. Guy Mittleman, Chair of the IACUC

Dr. Karyl Buddington, University Veterinarian
And Director of the Animal Care Facilities

Vice Chancellor for Research

4301 W. Markham St., #718
Little Rock, AR 72205-7199

501-686-5347
501-526-7465 (fax)

www.uams.edu

Lawrence E. Cornett, Ph.D.
lcornett@uams.edu



DATE: November 5, 2013

TITLE: Antibiotic-loaded chitosan devices for wound infection prevention

AUP FILE#: 3461

PRINCIPAL INVESTIGATOR Mark Smeltzer, Ph.D. **MAIL SLOT:** 511

NAME OF INSTITUTION: University of Arkansas for Medical Sciences

Dear Dr. Smeltzer:

The above mentioned new protocol submitted to the UAMS Institutional Animal Care and Use Committee (IACUC) was reviewed on September 20, 2013.

Revisions to the study were reviewed by the IACUC Chairman, and **Full Approval was received for the study on November 5, 2013.**

The Committee wishes to remind you that, under the provisions of the UAMS Animal Welfare Assurance Number #A3063-01 from the Office of Laboratory Animal Welfare, the principal investigator or project director is directly responsible for keeping the IACUC informed of any proposed changes involving the care and/or use of animals.

Please use the file number shown above regarding any questions or revision/addendum concerning this approved protocol.

Sincerely,

A handwritten signature in black ink, appearing to read "Bill J. Gurley", with a long, sweeping horizontal flourish extending to the right.

Bill J. Gurley, Ph.D.
Professor, College of Pharmacy
Chairman, Institutional Animal Care and Use Committee